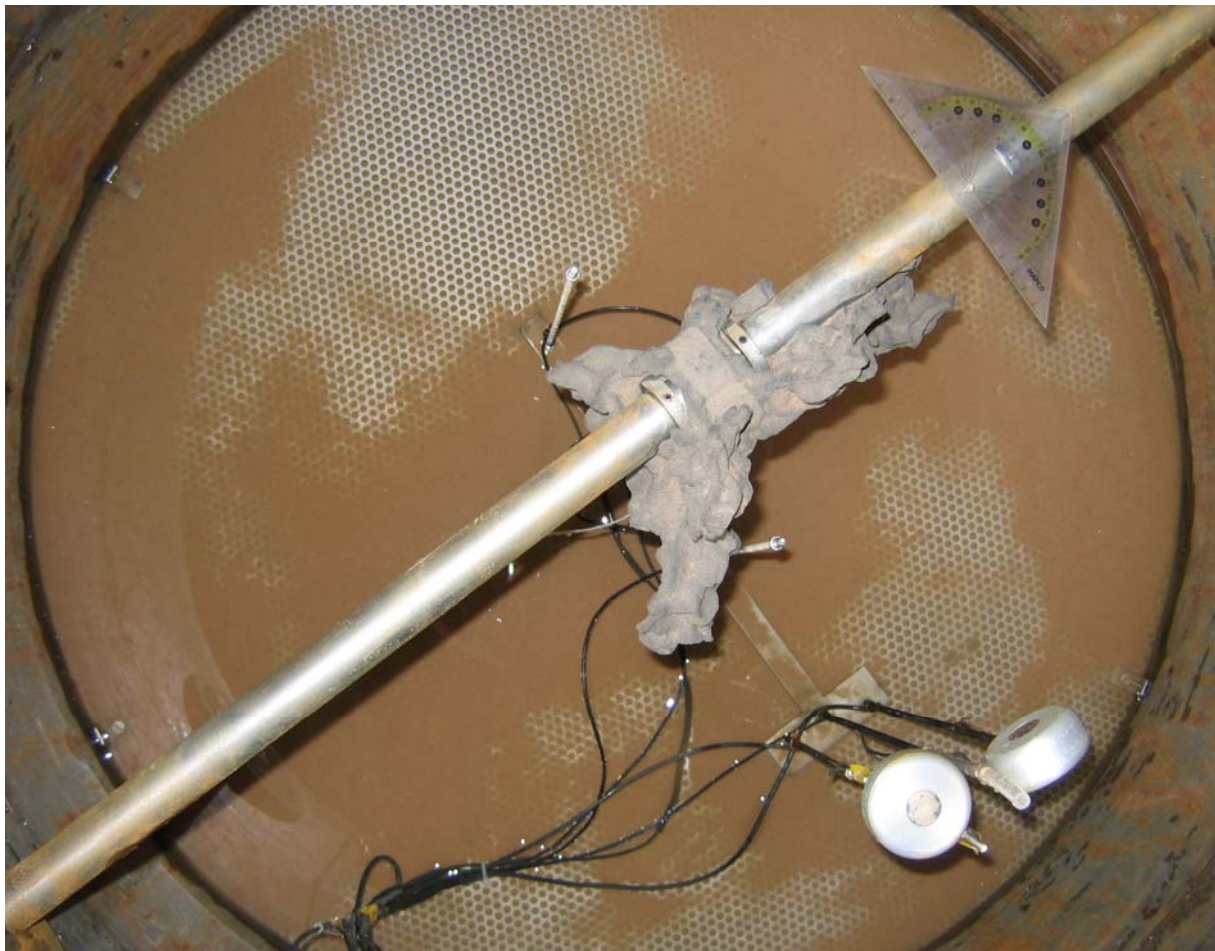

Compensation Grouting

Laboratory Experiments in Sand



Top view: Cylindrical container with excavated propagating grout fracture

Remco Kleinlugtenbelt
Std no. 9441101

M. Sc. THESIS, Civil Engineering
Compensation Grouting Experiments in Sand
October 2005

Colophon

Organisations

Delft University of Technology
Faculty Civil Engineering and Geosciences
Stevinweg 1
2628 CN Delft
Tel +31 15 278 5440

GeoDelft
Stieltjesweg 2
2628 CK Delft
Tel +31 15 269 3500

Student

Remco Kleinlugtenbelt
Graafseweg 17
6512 BM Nijmegen

Tel +31 6 4124 1898 (cell phone)
Email RKleinlugtenbelt@hotmail.com
Student No. 9441101

Committee

Chairman (TU Delft)

Prof. ir. A.F. van Tol
Chair Foundation Engineering
Room 1.18 (Civil Engineering)
Tel +31 15 278 5478
+31 15 269 3584 (GeoDelft)
Email A.F.vanTol@citg.tudelft.nl
A.F.vanTol@geodelft.nl

Supervisor (TU Delft)

Prof. ir. J.W. Bosch
Chair Underground Space Technology
Room 2.06 (Civil Engineering)
Tel +31 15 278 2844
+31 20 556 5428
Email J.W.Bosch@citg.tudelft.nl
Bosch@ivv.amsterdam.nl

Daily supervisor (TU Delft)

Ing. H.J.Everts
Chair Foundation Engineering
Room 0.10 (Civil Engineering)
Tel +31 15 278 5478
+31 15 269 3769 (GeoDelft)
Email H.J.Everts@citg.tudelft.nl
H.J.Everts@geodelft.nl

External supervisor (GeoDelft)

Ir. A. Bezuijen
Tel +31 15 269 3785
Email A.Bezuijen@geodelft.nl

Supervisor (TU Delft, separate department)

Dr. ir. P.J. Visser
Chair Hydraulic Engineering
Room 3.96
Tel +31 15 278 8005
Email P.J.Visser@citg.tudelft.nl

External supervisor

Ir J.K. Haasnoot
Tel +31 6 2397 6306
Email Haasnoot@CruxBV.nl

Preface

The final thesis of the Civil Engineering Master at Delft University of Technology consists of research on a civil engineering subject. This research is on an experiment performed in the context of the Noord/Zuidlijn, a metro line beneath surface level under the historical center of Amsterdam. Settlement might occur at foundation level during tunnel driving. A mitigating measure for settlement is compensation grouting; grout injections compensate the overcut of the tunnel excavation, thereby reducing settlement of the building.

A laboratory experiment was carried out on fracture grouting to increase the understanding of the compensation grouting technique. All the experiments were performed at the institute on geotechnical engineering GeoDelft and funded by the COB (Centrum Ondergronds Bouwen), the Dutch organization for underground construction.

Readers guide

Chapter 1 is an introduction on the compensation grouting issue. Chapter 2 describes the problems that have come across during research on compensation grouting and what the difficulties are in this study. Chapter 3 illustrates two experiments that have been done in the field of fracture grouting in Delft to see if these set-ups were useful for the compensation grouting experiment. A fracture grouting model made to analyze grout fractures is implemented in chapter 4, so an experiment can validate this model. The experimental set-up is given in chapter 5. The results and description of all 10 tests are presented in chapter 6. In chapter 7, some theoretical aspects concerning the experiment are discussed. The report finishes in chapter 8 with the conclusions and recommendations.

Acknowledgments

I would like to thank my counseling team consisting of Professor Bosch, Professor van Tol, Mr. Bezuijen, Mr. Everts and Mr. Haasnoot for their support and for coaching me during the execution of the tests and the writing of my report.

My appreciation goes to Mr. Essler, who gave me and my counseling team an out-of-the-box thought on the compensation grouting process and the experiment. He also brought me in contact with the people from Keller Australia, where I will go to work on a compensation grouting project after my graduation.

Also I would like to thank all the people at GeoDelft. Without them, I could not have performed the tests I did: Willem van Pernis, Ferry Schenkeveld, Jack van der Vegt, Gerard Kruse, Thijs van Dijk, Ruud van de Berg, Paul Schaminée, Goof Leendertse, Ton Veldhuis, Frans Kop, Percy Pourier, Lambert Smidt, and Willem van der Zon. They all made my stay in the 'Meethal' very pleasant.

Finally, I want to thank my friend Bram for his differential equation support. And last but not least, my girlfriend Lotte who did not only give support with the English language, she also gave me essential support, which is indispensable when accomplishing a final thesis.

Delft, 4 October 2005

Remco Kleinlugtenbelt

Summary

Introduction

The Noord/Zuidlijn (North/South Line) is a 9.5 kilometers long metro line tunnel bored underground through the historical city centre of Amsterdam. The Tunnel Bore Machine (TBM) will initiate unacceptable settlement of monumental buildings in the surroundings. At these locations, mitigating measures are defined. One of the measures that will be used is compensating grouting. Compensation grouting is a technique where from a vertical shaft horizontal injection pipes will be brought into the soil underneath the foundation of the protected building. A pump will inject the soil with grout (water cement mixture) through injection points.

The main objective of this research is to set up an experiment where, by means of grout injection, the geometry and the propagation of a grout fracture in sand can be examined. An analytical model has been made in a previous research to describe the propagation and stagnation of a fracture. The experiments can validate this model.

Central part

The grout fracture is modeled as a single tube where the shear force (Bingham fluid --> shear force per unit length is constant along the fracture length) and the minimum soil stress balance the driving grout-pump pressure. The diameter of the fracture is determined by the volume injected and the length of the fracture. Besides the friction of the fluid, there is another mechanism which stops the fracture propagating, the bleeding of the grout. Bleeding; under pressure water is squeezed out of the fresh grout into the sand. According to the model fractures of 30 meters will occur in a time span of 6 seconds.

The experiment consists of a cylindrical container with a diameter of 90 centimeters filled with sand. In the middle of the sand layer, there is an injection point installed. This is where at a constant flow rate the grout mixture will penetrate the sand. The important parameters to measure are the injection and pump pressures. In order to determine the volume balance the amount of drainage water pushed out of the sand sample and the heave on top of the sand sample are measured. Every test is unique with its own parameters. The parameters varied are the lay-out of the injection point, the injection rate and sand sample density. The rheology of the grout was measured for every test as well as the permeability of the bled grout layer. The tests were performed at a vertical total pressure of 100kPa. In the model the assumption is made that fracturing sand gives certain peak pressure-records. These peaks are reactions of additional fractures occurring after the initial opening of the rubber sleeve. The experiment does not confirm such a behavior only a clear fracture initiation pressure followed by a constant pressure when injection progresses are shown.

Conclusion

The main objective of the research has been achieved. A set-up of an experiment was made, where by means of grout injection the geometry and the propagation of a grout fracture in sand can be examined. Adjustments to the grout mixture were made to improve the behavior of the grout injection to create more of an actual fracture. The geometrical outline of the fracture was examined by excavation, which increased the understanding of the compensation grouting technique.

The compensation grouting laboratory experiments in sand have not given the expected outcomes as predicted by the model. Fortunately, a lot of experimental data is generated which can support further research.

Pre conditioning is done in the experiment by loading the sand and unloading it to get an over consolidated sand, creating a $K_0 \approx 1$. Pre conditioning generates larger horizontal soil stresses than vertical stresses. The larger horizontal stresses allow horizontal fractures. This aspect is an important part of the compensation grouting process. Creating the $K_0 \approx 1$ before injection was not accomplished but as soon injection started in the experiment, the horizontal stresses rose to a level higher than the vertical stresses, resulting in a K_0 larger than 1.

The additive, bentonite, has a large influence on the grout injections' material behavior. Bentonite that has steeped (hydrated) in water for 24 hours before adding the cement influences the permeability of the bled grout layer. This makes the mixture more capable of holding water. However, when bentonite hydrates for 24 hours it thickens the grout mixture and therefore the Water Cement mass Ratio (WCR) must increase to keep the grout mixture processible. Increasing the WCR adds more water to the mixture; this water can bleed again and consequently is not improving the efficiency (= volume heave/ volume injected grout).

The generated data can still be analyzed in more detail and on more aspects. The experiment has produced a considerable amount of data which can be used for a more comprehensive analytical analysis.

Content

| | |
|---|-----------|
| COLOPHON | 3 |
| PREFACE | 5 |
| SUMMARY | 7 |
| CONTENT | 11 |
| 1 INTRODUCTION | 15 |
| 2 PROBLEM ANALYSES AND OBJECTIVES | 19 |
| 2.1 PROBLEM ANALYSES COMPENSATION GROUTING | 19 |
| 2.2 OBJECTIVE OF THE GROUTING EXPERIMENT | 21 |
| 3 PREVIOUS HYDRAULIC FRACTURE EXPERIMENTS | 23 |
| 4 FRACTURE GROUTING MODEL IMPLEMENTED IN AN EXPERIMENT | 25 |
| 4.1 INTRODUCTION | 25 |
| 4.2 GEODELFT CONTAINER AND BASKARP SAND | 25 |
| 4.3 POWERSIM SIMULATION | 26 |
| 4.3.1 <i>The friction theory</i> | 28 |
| 4.3.2 <i>The bleeding theory</i> | 30 |
| 5 EXPERIMENTAL SET-UP | 35 |
| 5.1 INTRODUCTION | 35 |
| 5.2 SET-UP | 35 |
| 5.2.1 <i>Grout Pump</i> | 38 |
| 5.2.2 <i>Vertical Displacement of the Sand Sample</i> | 39 |
| 5.2.3 <i>Grout Pressure Measuring in Injection Pipe</i> | 40 |
| 5.2.4 <i>Overview of the Container with all the Transducers</i> | 41 |
| 5.2.5 <i>Injection System</i> | 42 |
| 5.3 EXPERIMENT PROCEDURE..... | 43 |
| 5.3.1 <i>Introduction</i> | 43 |
| 5.3.2 <i>Test Procedure</i> | 43 |
| 6 TESTS PERFORMED | 47 |
| 6.1 INTRODUCTION | 47 |
| 6.2 CLARIFICATION OF THE TEST RESULT | 47 |
| 6.3 OVER CONSOLIDATION | 47 |
| 6.4 MIXTURE | 50 |
| 6.4.1 <i>Permeability</i> | 51 |
| 6.5 DATA DIAGRAMS EXPLAINED | 52 |
| 6.6 TEST 1 WITH MODEL TE GROTENHUIS PARAMETERS..... | 55 |
| 6.7 TEST 2: A CHANGE IN THE INJECTION LAYOUT | 58 |
| 6.8 TEST 3 INJECTION RATE 10 L/MIN | 61 |
| 6.9 TEST 4 INJECTION RATE 20L/MIN | 63 |
| 6.10 TEST 5 MORE BENTONITE ADDED (7%) | 65 |
| 6.10.1 <i>Conclusion Tests 1-5 Leads to Test 6</i> | 67 |
| 6.11 TEST 6 PUMP UPGRADE 10BAR, 4 INJECTION HOLES | 68 |
| 6.12 TEST 7 PUMP UPGRADE 15 BAR | 70 |
| 6.13 TEST 8 LARGE VOLUME INJECTION (1 LITER) | 72 |

6.14 TEST 9 DENSE SAND 74

6.15 TEST 10 LOOSE SAND..... 76

7 DISCUSSION..... 79

7.1 THEORETICAL MAXIMUM EFFICIENCY OF THE INJECTION 79

7.2 CEMENT EFFICIENCY 82

7.3 PRESSURE RECORDS 83

8 CONCLUSIONS AND RECOMMENDATIONS..... 85

8.1 INTRODUCTION 85

8.2 CONCLUSIONS 85

8.2.1 *Set-up*..... 85

8.2.2 *Model Validation*..... 85

8.2.3 *Technical Achievements* 87

8.3 RECOMMENDATIONS 89

8.3.1 *Further Research*..... 89

8.3.2 *Practical Performance Compensation Grouting* 90

APPENDICES 91

APPENDIX A: 93

SUMMARY REPORT FRACTURE GROUTING IN THEORY 93

[TE GROTENHUIS, 2004⁴]..... 93

Introduction 93

Results Fracture Grouting in Theory..... 94

Conclusion Fracture Grouting in Theory..... 95

Recommendations Fracture Grouting in Theory 96

APPENDIX B: 97

REVIEW ALL TEN TESTS 97

REFERENCES..... 101

1 Introduction

The Noord/Zuidlijn (North/South Line) is a 9.5 kilometers long underground metro line. It begins above ground in Amsterdam-North and goes south. From the J. Van Hasseltweg station it goes underground through the historical city centre and comes above ground again in Amsterdam-South at the World Trade Centre Station (the end point of the new metro line). The bored section is 3.8 kilometers long. The Tunnel Boring Machine (TBM) follows the existing street patterns; therefore, almost no buildings will have to be demolished. Following the street pattern brings another major advantage, namely reducing the risk of settlement of the monumental buildings in Amsterdam.



Figure 1-1 Trajectory Noord/Zuidlijn Amsterdam [Noord/Zuidlijn¹]

Historic buildings are founded on wooden piles. These end-bearing piles are approximately 15 meters long in the inner city and rest on the first sand layer. Modern structures have a concrete piles foundation of approximately 20 meters long. Most of the modern buildings are founded on the second sand layer. Figure 1-2 schematically shows the Amsterdam situation.

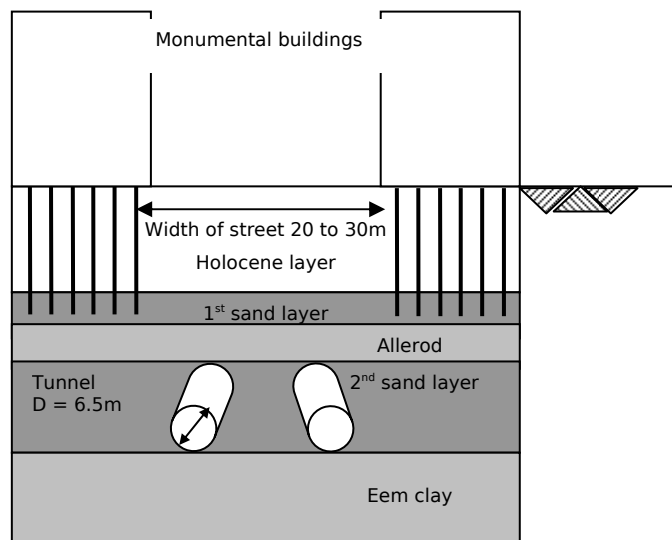


Figure 1-2 Characteristic soil profile of Amsterdam soil [Vliet 2001²]

The risk of unacceptable settlement is especially present in the curved parts of the tunnel trajectory. The head of the Tunnel Bore Machine (TBM) is a stiff cylinder of about 7m (see below). Therefore, overcut will always be larger when making a turn than when going straight.



Figure 1-3 Head Tunnel Bore Machine [Noord/Zuidlijn¹]

A settlement Risk Assessment has shown that there are several locations along the trajectory with a risk of unacceptable settlements. For these locations, mitigating measures are defined. One of the measures that will be used is the technique of compensating grouting.

Compensation grouting can be characterized by one of two types of grouting, fracture grouting and compaction grouting. Compensation grouting is a technique where from a vertical shaft horizontal injection pipes 'Tubes à Manchette' (TAM) will be brought into the ground, underneath the foundation. As seen in top view in Figure 1-4. Through injection points on the tubes will the soil be injected with grout, a water cement mixture.

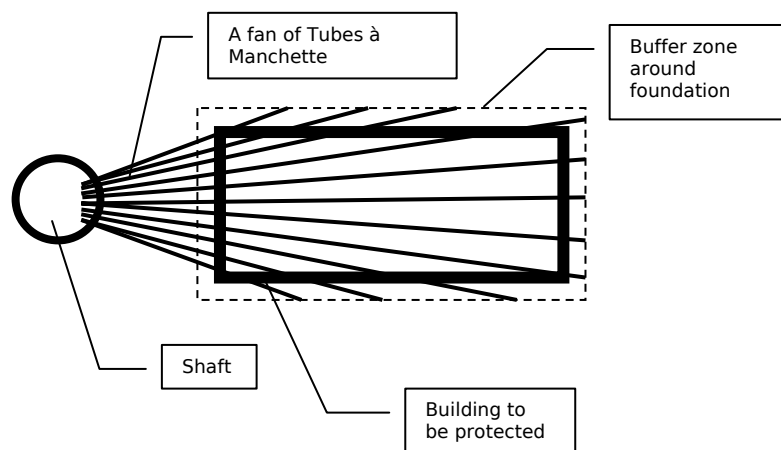


Figure 1-4 Schematic top view of the fracture grouting technique

The objective is to create horizontal fractures in the subsoil filled with grout. Grout used for this method is a liquid grout with a low viscosity compared to normally used grout mixtures. Generally, the fracture grout consists of cement, water and additives such as bentonite.

Compensation grouting has been a proven method all over the world to compensate settlement at tunneling projects. However, these projects in the United Kingdom, Japan and the United States are performed in cohesive soils. Amsterdam is one of the rare cases, together with the project in Antwerpen, where injection takes place in the silty soil. In Amsterdam the method of compensation grouting will be used in the cohesionless first sand layer as shown in Figure 1-2. This is one of the reasons for doing more research on the method. To assess the feasibility of the technique of compensating grouting for the Amsterdam situation, a full-scale test has been performed, the Compensation Grouting Trail (CGT). The results of the CGT showed that settlement of buildings founded on end bearing piles can be controlled. Compensation, immediately intervening during passage of the TBM, was less efficient because of the relatively high speed of the TBM. Additionally,

a large amount of grout had to be injected to control settlement during fast passing of the TBM. The Holocene layers above the first sand layer are an easy escape route for the injected grout, since fractures in soil layers follow the path with the lowest stress. The volume of grout lost due to vertical fractures makes compensation grouting less efficient.

The passage speed of the TBM could be adjusted since only a certain amount of grout can be injected in a particular time span to be efficient.

Grout efficiency has been calculated by the quotient of heave volume and the volume of injected grout [Kummerer 2003³].

$$\eta = V_h / \Delta V_0 \cdot 100\% \quad [1-1]$$

η = Grout efficiency [%]

V_h = Volume of Heave [m³]

ΔV_0 = Injected volume [m³] in a certain treated soil volume V_0

The objective of this research

A further analysis must be made for a better understanding of the technique of fracture grouting. It has been proven by the CGT that compensation grouting works but a lot of questions still exist regarding the process and the physical structure of fractures in sandy soils.

Several studies have already been performed on the CGT and even more research is appreciated. An example is the study of te Grotenhuis^[4] who developed a model to describe propagation of fractures in sand. The experiments in this thesis are closely related to his analytical model. The recommendation of te Grotenhuis' thesis is to set up an experiment validating his analytical model.

2 Problem Analyses and Objectives

2.1 Problem Analyses Compensation Grouting

As discussed in the introduction, compensating grouting is a mitigating measure for the settlement caused by the TBM. Compensation grouting is divided into two different types of grouting; compaction grouting and fracture grouting. For the difference in the two principles, see Figure 2-1.

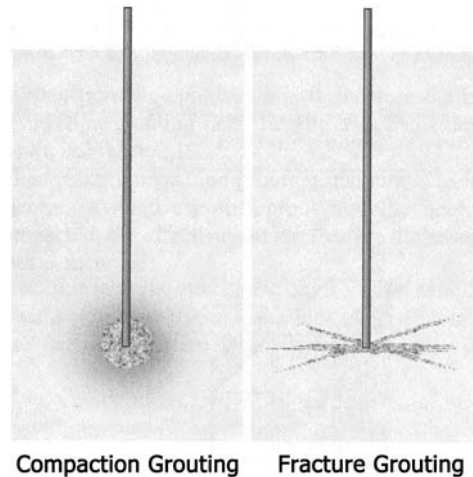


Figure 2-1 Principal difference compensation grouting techniques [Stoel⁵]

The principle of compaction grouting is creating a homogeneous expansion of the grout similar to an inflated balloon. Very stiff, high viscosity grout is used. The application of compaction grouting is used primarily for the compensation of shallow foundation considering an uplift force to compensate settlement. The use of this technique to compensate settlements of piles foundation is less frequent [Stoel⁵]. This is because of the restriction of multiple injections.

The principle of fracture grouting is to create fractures in the subsoil. The grout initially forms a ball. As injection progresses the grout follows the path of the lowest stress and sets into thin fractures. This technique can create a surface heave in a large area. Low viscosity grout is used. The fracture grouting technique has proven to be effective as can be seen in London's Green park station and Tokyo's Koto-ku. [Cheong et al⁶]

Considerable uplift force to compensate settlement is created by both techniques. However, fracture grouting is preferable in Amsterdam because of the possibility of re-grouting to compensate an additional settlement. Nevertheless, the situation in Amsterdam is in one important manner different from the places where the technique of compensation grouting has been successful. These latter cases were in cohesive soils whereas the compensation in Amsterdam has to be performed in the cohesionless first sand layer. Another difference between the earlier compensation grouting projects and the Amsterdam situation is the type of foundation. In Amsterdam grouting occurs underneath a pile foundation.

A problem at the CGT was the fracture length, which affects the efficiency. Very large fractures of more than 20m appeared, as seen in the data of this trial [Haasnoot et al⁷]. A fracture propagating away from the foundation of the 'protected building' reduces the efficiency of the technique, so a limitation of the fracture length is desirable.

Hardening of the injected grout takes time. Repetition of injections is also time consuming, therefore, it is favorable to make the injections as efficient as possible to save time and grout. Another important issue is the speed of the TBM. Is it possible to inject grout and compensate settlement during passage of the TBM?

The length of a fracture seems to be a problem but when one is capable of controlling the fracture path and the diameter of a fracture, then the process is much more controllable and more likely to use often as a mitigating measure.

Grout consists of almost 50 mass percentages of water, giving it a water cement ratio (WCR) of 1. During the grout injection this water is 'lost' to the surrounding soil. This process is called bleeding. It has been understood that fine materials like bentonite are able to build up a filter cake and in that way retain the water for a longer time when under pressure of the pump. This makes the injection more efficient as less fluid is lost to the soil by bleeding. See Figure 2-2 below.

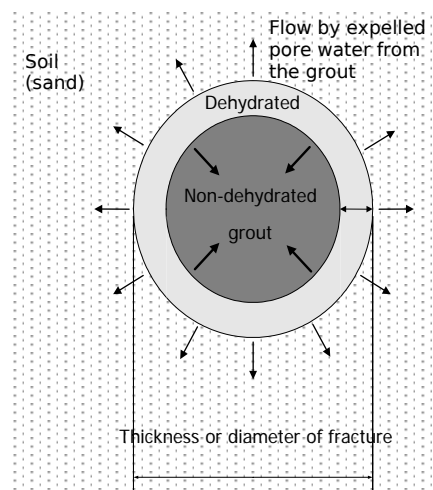


Figure 2-2 Simplified sketch of dehydration (bleeding) grout in propagating fracture [te Grotenhuis, 2004⁴]

The problem analysis of this thesis subject is to find out how a grout injection behaves, which means fracture propagation and fracture growth in diameter, while injected at a controlled flow. Examine possibilities to influence length and exterior of the fracture this, means borehole expansion and fracture propagation, by changing the rheology parameters of the grout mixture. This is done in order to control the settlements at foundation level along the trace of the Noord/Zuidlijn in Amsterdam.

2.2 Objective of the Grouting Experiment

In a wider perspective, the purpose of the CGT and further research is to assess the feasibility of compensation grouting, increase the efficiency of the technique, and to understand the process of compensation grouting so it can be applied effectively in different soil situations such as clay (cohesive materials) and sand (cohesionless material).

The main objective of this research is to set up an experiment where, by means of grout injection, the geometry and the propagation of a grout fracture in sand can be examined. This will give a better understanding of the technique of compensation grouting. An analytical model has been made to describe the propagation and stagnation of a fracture. The experiments can validate the model to be used in practice and are useful for making an injection strategy.

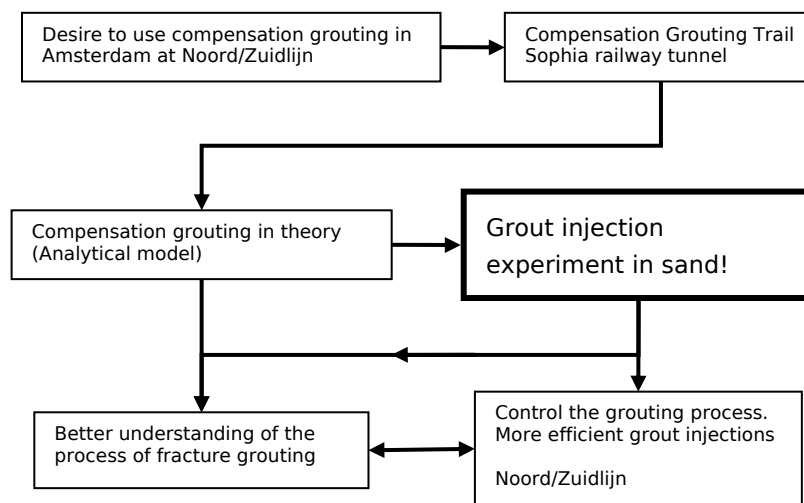


Figure 2-3 schematic outline of the objective of this research

In the figure above the compensation grouting laboratory experiments in sand is set in perspective to other research and with what intention and purpose this experiment is done.

3 Previous Hydraulic Fracture Experiments

An inventory of experimental set-ups is made to determine the most suitable setting for the experiments. The faculty of Applied Earth Science is well accommodated for an experimental study of hydraulic fracturing in sand. A set-up is available for fracturing of sand under very high pressures, modeling a depth of 2 to 3 kilometers (20–30 MPa). See Figure 3-1 below.

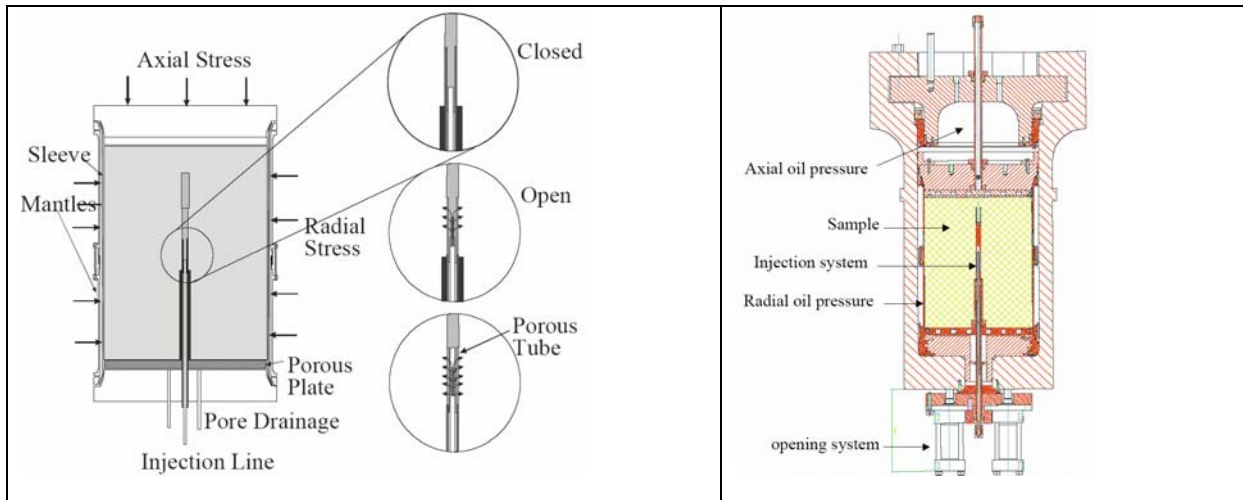


Figure 3-1 Sand sample in biaxial cell. The enlargement shows the injection system, both in the closed and open state [de Pater et al, 2003⁹]

For the experiment on fracture grouting in low stress conditions, in the shallow sub-soil of a maximum depth of 20 meter, are these facilities not suitable. In order to use a Tube à Manchette (TAM) and grout instead of a grout mixture a larger installation is needed. The robust setting of the aluminum protection cylinder is not necessary for grout injections with a vertical effective stress at a maximum of 0,2MPa pressure.

GeoDelft [A. Bezuijen 2003⁹] has performed Hydraulic fracture experiments at low stresses in sand. This set-up seems very useful for the fracture grouting experiments see (Figure 3-2 below). Some changes must be made in order to inject grout trough a TAM.

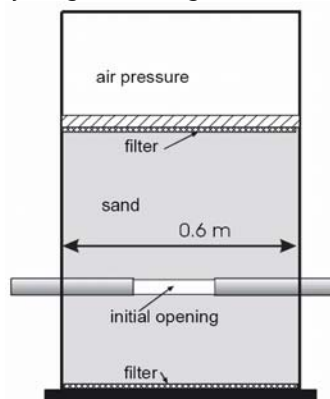


Figure 3-2 Experimental set-up for horizontal borehole tests [Bezuijen, 2003⁹]

Interpreting the experimental set-up of A. Bezuijen a set-up for the compensation grouting experiments is made. The compensation grouting set-up is presented in Chapter 5. It is closely related to the experiment of horizontal borehole tests. The most important differences are the injection fluid, the technique of injection and the size of the cylindrical container.

4 Fracture Grouting Model Implemented in an Experiment

4.1 Introduction

The model of te Grotenhuis is used for the prediction of the fracture pattern. A grout mixture that can be used in the experiment and thus help control the important parameters such as fracture length and effective diameter is designed. All parameters in this model are controllable. The challenge is to create a grout mixture that takes into account the boundary values the container and the sand sample give. Boundary values are: a maximum fracture length of 45cm and a permeability of the bled grout layer 50 times as large as the permeability of the sand. Also the soil pressures are an important factor in fracture length according to the model.

4.2 GeoDelft Container and Baskarp Sand

By using the geo-centrifuge cells, to make a container, from GeoDelft and Baskarp sand, (see for properties of the Baskarp sand paragraph 6.2) two boundary conditions of the experiment have already been set as held before. The main reasons for using this type of container for the test are availability and the fact that it gives the opportunity to keep the test reproducible. GeoDelft generally uses Baskarp sand in all its experiments, which makes it obvious to use the same sand for this experiment. In practice, the soil type is not a parameter that can be controlled. All material properties of Baskarp sand are known, and therefore, no further research on the sand is necessary. The question remains whether or not it is possible and valid to use the analytical model. Parameter variation studies of the analytical model give the dominant parameters in the model. In Table 4-1 all the parameters used are given with their dependency (formula). The last column (Table 4-1) gives the value of the constants te Grotenhuis used in his calculations.

The Model te Grotenhuis uses states:

The grout fracture is modeled as a single tube. The shear force (Bingham fluid --> shear force per unit length is constant along the fracture length) and the minimum soil stress balance the driving pump-pressure. The diameter of the fracture is determined by the volume injected and the length of the fracture. Besides the friction of the fluid, there is another mechanism which stops the fracture of propagating, the bleeding of the grout. A fracture silts up by losing water to the sand. See for a more extensive explanation of the model the summary of te Grotenhuis' report in Appendix A.

4.3 Powersim Simulation

Table 4-1 Summary of all parameters in model

| RtG | Powersim | Description | Dimension | Formula | Value |
|------------------|----------------|---|-------------------|--|-----------------------|
| s | s | length fracture | m | $= \frac{p_{ext} - \sigma_{min}}{4\tau} \cdot d$ | |
| d | d | diameter fracture (Volume controlled) | m | $= \sqrt{\frac{4 \cdot V}{\pi \cdot s}}$ | |
| | Stress ratio | | - | $= \frac{p_{ext} - \sigma_{min}}{\tau}$ | |
| p _{ext} | p_ext | fracture extending pressure | kN/m ² | $= \sigma_{min} + p_d$ | 700 |
| σ _{min} | sigma_min | minimal principal stress | kN/m ² | | 240 |
| τ | tau | shear stress | kN/m ² | | 0.025 |
| Q | Q | injection rate | m ³ /s | | 1.67·10 ⁻⁴ |
| t | Time | time | s | | |
| V | V | volume | m ³ | Q·t | |
| x _e | Xe | thickness bleded layer | m | $= sdf \cdot \sqrt{2k \frac{1 - n_i}{n_i - n_e} \Delta\phi \cdot t}$ | |
| k | k | permeability bleded layer | m/s | | 5·10 ⁻⁹ |
| | Porosity_ratio | porosity ratio | - | $= \frac{1 - n_i}{n_i - n_e}$ | 1.03 |
| n _i | ni | initial porosity non-bleeded grout | - | | 0.75 |
| n _e | ne | final porosity grout after bleeding | - | | 0.5 |
| Δφ | delta_psi | pressure head difference | m | | 54 |
| sdf | S_D_F | Spatial Dehydration Factor | - | | 3.5 |
| d _{eff} | D_eff | effective thickness of propagating fracture | m | $= d - x_e$ | |

When using Powersim, a program for the calculation of first order differential equations, it becomes possible to easily vary the parameters of the model. The values te Grotenhuis calculated have been reproduced here, and one can conclude that the Powersim model correctly simulates the propagation and stagnation of a fracture as done in te Grotenhuis' model. Figure 4-1 schematically visualizes the Powersim model.

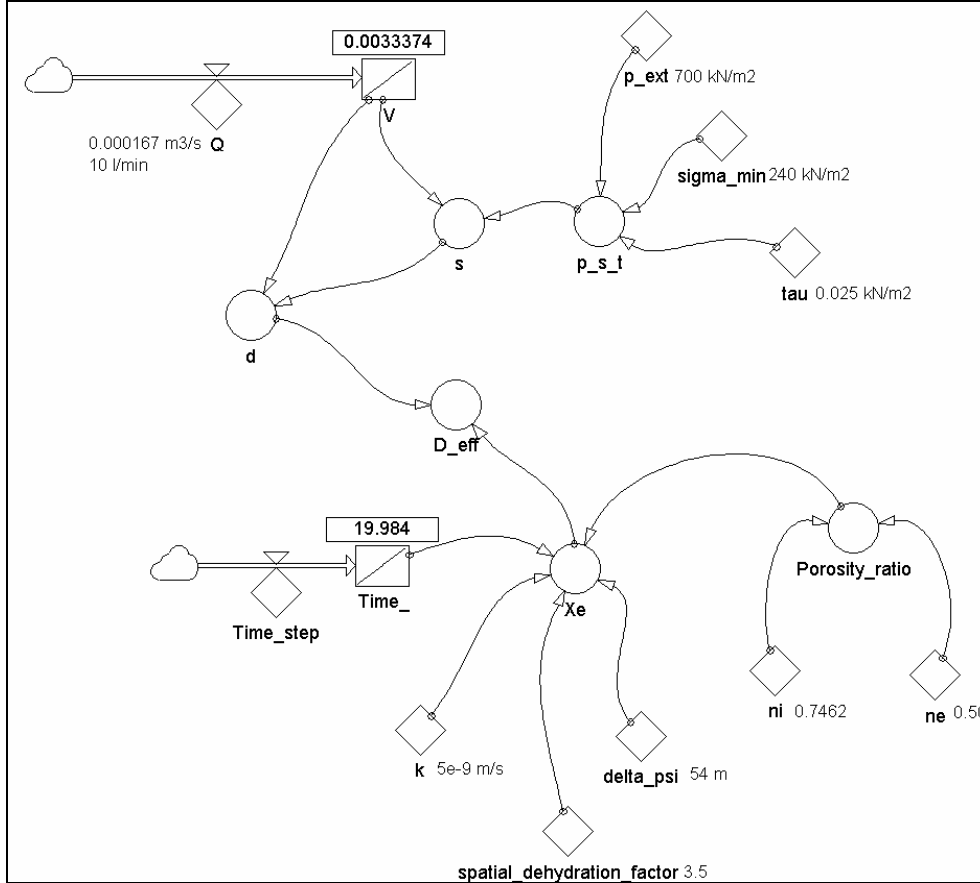


Figure 4-1

The squares \square V and \square_{Time} represent a stock level, a value that grows in time. Obviously, time does grow in time. V , the volume of grout injected, grows in time with the injection rate Q . Diamonds \diamond k represent a constant. All Circles \circ stand for the values calculated and the arrows for the relation between the parameters. Hidden in the circles is the calculated formula. The diagrams below show the relation between fracture length in time and diameter growth in time.

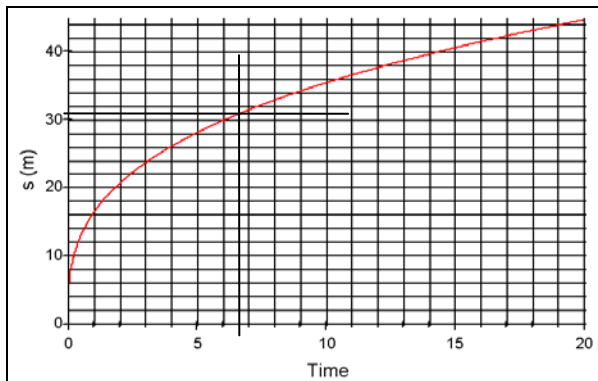


Figure 4-2 Fracture growth s in time

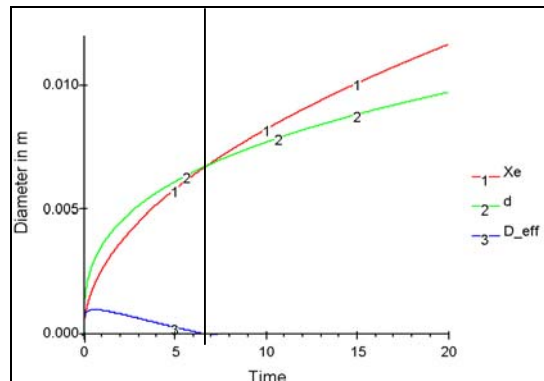


Figure 4-3 Growth of d , x_e and d_{eff} in time

In both diagrams the time when $d_{\text{eff}} = 0$ is marked by a black line. $d_{\text{eff}} = 0$ means that the fracture stops propagating. While keeping the pressure high it is assumed that the fracture does not propagate in the original direction anymore but finds another way into the sand along another fracture path or a branch of the main fracture. The initial fracture length before starting to another direction is as can be seen from Figure 4-2 30meter length in 6seconds with a diameter of 7mm. In order to be able to test and validate the model, fracture length 's' must be controllable, assuming the model is correct. It is possible to shorten 's' so the container of a diameter of 90cm can be used. In addition, the parameters used in the experiment must stay within the range of the parameters used for compensation grouting in practice. The model makes it possible to examine two ways of approaching the shortening of the fracture length 's' for testing in the experimental set-up, the friction theory side and the bleeding theory side.

4.3.1 The friction theory

When grout is injected into a single channel, injection proceeds until the grout stops because the shear force along the wall of the channel balances the driving pressure. The model assumes that the grout behaves as a Bingham fluid which means that the shear force per unit area of contact between the grout and the fracture channel wall is constant along the length of the fracture. [Stille et al. 1992¹⁰]

$$\text{Fracture length} \quad s = \frac{p_{\text{ext}} - \sigma_{\text{min}}}{4\tau} \cdot d \quad [4.1]$$

- A smaller injection rate brings less volume in the soil and thus automatically creates a smaller diameter 'd' and a shorter length 's' of the fracture.
- If the grout experiences more friction (larger τ), it will not propagate as far into the sand because the pump pressure cannot overcome the friction due to shear stress. The fracture will not fracture propagate any further. The injected grout will be more likely to go into a new fracture direction.
- The σ_{min} determines the total pressure in the surrounding soil. The lower σ_{min} the easier it is to keep propagating a fracture.

Reviewing these theories in the formulas used:

The injected Volume V should be less.

$Q = 0.000167 \text{ m}^3/\text{s} \rightarrow 10\text{l}/\text{min}$ in the Compensation Grouting Trial (CGT)

Take for experiments 1l/min or 0.5l/min.

Stress ratio $\frac{p_{\text{ext}} - \sigma_{\text{min}}}{\tau}$ should go down. $\rightarrow \tau$ increases (yield stress raise)

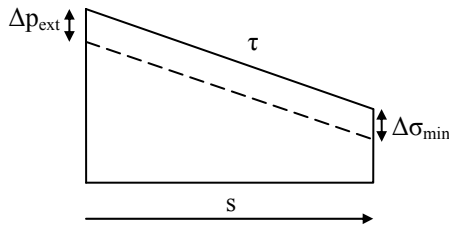
$p_{\text{ext}} - \sigma_{\text{min}}$ should decrease $\rightarrow p_d = p_{\text{ext}} - \sigma_{\text{min}}$

p_d is a result of the injection rate. The question how p_d varies with the injection rate (Q) is still unknown.

$\sigma_{\text{min}} = 240 \text{ kN}/\text{m}^2$ (total pressure) equals 17m below surface level. 1m under surface level gives a $\sigma_{\text{min}} = 20.5 \text{ kN}/\text{m}^2$ (total pressure). p_{ext} can be smaller. A rule given by Bezuijen is that fracture initiation starts at 3 to 5 times the soil pressure. $p_{\text{ext}} = 5\sigma_{\text{min}}$

4.3.1.1 Dependent relation between σ_{min} and p_{ext}

There is thought of a relation between minimum soil stress (σ_{min}) and injection pressure (p_{ext}). This gives the expected pump pressure when the soil pressure is known. This is an assumption made by te Grotenhuis (RTG) but the p_{ext} does also depend on the injection rate (Q)



| Symbol | Clarification | SI-Unit |
|------------------|---------------------|-------------------|
| σ_{min} | Minimum soil stress | N/m ² |
| τ | Shear stress | N/m ² |
| s | Fracture length | m |
| Δp_{ext} | Injection pressure | N/m ² |
| Q | Injection rate | m ³ /s |

Table 4-2

Figure 4-4 $\Delta\sigma_{min} = \Delta p_{ext}$

Theorema te Grotenhuis:

The grout fracture is modeled as a single tube. The shear force (Bingham fluid --> shear force per unit length is constant along the fracture length) and the minimum soil stress balance the driving pump-pressure.

$$p_{ext} = \sigma_{min} + \tau \tag{4.2}$$

The pump produces a pressure p_{ext} . The pump pressure has to overcome the shear stress τ and soil stress. For this reason, the fracture can only reach a certain length s.

What happens if σ_{min} is lowered and τ stays the same? p_{ext} reduces with the same absolute numbers as σ_{min} , as can be concluded from Figure 4-4

Consider $\sigma_{min} = 0$

As can be expected p_{ext} should also become 0 and should not drop with the same absolute value as σ_{min}

After all, if soil pressures are 0 pump pressures cannot build up because of a lack of backpressure from the soil.

Conclusion: p_{ext} does not reduce with the same absolute numbers as σ_{min} as shown in Figure 4-4. p_{ext} and σ_{min} are proportionate to one another.

For example: $5 \cdot \sigma_{min} \approx p_{ext}$ [te Grotenhuis⁴]

In this correlation, a lower soil stress σ_{min} will shorten the fracture length s. As shown in Figure 4-5

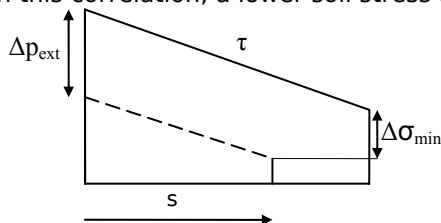


Figure 4-5 $\Delta p_{ext} = 5 \cdot \Delta\sigma_{min}$

4.3.2 The bleeding theory

$$\text{Bleeded layer } x_e = \sqrt{2 \cdot k \frac{1-n_i}{n_i-n_e} \cdot \Delta\varphi \cdot t} \quad [4.3]$$

A fast bleeding of the fracture means a more rapid growth in time of x_e , which means an earlier stagnation of the fracture and consequently a shorter fracture length 's'

- A larger permeability, k , of the bled layer makes x_e grow faster in time.
- A larger injection rate Q gives a higher-pressure head $\Delta\varphi$. However, in this model, the pressure head is related to: $\Delta\varphi = \sigma_{\min} + \frac{1}{2}(p_{\text{ext}} - \sigma_{\min})$. So according to the model, $\Delta\varphi$ cannot be influenced by the injection rate Q .
- It is possible to change the porosity ratio. n_i can become smaller, making a dryer and thus smaller WCR, which leads to a more viscous mixture. n_e is measured in the grout classification tests for rheology and permeability.

The whole theory of bleeding holds as long as the permeability of the surrounding soil is larger than 50 times the permeability of the bled layer. [Bezuijen 2003¹¹] If this is not the case: the permeability of the sand layer is smaller than the permeability of the bled grout layer and it therefore has to be included in the model for bleeding grout. See for an explanation of this the next paragraph.

This information gives a boundary value of the permeability of the bled layer x :

$$50 \cdot k_{\text{grout}} < k_{\text{sand}} \quad [4.4]$$

4.3.2.1 Theory on bleeding grout

Fresh grout in an unconfined cell under pressure will squeeze out the water towards the unconfined site (bleeding). The rate of bleeding depends on the grout properties (porosity and permeability) and the resistance of the soil where the water drains away. An analytical model is developed to quantify this phenomenon. [Bezuijen, 2003¹¹]

Underlying assumptions are:

1. Grout is homogeneous and has an initial porosity n_i
2. A constant pressure on the grout is applied
3. The grout bleeds to an end porosity n_e
4. The water can only drain away on one side of the grout. The other side is impermeable
5. On the permeable side, the water experiences a flow resistance R which depends on the soil properties
6. Until the end porosity n_e is reached, the effective stresses in the grout are assumed to be zero.

From the last assumption (6) follows that the bleeding of grout differs from the consolidation of clay. When clay consolidates, it is assumed that the effective stress increases linear with the compaction of the sample. The assumption chosen here, namely that effective stresses do not change and have no influence, is an approximation. In fact, there will be an increase of the effective

stresses, but measurement results from the grout pressure measurements at “Sophia” railway tunnel prove this approximation is justified.

Using the above-mentioned assumptions the following situation occurs. The grout placed under pressure will bring an increase to the pore water pressure in the grout. The water will flow to the unconfined site. At the border of sand and grout, the porosity of the grout will change from n_i to n_e . The porosity in the rest of the grout (n_i) will remain the same (Effective stress in the grout is zero, water pressure is constant consequently there is no flow of water in de rest of the grout sample). In the next phase, the water is squeezed out right above the previously bled grout layer with porosity n_e . In this manner, a front of bled grout begins. Only through this front is water able to drain away. Gradually the flow will slow down because the water has to flow through previously bled zone (See Figure 4-6).

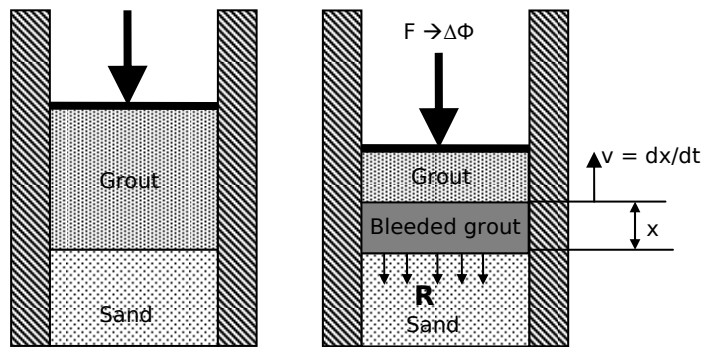


Figure 4-6 one dimensional bleeding test

The force F leads to an increase of the head difference, $\Delta\phi$. This head difference is used to overcome the flow resistance in the bled grout zone and the resistance R in the sand. This leads to equation

$$\Delta\phi = \Delta\phi_1 + \Delta\phi_2 \tag{4.5}$$

$\Delta\phi_1$: pressure head difference over the grout [m]

$\Delta\phi_2$: pressure head difference over the flow resistance R (the sand) [m]

According to Darcy, for the flow of water through the bled grout layer holds:

$$q = k \cdot \frac{\Delta\phi_1}{x} \tag{4.6}$$

With:

q : specific discharge of water from grout [m^3/s per m^2]

k : permeability of the bled grout [m/s]

x : thickness of the bled grout layer [m]

In general, the flow resistance R is defined as:

$$\Delta\phi = R \cdot q \tag{4.7}$$

R : flow resistance [s]

For this particular situation remains:

$$q = \frac{\Delta\phi_2}{R} \quad [4.8]$$

Further, the continuity condition holds

$$q = \frac{n_i - n_e}{1 - n_i} \frac{dx}{dt} \quad [4.9]$$

n_i : initial porosity grout before bleeding

n_e : end porosity grout after bleeding

This relation indicates the correlation between the water discharge from the grout and the velocity of the boundary line growing towards the fresh grout (see Figure 4-6). Put differently, how does x develop over time?

Combination of equation [4.5], [4.6], [4.8], [4.9] leads to the following differential equation:

$$\left[R + \frac{x}{k} \right] \frac{dx}{dt} = \frac{1 - n_i}{n_i - n_e} \Delta\phi \quad [4.10]$$

This equation can be solved with boundary condition $x=0$ at $t=0$:

$$Rx + \frac{1}{2k} x^2 = \frac{1 - n_i}{n_i - n_e} \Delta\phi \cdot t \quad [4.11]$$

or:

$$x = \left(-R + \sqrt{R^2 + \frac{2}{k} \frac{1 - n_i}{n_i - n_e} \cdot \Delta\phi \cdot t} \right) k \quad [4.12]$$

In the experiments performed here, the flow resistance R is negligible because of the large difference in permeability of the sand and the bled grout. Water drains away into the sand much easier than it does through bled grout. Therefore, the measuring outcome can be fitted to:

$$x = \sqrt{2 \cdot k \frac{1 - n_i}{n_i - n_e} \Delta\phi \cdot t} \quad [4.13]$$

4.3.2.2 Two dimensional radial bleeding

Assuming the fracture is a circular tube bleeding will occur 2 dimensional radial [Bezuijen, Kleinlugtenbelt, 2005].

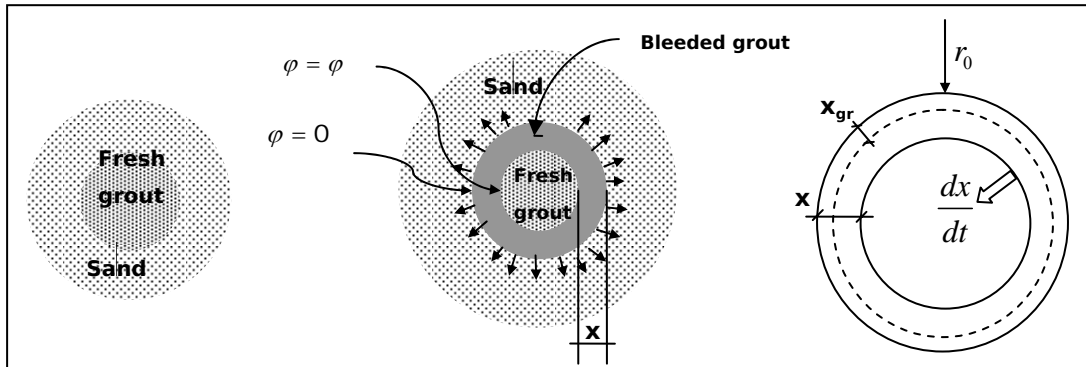


Figure 4-7 Schematical presentation of a 2 dimensional radial bleeding fracture

Similar to equation, [4.6] (according to Darcy) the flow of water through the bleded grout layer holds:

$$q = 2\pi \cdot k \cdot x_{gr} \cdot \frac{d\varphi}{dx_{gr}} \tag{4.14}$$

Over the distance x integrated gives the following differential equation:

$$d\varphi = \int_{(r_0-x)}^{r_0} \frac{q}{2\pi \cdot k \cdot x_{gr}} \cdot dx_{gr} \tag{4.15}$$

Integrated this gives:

$$q = \frac{2\pi \cdot k \cdot \varphi}{\ln \frac{r_0}{r_0 - x}} \tag{4.16}$$

With:

- q : specific discharge of water from grout [m³/s per m²]
- k : permeability of the bleded grout [m/s]
- x : thickness of the bleded grout layer [m]
- φ : pressure head over the grout [m]
- r₀ : see Figure 4-7 [m]

Further, similar to equation [4.9], the continuity condition holds:

$$q = \frac{n_i - n_e}{1 - n_i} \cdot 2\pi \cdot (r_0 - x) \cdot \frac{dx}{dt} \tag{4.17}$$

- n_i : initial porosity grout before bleeding
- n_e : end porosity grout after bleeding

This relation indicates the correlation between the water discharge from the grout and the velocity of the boundary line growing towards the fresh grout (see Figure 4-7). Put differently, how does x develop over time?

Combination of equation [4.14], [4.17] leads to the following differential equation:

$$\left[\frac{(r_0 - x) \ln\left(\frac{r_0}{r_0 - x}\right)}{k} \right] \frac{dx}{dt} = \frac{1 - n_i}{n_i - n_e} \cdot \Delta\varphi \quad [4.18]$$

This equation can be solved numerically with boundary condition $x=0$ at $t=0$:
And the results can be seen in Figure 4-8

Defining two parameters:

$$\chi = \frac{x}{r_0}$$

$$T = t \cdot 2k \cdot \frac{\Delta\varphi}{r_0^2} \cdot \left(\frac{1 - n_i}{n_i - n_e} \right)$$

The results can be interpreted. The second parameter T can be interpreted as time relative to the time it takes for the one dimensional model to grow to a thickness of $x=r_0$.

Three conclusions can be drawn from the plot in Figure 4-8.

- The time it takes for a certain thickness of grout to develop is nearly the same for both models when $x/r_0 < 1/4$.
- The 2 dimensional process silts up twice as fast as the 1dimensional process.
- The layer x in the 2 dimensional case is at the most $\sqrt{2}$ times as thick as the 1 dimensional

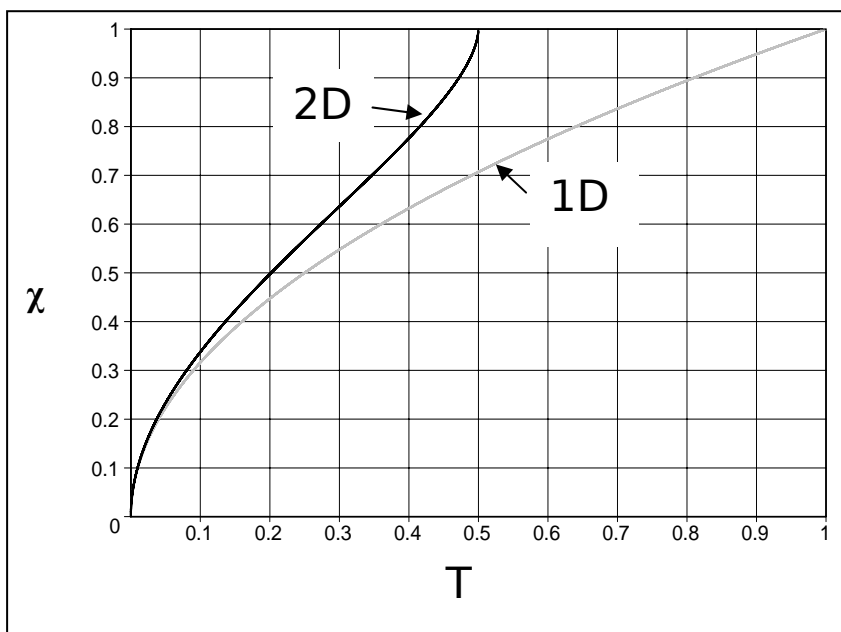


Figure 4-8 1D and 2D relative growth of the bled layer [A.A. Soethoudt 2005]

5 Experimental Set-up

5.1 Introduction

The experimental set-up is explained in the following chapter. First a total view of the set-up is given whereas in the sub paragraphs every single element of the set-up is described.

5.2 Set-up

The experiment consists of a cylindrical container (see Figure 5-1) filled with sand. At 39 cm from the bottom, an injection pipe is installed. In the middle of the container, there is an injection point on the injection pipe (TAM). This is where at a constant flow rate the grout mixture will penetrate the sand. The important parameters to measure are the injection and pump pressure. In order to determine the volume balance the amount of drainage water and the heave of the PVC-piston plate at the top of the sand sample are measured.

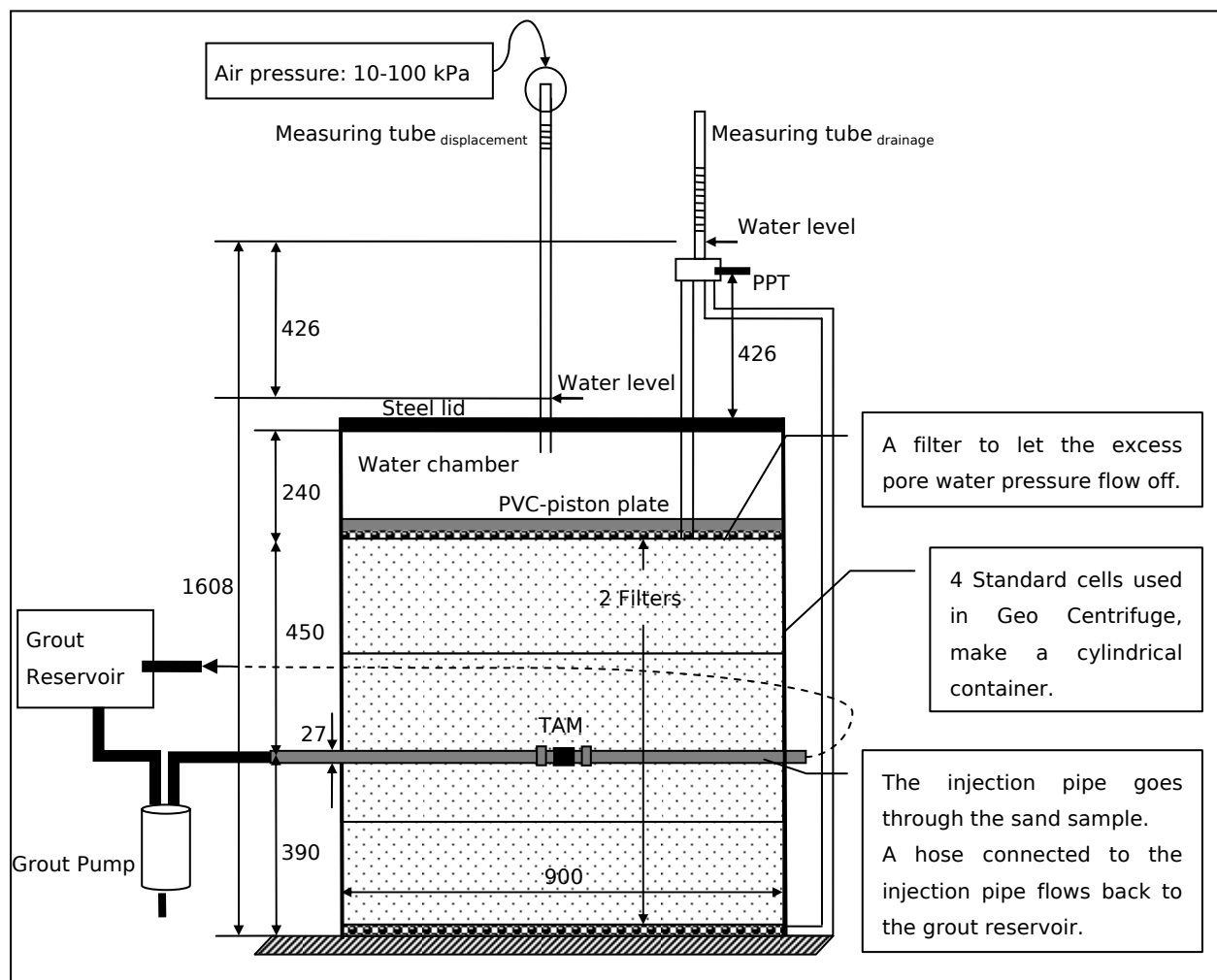


Figure 5-1 Schematic cross-section of the test set-up

The container is filled with saturated sand. During filling the injection pipe is already installed. The sand is loaded to a desired confinement pressure. This is done by the air pressure onto the water level in the measuring tube displacement. The pressure is passed on to the water in the water chamber, which puts the pressure on the PVC-piston plate. The PVC-piston plate is placed on the filter that has a direct connection to the sand.



Figure 5-2 Photo of the experimental set-up

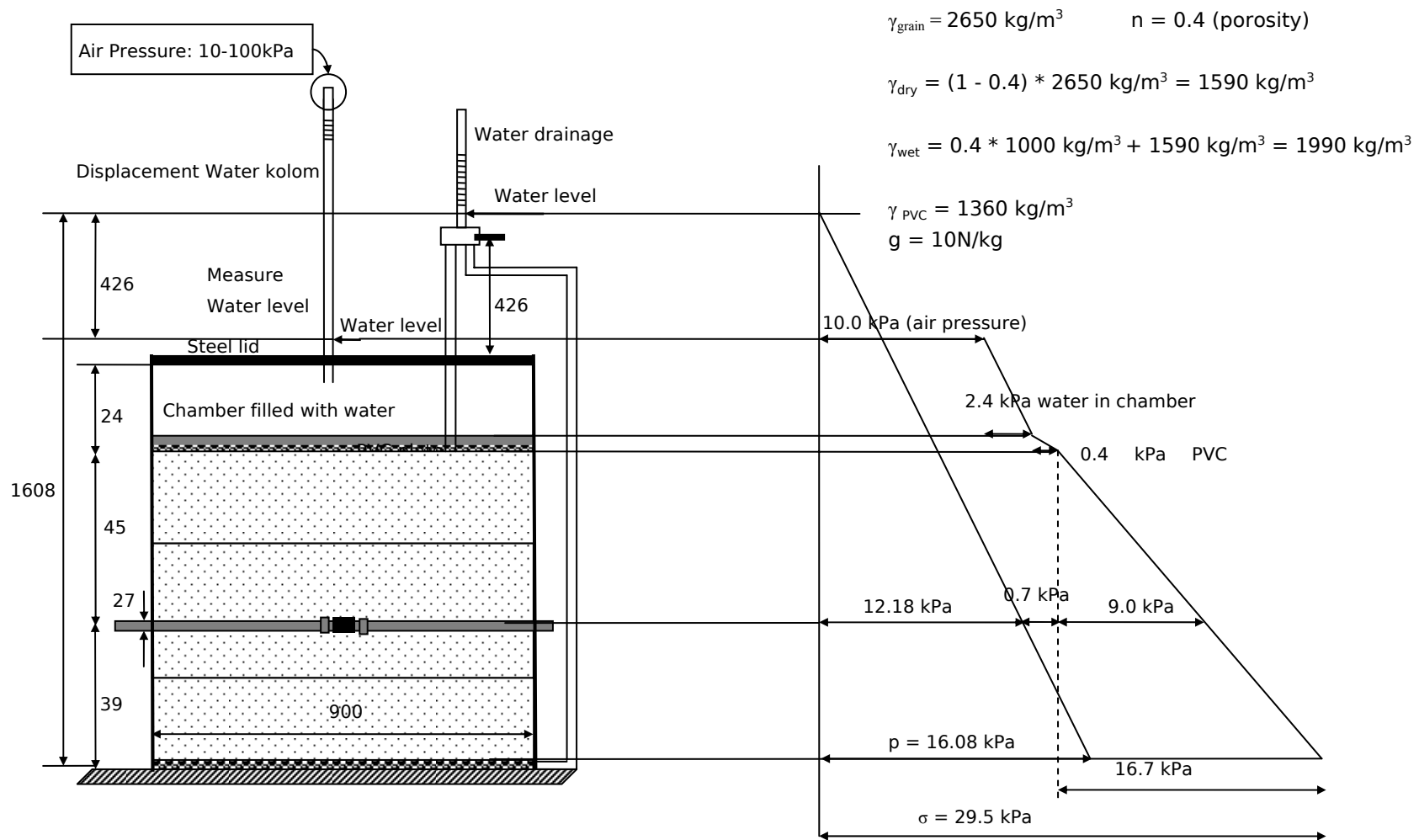


Figure 5-3 Schematic cross-section of the test set-up and stresses in the cell

5.2.1 Grout Pump

The whole injection system is flow rate controlled. Grout pressure will rise as injection progresses.

| | | |
|--------------------------|---|-------------------------------------|
| Plunger-Pump | | |
| Soil pressure 100 kPa | Maximum pump pressures by the RTG Model and in literature 500 kPa | System maximum pressure 1500 kPa |

Table 5-1 Estimated pump pressures

To get a constant injection rate the piston in the cylinder of the water plunger-pump moves up at a constant rate. A casing filled with grout and a water bladder are used (Figure 5-4) to inject the grout when the water by means of the oil pressure is pressed into the water bladder the grout is forced into the injection system. This system is designed to keep grout out of the water plunger-pump, so the cement grains cannot damage the interior of the cylinder of the water plunger-pump.

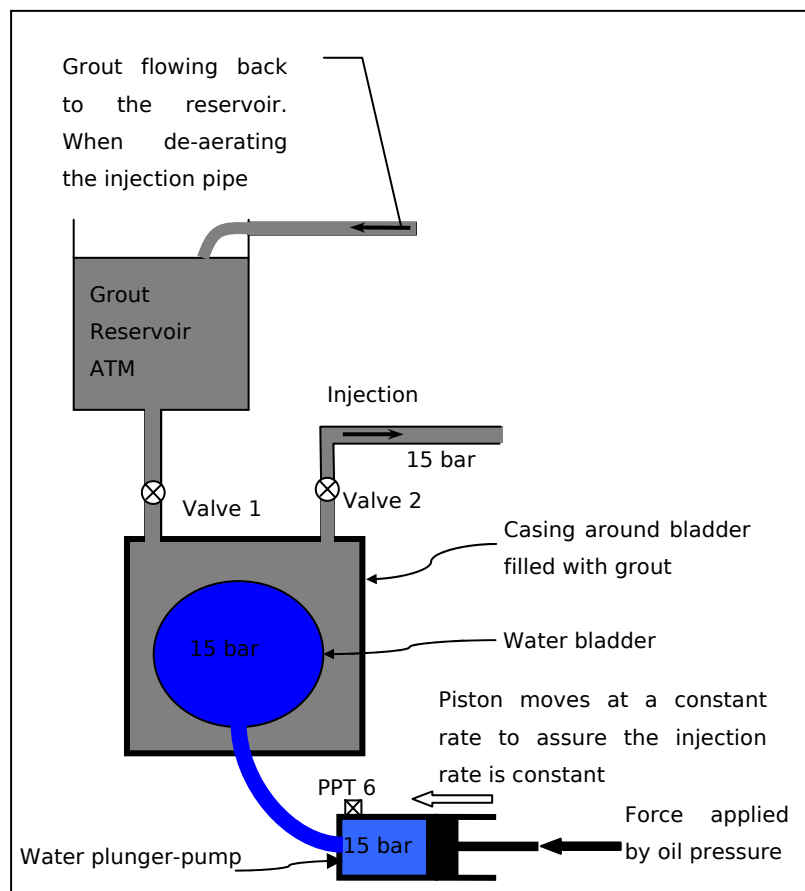


Figure 5-4 Schematized water plunger-pump system. Photo (right) of casing filled with grout

| Injection rate [ml/s] | Time [s] | Injected Volume [ml] |
|-----------------------|----------|----------------------|
| 16.7 | 10 | 167 |
| 167 | 2 | 333 |
| 167 | 6 | 1000 |
| 333 | 2 | 667 |

In Table 5-2 Injection rates and durations are given these are the injection rates the water plunger-pump had to perform.

Table 5-2 Injection rates and durations

5.2.2 Vertical Displacement of the Sand Sample

The injected volume in proportion to the total volume of the sand sample is very small, approximately 1 liter injected grout to 500 liter sand in the container. The expected heave on top can be calculated from this.

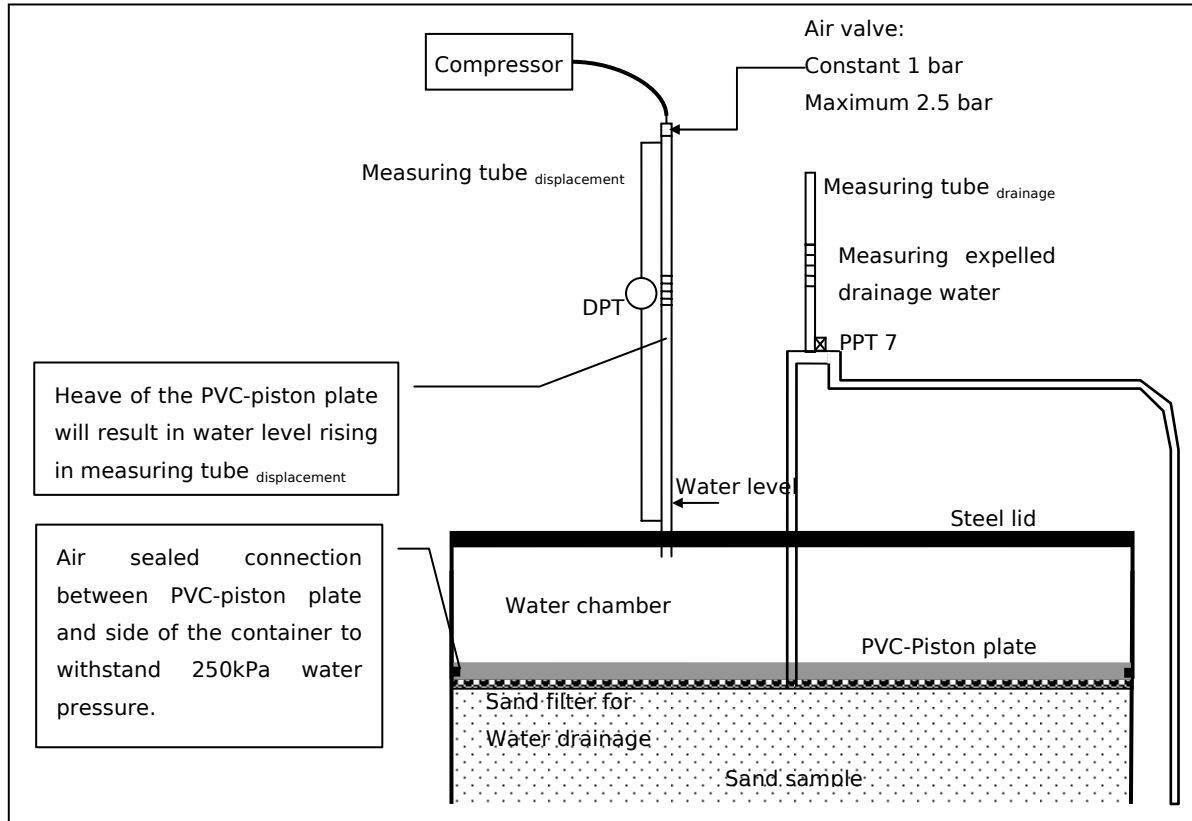


Figure 5-5 Detail top of the container

Calculation

| Diameter container [m] | Area container [m ²] | Volume injected [m ³] | Heave at PVC-piston plate [mm] |
|------------------------|----------------------------------|-----------------------------------|--------------------------------|
| 0.9 | 0.64 | 1·10 ⁻³ | 1.6 |

Table 5-3 Calculated heave of the PVC-piston plate because of injecting volume

If the sand sample is not being compacted during testing the PVC-piston plate will raise the 1.6mm from Table 5-3 the sand is compacted during injection so the PVC-piston plate will raise even less. It seems difficult to measure these figures with mechanical measuring devices. However, it is necessary for the volume balance to measure the heave of the PVC-piston plate. And it is a compensation grouting experiment so it is important to measure heave on top. Therefore, a method to measure the heave of the PVC-piston plate is necessary. As drawn in Figure 5-5 the heave of the PVC-piston plate will change the volume of the water-filled chamber; since water is incompressible, the level of water rise in the small pipe on top will give the heave of the PVC-piston plate. A DPT (Differential Pressure Transducer) detects the changes in water level. The level changes can be made sensitive by making the cross section of the pipe smaller (Table 5-4). The air, kept at a constant pressure, is in direct contact with the chamber filled with water. As a result, the water will pass the pressure through the PVC-piston plate on to the sand sample.

| | | | | |
|--------------------|-----|-----------------|--------|-----------------|
| diameter pipe | 20 | mm | | |
| Cross section pipe | 314 | mm ² | | |
| Volume change | 790 | mm ³ | 125000 | mm ³ |
| water level raise | 2.5 | mm | 398 | mm |

Table 5-4 Water level raise in measure pipes at DPT

The volume of air above the water level in the measuring tube displacement changes due to the raise of water level in the tube. The calculations in Table 5-5 are done to verify if volume changes do not influence the pressure on top of the measuring tube displacement. A valve is connected on top of this tube to let this overpressure flow off, in order to regulate the air pressure in the measuring tube displacement.

| | | | | | |
|--|-----|-----|----------------|-----|-----|
| Volume change due to heave of PVC-piston plate | | | 125 ml | | |
| P ₁ | 100 | kPa | P ₂ | 200 | kPa |
| V ₁ | 250 | ml | V ₂ | 125 | ml |

Table 5-5 Pressure changes according to the 'ideal Gas Law'

The valve connected on top of the Measuring tube displacement can lever these changes.

5.2.3 Grout Pressure Measuring in Injection Pipe

The grout pressures in the injection pipe are of significant importance. The pressure in the grout plunger-pump gives information on the pressure during injection, but because of friction in the hoses and injection pipe it is desirable to measure the grout pressure as close as possible to the injection opening. A Pore Pressure Transducer (PPT) is connected to the injection pipe outside the container and in front of valve-3, which closes off during testing. The grout does not flow between the injection opening and valve-3, therefore, the pressure can be measured outside the container. During de-aerating the injection pipe valve-3 is opened.

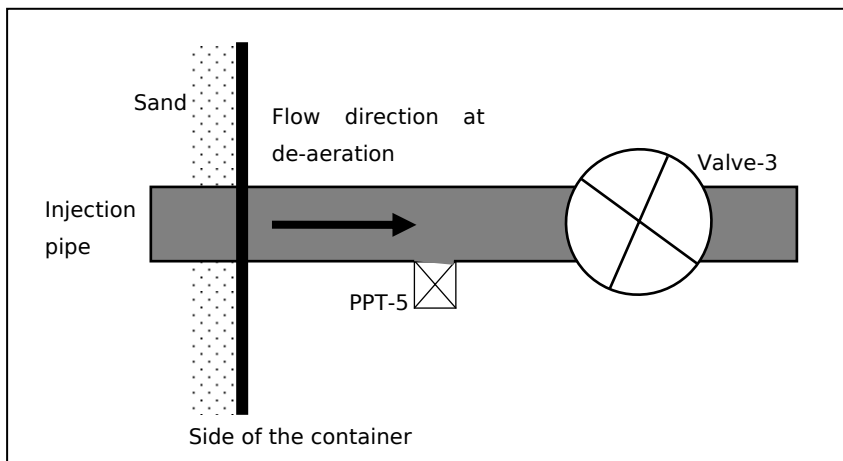


Figure 5-6 System to measure grout pressure in injection pipe

5.2.4 Overview of the Container with all the Transducers

To measure the horizontal and vertical total stresses, two Total Pressure Transducers (TPT) are installed at sufficient distance from the side of the container to reduce the effect of friction of the sand to the wall of the container. This friction could influence the TPTs measurements. The TPTs are also installed at sufficient distance from the injection opening. The container is also equipped with Pore Pressure Transducers (PPT) to measure water pressures. To 'catch' the fracture pressure in the container, PPTs are installed at places where the fracture most likely goes to. PPT2 is placed as close to the injection opening as possible. In the results this is the PPT which shows the fiercest reaction to injections. Table 5-6 shows a summary of the location of the transducers.

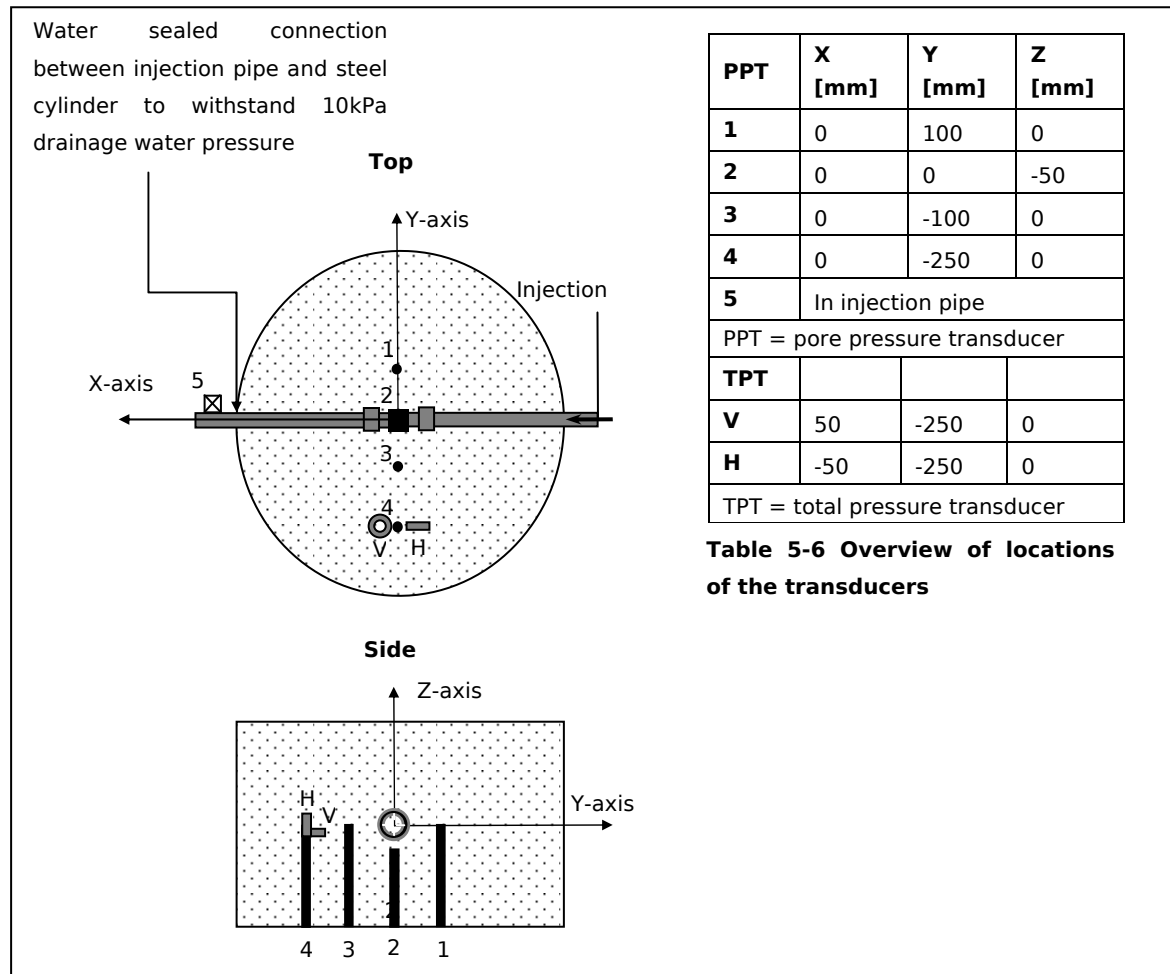


Figure 5-7 Positioning of the pressure transducers

5.2.5 Injection System

A Tube à Manchette as used in the field is shown in the photo below. A rubber sleeve protects the four injection holes so grout will not flow back into the pipe. It will also prevent sand grains from moving into the injection pipe. The steel blockades next to the rubber sleeve are used (in practice) to protect the rubber sleeve when the injection pipes are brought into the soil. In the experiment there is thought of that the steel blockades are able to prevent the grout from escaping along the pipe. They form a barrier to obstruct the grout from flowing along the pipe. The idea in this is to force the grout in some way into the sand.



Figure 5-8 Injection system used in practice (diameter = 60mm).

A simplification of this device (Figure 5-9) easier to use in the experiment would be a pipe like this with only one injection point (test 1 had only one injection hole of 5mm). The type of pipe used in the experiment is a tube with a pipe wall of 2.5mm, which can withstand a pressure of 15bar. The four injection holes measure 7mm in diameter (layout of the injection pipe in tests 6 - 10). In tests 2 - 5 the injection opening consists of two holes of 7mm. The rubber sleeve is a rubber inner tube of a bicycle. The steel rings around the pipe next to the rubber sleeve are used in the experiment to prevent a grout canal from originating along the pipe.

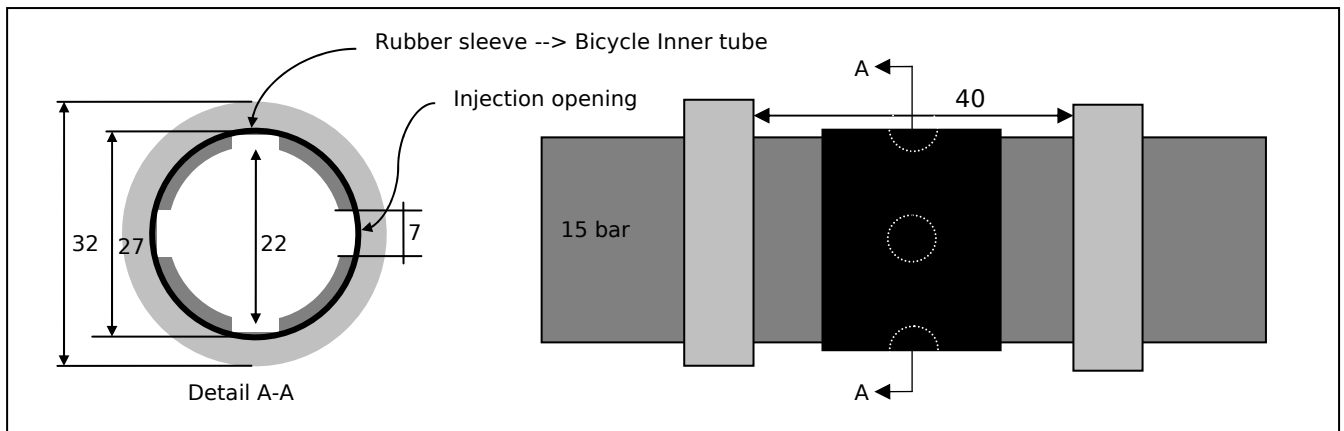


Figure 5-9 Injection system designed for the experiment

Assuming the grout escapes through one hole the injection velocities can be calculated from that, see Table 5-7.

| | | | | |
|---|------|------|-------|------|
| Injection rate [l/min] | 1.0 | | 20.0 | |
| Diameter injection opening [mm] | 5 | 7 | 5 | 7 |
| Fluid flow velocity in injection opening [m/s] | 0.85 | 0.43 | 16.98 | 8.66 |

Table 5-7 flow velocities at injection rate at different sizes of the injection hole

5.3 Experiment Procedure

5.3.1 Introduction

When all the preparations for the experimental set-up are done, a test can be performed. The set-up is ready for use once all transducers are calibrated and hoses and pipes are connected. The points described in detail in the next paragraph are all the steps that are needed to fulfill a complete test.

5.3.2 Test Procedure

1. Fill up the container to 60cm (See sand sample preparation for height explanation) with de-aired water. Figure 5-10
2. Scatter with the help of a rotating sieve a precisely weighed amount of dry Baskarp sand (948kg) in the container filled with de-aired water. Figure 5-11



Figure 5-10 Dry sand scatter set-up



Figure 5-11 Detail rotating sieve

3. Install a plate on top of the freshly scattered sand as an overburden during densification.
4. Densify the sand sample by letting the container drop from a height of 5 centimeters.
5. Make porosity and density measurements of the sand sample in the container by monitoring the height of the sand sample after every drop. Figure 5-12

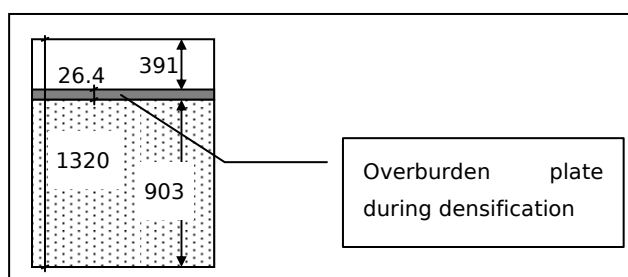


Figure 5-12 Schematized container with measured heights [mm] to calculate sand density

6. At a desirable sand density, the sand sample is flattened at a vertical distance of 45cm from the injection pipe. Figure 5-13



Figure 5-13 Flattening the sand surface

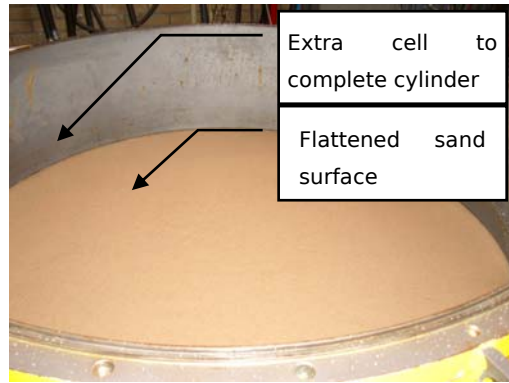


Figure 5-14 Flattened sand surface with extra cell ring

7. Place the filter on the flattened sand surface. Figure 5-15
8. Place the PVC-piston plate on top of the filter and install the water drainage pipes with the measuring tube_{drainage}. Close off the rim of the PVC-piston plate with a rubber ring so the water chamber can be brought under pressure without leaking water to the pore water in the sand sample. Figure 5-16



Figure 5-15 Filter on the flattened sand

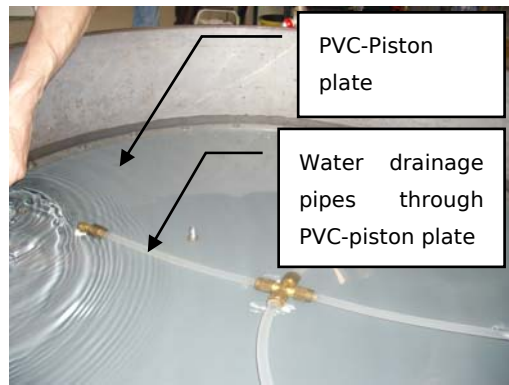


Figure 5-16 PVC-piston plate

9. Fill the water chamber.
10. Place the steel lid onto the cylindrical container to confine the water-chamber and install the air pressure valve onto the measuring tube_{displacement}. Figure 5-17

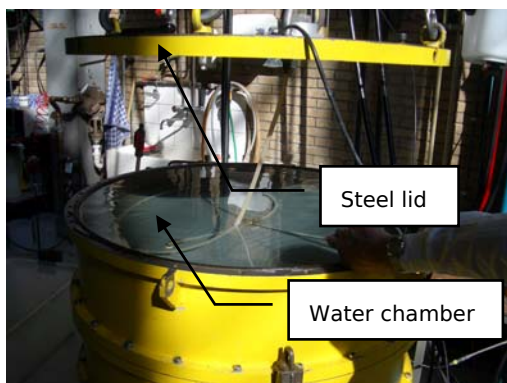


Figure 5-17 Close the container

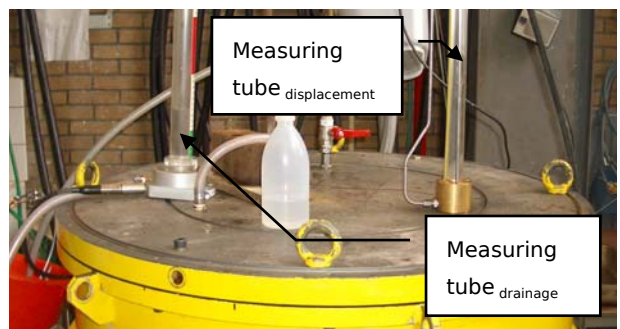


Figure 5-18 Measuring tubes

11. Fill up the water chamber up to the measuring tube ^{displacement}.
12. De-aerate the water chamber by letting air come out through a plugged hole in the steel lid.
13. The set-up is ready for use and desirable stresses can be applied by the air pressure valve.
14. This is the point to start the measurement. The information from the transducers in the container is filed in the computer.
15. Apply the overburden, a vertical pressure, of 250kPa. The water chamber has to be filled with water under pressure. The water main is just for this. The waterworks supply an average water pressure of 250kPa.
16. While doing this the sand sample is pressurized, this causes water to be squeezed out of the sand sample. This is observed by a level raise in the measuring tube ^{drainage}.
17. Verify the vertical and horizontal stresses.
18. Release vertical pressure to 100kPa, which is what all tests start with. Releasing the overburden from 250kPa to 100kPa causes the sand sample to suck water from the measuring tube ^{drainage}.
19. Make the grout (cement, water, and bentonite) mixture. Figure 5-19
20. Measurements of rheological parameters of the grout mixture with Fann V-G meter.
21. Measurements of water expulsion with pressure cell to determine the permeability of the bled zone. Figure 5-20



Figure 5-19 Mixing grout



Figure 5-20 Pressure cell

22. Keep a grout sample out of the injection experiment to verify hardening time.
23. Fill the grout reservoir.



Figure 5-21 Empty bladder



Figure 5-22 Bladder filled with grout

24. Open Valve 1, 2 and 3 and let the grout flow under the head difference from the grout reservoir into the bladder.
25. De-aerate the injection system in the following manner:
Fill injection system with grout from the reservoir with help of the water plunger-pump by following the steps below.

- Close Valve-2, open Valve-1
 - Move the water plunger-pump piston back in order to suck grout from the reservoir into the bladder
 - Close Valve-1, open Valve-2
 - Move the water plunger-pump piston forward in order to push grout from the bladder into the injection system.
26. Repeat these steps until grout flows back into the grout reservoir.
Grout flowing back to the grout reservoir de-aerates the injection pipe, as the grout presses the air out of the system.
 27. Close valve 3.
 28. Preset the water plunger-pump at a constant injection rate (10 liter per minute) with a fixed stroke to control the total volume injected.
 29. Start the measuring system by filing the results from PPT 1-6, DPT 1, TPT V-H to the computer.
 30. Start the water plunger-pump. The water plunger-pump stops itself as soon as the preset stroke is reached
 31. Release the pressure of the water plunger-pump by pulling back the piston.
 32. Open valve 1, 2 and 3.
 33. Flush out the injection system with clean water. (at a low pressure (0.5bar max) so the rubber sleeve stays closed)
 34. Remove grout from the pipes; transport the content of the grout reservoir to the waste container.
 35. Close valve 1,2 and 3
 36. Give the grout fracture time to harden overnight.
 37. Lower the water level in the sand sample (drainage)
 38. Release the vertical soil pressure from 100kPa to 0kPa
 39. Disassemble container for analysis of the grout fracture
 40. Dig up the sand.
 41. Dry the sand for use in the next test
 42. General cleanup

6 Tests Performed

6.1 Introduction

The previous chapters have given an extensive description of the compensation grouting experiment, including the objective of the experiment on grout injections in sand, the lay out of the set-up, and the test program with its procedure. In this chapter, each test will be discussed separately. Ten tests were performed from April to July 2005, each test taking about one week of work.

6.2 Clarification of the Test Result

Every test is unique with its own parameters but a lot of circumstances are the same in every test. These similar factors are first given before every test is discussed. In Table 6-1 the relative densities of the sand and the average vertical and horizontal total stresses at the injection opening are given. The same sand density is used in every test, except in tests 9 and 10, where a deliberately lower and higher density is used. The drainage water pressure at the injection point at the start of all tests is 10 kPa. From test 5 on, a stronger pump is used for injection. This can be seen from the peak pump pressures, which are noticeably higher because a stronger pump could achieve a higher pressure. Numbers written in bold in Table 6-1, Table 6-4 and Table 6-6 indicate that changes have been made in comparison to the previous test. For example in Table 6-1: test 9 uses a higher relative density (75%) than test 8 (60%).

6.3 Over Consolidation

The Relative Density and Total Vertical stress are enforced before the experiment starts. The total horizontal stresses follow from the enforced vertical total stress.

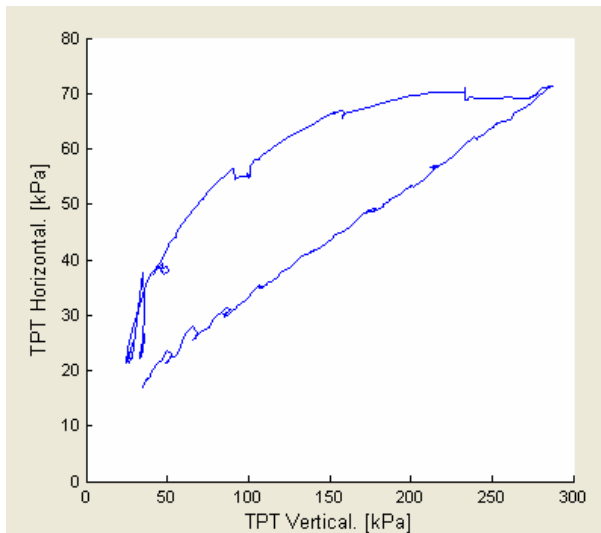


Figure 6-1 Load-unload cycle of vertical and horizontal Total Pressure Transducers (test 2)

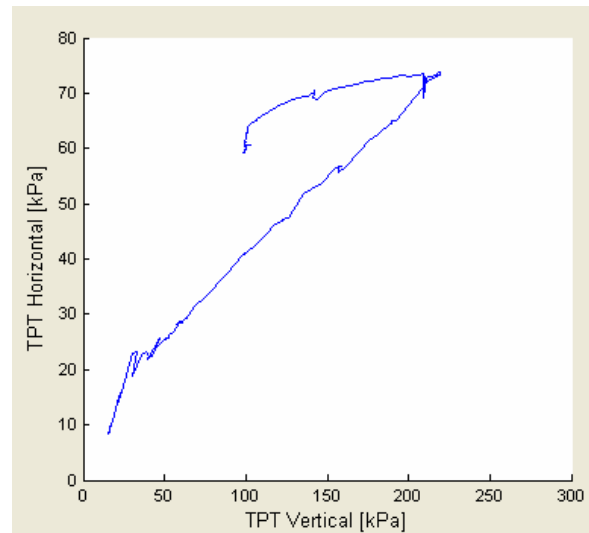


Figure 6-2 Same phenomenon as Figure 6-1 (test 3) The effective stresses are calculated by subtracting 10kPa water pressure

See Figure 6-1 and Figure 6-2 for the relation between the linear raise of the horizontal stress and the vertical pressure increase. At the highest vertical pressure of 220 to 280 kPa, the vertical pressure is released. The horizontal pressure does not follow the same path as when the vertical

pressure was increasing. This load-unload cycle can be distinguished from the different path going up compared to the path down. Before the test starts, a situation is created where a higher horizontal stress is enforced than before the pre-stressing of the soil. This over consolidating is done to get a more isotropic stress situation. When compensation grouting is performed, the soil is preconditioned by pre-injections, which creates a situation of stresses in the soil of larger horizontal than vertical stresses. The pre-stressing for higher horizontal stress simulates the preconditioning phase. Although the situation of a $K_0=1$ is not achieved, the horizontal stress at loading is lower than in the unload path. In Table 6-1 are the stresses per test listed. These are the stresses where the test started of with. During injection these stresses raise as can be seen from the diagrams Pressure Transducers.

| Test | Relative Density (Void ratio D_r) [%] | Total Vertical stress at injection opening [kPa] | Total Horizontal stress at injection opening [kPa] | Peak Pump pressure [kPa] |
|------|--|--|--|--------------------------|
| 1 | 60 | 27 | 27 | 500 |
| 2 | 60 | 28 | 23 | 400 |
| 3 | 60 | 24 | 21 | 500 |
| 4 | 60 | 24 | 20 | 500 |
| 5 | 60 | 24 | 20 | 500 |
| 6 | 60 | 50 | 35 | 1000 |
| 7 | 60 | 100 | 34 | 1400 |
| 8 | 60 | 116 | 42 | 1500 |
| 9 | 75 | 24 | 35 | 1540 |
| 10 | 40 | 100 | 40 | 870 |

Table 6-1 Properties sand sample

The sample preparation is copied from the preparation technique at GeoDelft to make sand models for centrifuge tests. This technique has proven to result in homogenous samples [van der Poel and Schenkeveld, 1998] and was also used in the tests described by Bezuijen (2003). In brief, the following procedure is used: the sand is dried and the cylinder is filled with de-aired water. The sand is ‘rained’ in the container with a constant speed, which results in a loose sand sample. Densification is reached by lifting the container a few centimeters of the ground and letting it drop. This causes a shock wave through the sand sample that leads to a homogenous densification. This process is repeated until one reaches the desired densification.

| | max | min |
|----------|-------|-------|
| e | 0.883 | 0.515 |
| n | 0.469 | 0.340 |

The relative densities are calculated with the maximum and minimum void ratio (e) as stated in Table 6-2

Table 6-2 Maximum and minimum void ratio (e) and porosity (n) of the Baskarp sand.

A grain size distribution of the Baskarp sand is sieved at GeoDelft. For comparison and to apply the geometrical closed filter rules, the sieve diagram for the cement used in the experiment is also plotted.

The difference in fresh and used Baskarp sand is that fresh Baskarp sand is taken directly from a new bag of sand, whereas the used sand has been previously used in one or more tests. The reason for comparing these two situations is that used sand has been rained in water and shoveled around

into the oven and in containers. Therefore, the suspicion arose that the fine parts could be washed or blown out of the sand. Less fine parts in the sand sample have an influence on the permeability of the sand which hampers the drainage water of flowing out the sand sample. However, no evidence for this was found.

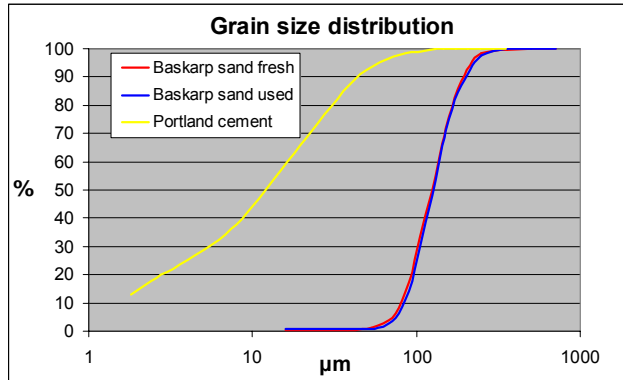


Figure 6-3 Grain size distribution, cement and Baskarp sand

Demands for closed filters:

[Schierck¹²]

Stability, no movement of the small grains of cement into the pores of sand:

$$\frac{d_{15s}}{d_{85c}} < 5; \quad 90/36 = 2.5$$

Permeability, the permeability of the sand must be larger than the permeability of the bled grout:

$$\frac{d_{15s}}{d_{15c}} > 5; \quad 90/2.2=41$$

These demands are for closed filters used in bed, bank and shoreline protection dams. The reason the permeability of the filter layer (sand) must be larger than the base layer (cement) in those cases is:

In a dam it is prevented that water pressure can build up and consequently might press a filter layer away. In this experiment it is important that water can flow away in the sand so the relation for the x as calculated in 4.3.2.1 can hold. As stated before that the permeability of the bled grout layer x must be 50 times smaller than the permeability of the sand:

$$50 \cdot k_{grout} < k_{sand}$$

This still hold

Compared to the closed filter rules would this lead to: (since the permeability is approximately quadratic in proportion to the grain diameter).

$$\frac{d_{15s}}{d_{15c}} > \sqrt{50} \approx 7$$

This is smaller than the 41 calculated before.

6.4 Mixture

The rheology of the grout was measured for every test. Yield stress and viscosity (Fann Viscometer see Figure 6-5) are measured as well as the permeability of the bled grout (Pressure cell Figure 5-20). In Figure 6-4 all the different grout mixtures used in the 10 tests (test 8 has no rheology measurements because of absence of the Fann viscometer) are illustrated with their viscosities and yield stresses. It is assumed that grout behaves as a Bingham fluid. A linear trend-line is drawn through the horizontally situated dots. The crossing with the y-axis is assumed to be the yield stress of the grout mixture. The slope of the trend line is taken as the viscosity.

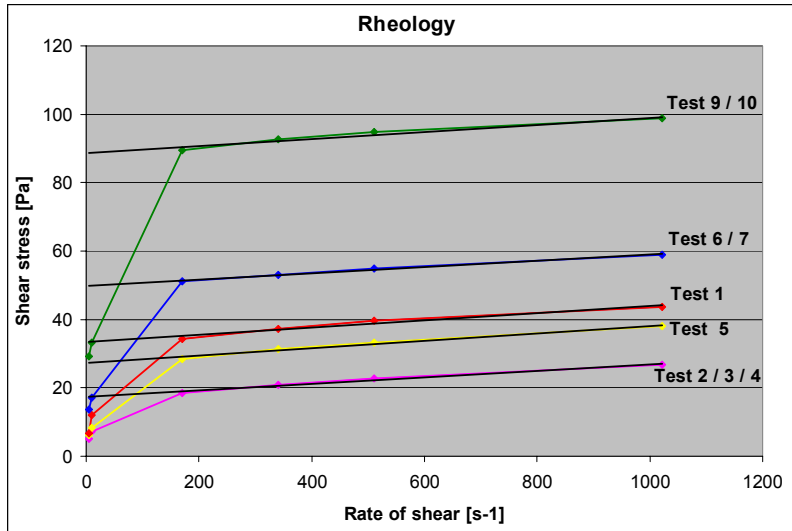


Figure 6-4 Rheology of the grout mixtures used in the tests



Figure 6-5 Fann Viscometer

The differences in yield stress of the grout mixtures are explainable by the ingredients and the mixture procedure. In Table 6-3 the properties of the grout mixture are given for every single test. Some tests have the exact same properties and for that reason the average of the results of rheology measurements are taken and plotted in Figure 6-4 as one line. See for example tests 2, 3 and 4.

| Test | WCR [-] | Bentonite mass percentage of water [%] | Permeability Bleeded grout [m/s] x 10 ⁻⁸ | Viscosity [Pa·s] x 10 ⁻³ | Yield stress [Pa] | Hours hydration Bentonite [hour] |
|------|------------|---|--|--|----------------------|-------------------------------------|
| 1 | 1 | 5 | 10 | 10 | 33 | - |
| 2 | 1 | 5 | 9.4 | 9 | 18 | - |
| 3 | 1 | 5 | 11 | 9 | 17 | - |
| 4 | 1 | 5 | 10 | 9 | 17 | - |
| 5 | 1 | 7 | 5.3 | 12 | 27 | - |
| 6 | 1.2 | 5 | 2.3 | 9 | 50 | 20 |
| 7 | 1.2 | 5 | 2.3 | 9 | 50 | 22 |
| 8 | 1.4 | 5 | 1.2 | Not measured | Not measured | 24 |
| 9 | 1.4 | 5 | 0.4 | 10 | 88 | 43 |
| 10 | 1.4 | 5 | 0.7 | 11 | 89 | 47 |

Table 6-3 Properties Grout mixture

Grout with a WCR of 1 has been used in Test 1, 2, 3 and 4 and an additive of 5% (mass percentage of water) bentonite. The only difference is the amount of volume mixed. For test 1 an amount of 8 liters of grout is made and for tests 2, 3 and 4 an amount of 6 liters of grout is prepared (this is done to save cement). The high shear mixer has only a certain capacity and has difficulty mixing more volume. Grout that has been stirred less could give a higher yield stress.

Test 5 (7%) has the same properties as tests 2, 3 and 4 (5%) except for the percentage of bentonite added to the grout. Adding more bentonite gives the grout mixture a higher yield stress. The reason for putting more bentonite into the grout was the ability of bentonite to hold water to the mixture, which reduces the bleeding.

The grout mixed for test 6 had 5% bentonite added to it. The difference with tests 1-5 is that the bentonite was steeped in water for 20 hours before the cement was added to the water. This steeping, from now on called hydrating, gives the bentonite an opportunity to swell and to react with water so it will hold more water when it is injected under pressure of the grout pump.

The motivation for the higher WCR in tests 6 and 7 is to make the mixture easier to pump lower yield stress than when using a grout with a WCR of 1.

During test 8 the measuring equipment was not on hand so no results of that mixture are available. Nevertheless, one can imagine the yield stress to be between the outcome of test 5 and tests 6/7.

The mixtures for tests 9 and 10 were hydrated for a longer period because the mixture was ready to use but the experimental set-up was not ready yet. Letting bentonite hydrate for a longer time gives a larger yield stress and a smaller permeability to the bled grout layer, which is favorable for the efficiency of the grouting.

| | | WCR [-] | | | | |
|------------------|--------|---------|------|------|------|------|
| | | 1.00 | 1.10 | 1.20 | 1.30 | 1.40 |
| n_i | [-] | 0.74 | 0.76 | 0.77 | 0.79 | 0.80 |
| e | [-] | 2.86 | 3.15 | 3.43 | 3.72 | 4.00 |
| γ_{grout} | [kg/l] | 1.48 | 1.45 | 1.42 | 1.39 | 1.37 |

Table 6-4 initial porosity and density of grout mixtures with different WCR

6.4.1 Permeability

The permeability of the bled grout layer is calculated by the theory of bleeding grout mentioned in Chapter 4. The results are given in Table 6-3. The addition of bentonite or giving bentonite the ability to react with water gives a smaller permeability of the bled layer. The differences in permeability, when not caused by adding more bentonite or hydration of the bentonite, for example in tests 9 and 10, are attributed to measurement inaccuracies.

6.5 Data Diagrams Explained

The data of every test is grouped in four diagrams. These diagrams are classified in: Total Volume, Pump and injection pressure, Pressure Transducers and Water Columns.

Total Volume diagram

From this diagram, a volume balance can be made. The total volume injected (The area of the water plunger-pump multiplied by the stroke of the piston) in a certain time period is the injection rate. The quantity of drainage water plus the amount of heave of the PVC-piston plate are summed and plotted next to the amount injected. When there is no air in the sand sample that can interrupt with the measuring devices, all volume changes in the sand are monitored.

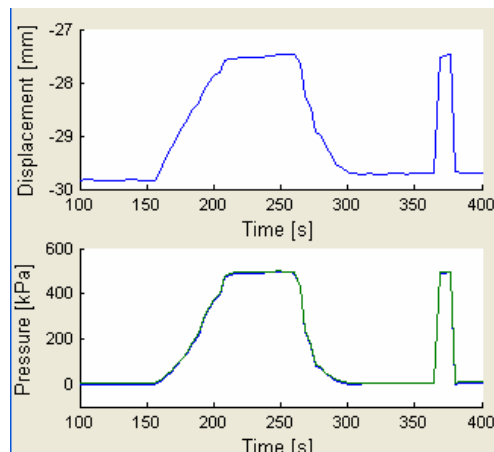


Figure 6-6 Stiffness test of the injection system, a fast and slow plunger stroke.

The disturbance in measuring the volume injected is the stiffness of the injection system. In Figure 6-6 the results of the stiffness test of the injection system are plotted. The water plunger-pump piston makes a pre-set stroke while the injection holes are closed. Therefore, the pressure in the water plunger-pump and in the injection pipe increases rapidly, to the maximum pressure the water plunger-pump can produce. The volume lost to this phenomenon is:

- Area piston: 113.097 cm²
- Stroke: 0.24 cm (-29.8 mm to -27.4mm)
- Volume: 27.1 cm³ (ml)

Pump and injection pressures diagram

In this diagram, the pressure in the water plunger-pump and the pressure in the injection pipe are plotted. In general, when the plunger moves up, both the pressures run up relatively fast; this can also be deduced from the stiffness test in Figure 6-6. During injection, the moment the grout is able to open the rubber sleeve around the injection opening a pressure drop is detected. The injection pressure lags somewhat behind the pump pressure because of the friction in the injection pipe system.

Pressure Transducers Diagram

All the results of the pressure transducers are plotted in one diagram. All tests went through the procedure of over consolidation as described in paragraph 6.3. V (Vertical total pressure transducers) shows the total pressure the test starts with. It was not possible to inject the grout at a vertical total stress of 100kPa in every test because of insufficient capacity of the pump. To be able to inject anyway, the vertical pressure was lowered to a value to where the pump was able to open the rubber sleeve around the injection opening. From test 6 on, a stronger pump was used.

Water Columns diagram

The water columns, measuring tube _{drainage}, and measuring tube _{displacement}, have a relation to each other. The grout injection causes either drainage water flowing off or displacement on top of the sample, or both. If the water level in the tube _{displacement} rises, the grout injection is efficient and compensation grouting has occurred. The tube _{drainage} states something about the relocation of the

sand grains in the sand sample. Grains are pushed closer to each other when injection occurs and as a result, drainage water is pressed out of the sand. In addition, the bled water from the grout also causes a raise of the water level in the measuring tube _{drainage}. The measuring tube _{drainage} is shorter than 45 cm in tests 1-6, which means it can measure volumes of drainage water up to 318ml (diameter: 3cm, length: 45cm).

| Maximum volumes measuring | Measuring tube _{drainage} | Measuring tube _{displacement} |
|---------------------------|------------------------------------|--|
| Test 1-6 | 318 ml | 314 ml |
| Test 7-10 | 672 ml | 314 ml |

Table 6-5 Maximum volumes measuring

After test 6 the measuring tube _{drainage} is extended by 50cm so it can measure the double amount of drainage water flowing out of the sand sample. Where the purple line *drainage* runs off horizontally in the Water Columns diagram (test 5 and 6 at 320 ml, tests 8 at 670ml), the tube _{drainage} overflowed. In Table 6-6 the injection rates and injected volumes of all the tests are given.

In the next ten paragraphs, every test is described in more detail. From the first to the last test, a whole path of attempts to create a long thin fracture was gone through. This is the reason for changes in the injection rate and the layout of the injection point.

| Test | Injection rate [ml/s] | Injection time [s] | Volume injected [ml] | Lay out Injection Opening | Area injection opening [mm ²] | Injection Velocity [m/s] |
|------|-------------------------|--------------------|----------------------|-------------------------------|---|--------------------------|
| 1 | 16.7 = 1 liter / minute | 10 | 167 | 1 hole 5mm rubber sleeve 40mm | 20 | 0.85 |
| 2 | 16.7 | 10 | 167 | 2 holes 7mm | 77 | 0.22 |
| 3 | 167 | 2 | 333 | 2 holes 7mm | 77 | 2.17 |
| 4 | 333 | 2 | 667 | 2 holes 7mm | 77 | 4.33 |
| 5 | 167 | 4 | 667 | 2 holes 7mm | 77 | 2.17 |
| 6 | 167 | 4 | 667 | 4 holes 7mm | 154 | 1.08 |
| 7 | 167 | 4 | 667 | 4 holes 7mm | 154 | 1.08 |
| 8 | 167 | 6 | 1000 | 4 holes 7mm | 154 | 1.08 |
| 9 | 167 | 4 | 667 | 4 holes 7mm | 154 | 1.08 |
| 10 | 167 | 4 | 667 | 4 holes 7mm | 154 | 1.08 |

Table 6-6 Properties injection pipe (test 2 - test 10 rubber sleeve 20mm)

At every test, the grout efficiency is calculated by the following quotient:

$$\eta = \frac{V_h}{\Delta V_0} \cdot 100\% \quad [6.1]$$

η = Grout efficiency [%]

V_h = Volume of heave [m³]

ΔV_0 = Volume of injected grout [m³] in a certain treated soil volume V_0

| Test | V_h [ml] | ΔV_0 [ml] | η [%] | Drainage [ml] | Remark |
|------|---------------|----------------------|---------------|------------------|--------------------------------------|
| 1 | 3 | 50 | 6 | 4 | |
| 2 | 103 | 167 | 62 | 0 | No drainage measured |
| 3 | 140 | 333 | 42 | 167 | |
| 4 | 246 | 667 | 37 | 283 | |
| 5 | 287 | 667 | 43 | 312 | Drainage overflow |
| 6 | 225 | 667 | 34 | 335 | Drainage overflow |
| 7 | 175 | 667 | 26 | 450 | |
| 8 | 200 | 1000 | 20 | 671 | Drainage overflow |
| 9 | 281 | 667 | 42 | 188 | Measuring tube displacement overflow |
| 10 | 38 | 667 | 6 | 619 | |

Table 6-7 Efficiency calculated for every test.

6.6 Test 1 with Model te Grotenhuis Parameters

The first test, as presented in chapter 4, emanated from the analytical model. This was the reason for small injection rates and small volumes injected in the first test. The motivation for a 1-hole injection was to make the injection from a controllable defined point. After realizing the grout was not able to penetrate the sand, the layout of the injection point was changed. The first test of the series did not fail, but to say it was a success is overstating it. The grout was unable to penetrate the sand. Nevertheless, the measurements were promising. From the measuring tube displacement it was concluded that displacements from the PVC-piston plate were measurable.

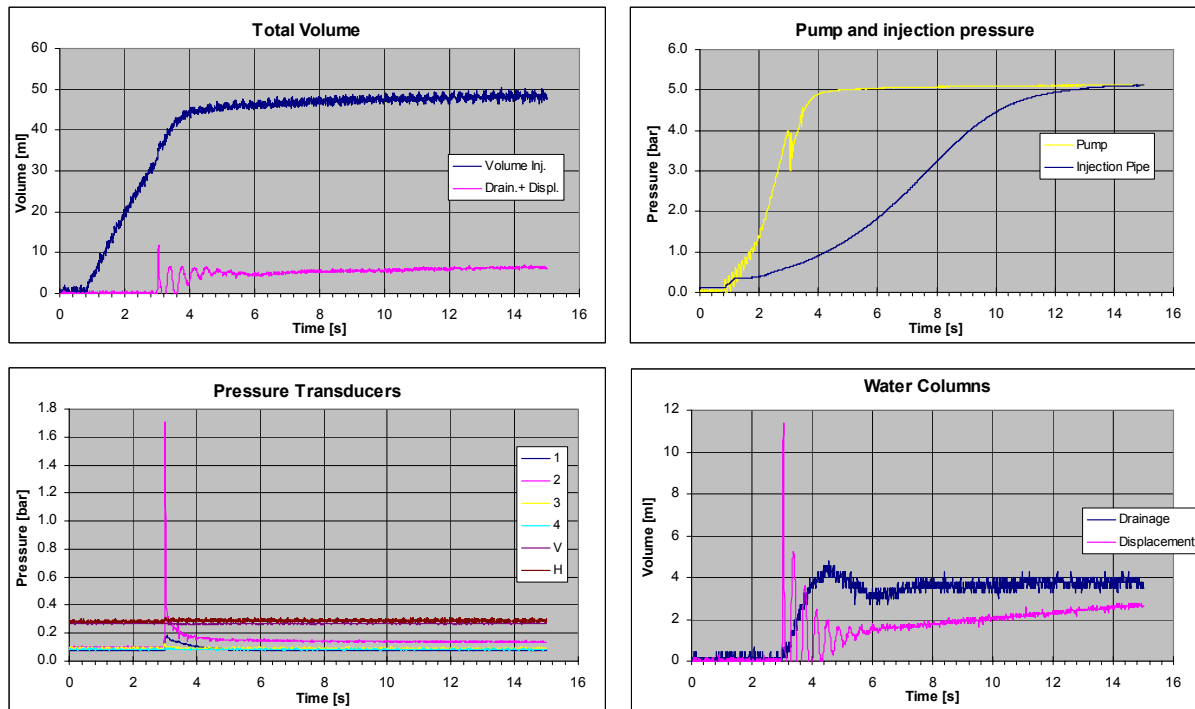


Figure 6-7 Results Test 1

Total Volume diagram:

The volume balance cannot be made because the grout did not penetrate the sand. The amount of volume lost to the limited stiffness in the system is 27ml (Figure 6-6), which is half of the total injected volume in this test. This means that half the injected volume measured is an inaccuracy owing to limited stiffness of the injection system. Therefore, on that ground the measurement is inaccurate.

Pump and injection pressures diagram

At the point in time $t=3s$ the rubber sleeve opens; this can be concluded from the pressure drop in the pump and from the leap in pressure in PPT 2 in the Pressure Transducers diagram. After the opening, the pressure rises to the maximum pump pressure of 5bar. The pressure in the injection pipe follows slowly because the filter in the pressure transducer is blocked by cement grains.

Pressure Transducers diagram

The aim was to start the injection at a vertical total pressure of 100kPa. When this was not possible the vertical pressure was halved twice, since at 50kPa the pump was still not able to inject. The PPTs 1 through 4 all give a vertical water pressure of 10kPa. At $t=3s$ PPT 2 shows a jump as a reaction to the injection.

Water Columns diagram

The displacement plot encounters a pulse at the opening of the rubber sleeve. After that the water column oscillates with 2.5 Hz, which made possible the oscillation of the PVC-piston plate floating on the drainage water between the PVC-piston plate and the sand.

The layout of the injection system in test 1 is shown in the pictures below.



Figure 6-8 Test 1, underneath the rubber sleeve one 5mm hole is made



Figure 6-9 Test 1, the rubber sleeve is closely connected to the steel blockade rings

After excavation of test 1 (Figure 6-10) the following result could be observed: the rubber sleeve was filled with grout, but there was no injection because the 5bar maximum pump pressure was not enough to force the grout into the sand.

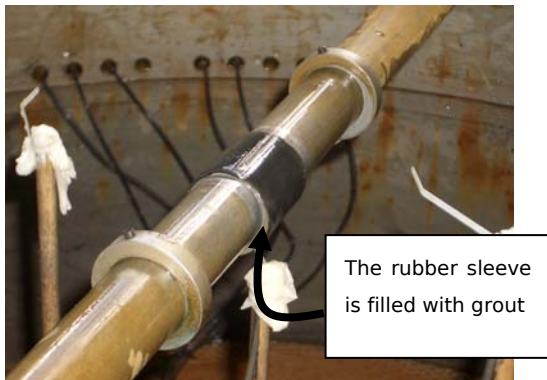


Figure 6-10 Test 1 Rubber sleeve filled with grout but no injection into the sand.

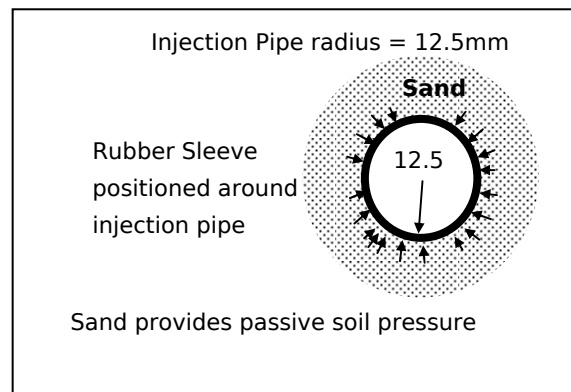


Figure 6-11 Pressure comparisons rubber sleeve and injection hole.

The 5 bar pressure through the 5mm hole is not enough to initialize an opening for injection. A calculation is done to compare the Force on the rubber sleeve (Pressure * Area) to the Force which the grout can pass on through the injection hole on to the rubber sleeve.

Horizontal pressure = Vertical pressure = 25 kPa (Test 1)

Pressure in injection pipe = 500 kPa

Pressure Ratio: 500kPa / 25kPa = 20

$$\text{Area Rubber sleeve} = l \cdot 2 \cdot \pi \cdot r_{\text{injection pipe}} = 40\text{mm} \cdot 2 \cdot \pi \cdot 12.5\text{mm} = 31.4 \text{ cm}^2$$

$$\text{Area Injection opening} = 1 \text{ hole} \cdot \pi \cdot r_{\text{injection hole}}^2 = 1 \cdot \pi \cdot (3.5\text{mm})^2 = 0.20 \text{ cm}^2$$

Area Ratio: 31.4cm² / 0.20cm² = 157

This does not state anything concerning the pressure needed to initiate opening of the rubber sleeve but it does show the large force on the rubber sleeve compared to the size of the injection hole.

6.7 Test 2: A Change in the Injection Layout

First, a solution was found so the grout was able to penetrate the sand with the pump pressure available. The one thing that could be adjusted easily was the injection point layout. Overburden was already at a minimum and from test 1 was learned that a less viscous grout would not help because water was not able to open the rubber sleeve either. For this reason, some actions were taken to change the injection opening. The following measures were taken:

- Cutting the rubber sleeve in half so it was not connected to the steel blockade rings anymore see Figure 6-12
- Two injection openings with a diameter of 7mm each instead of one hole of 5mm.

This new layout of the Tube à Manchette is used in test 2.

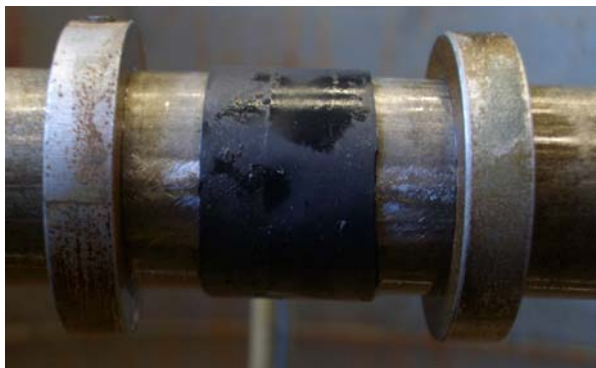


Figure 6-12 New lay out Tube à Manchette.

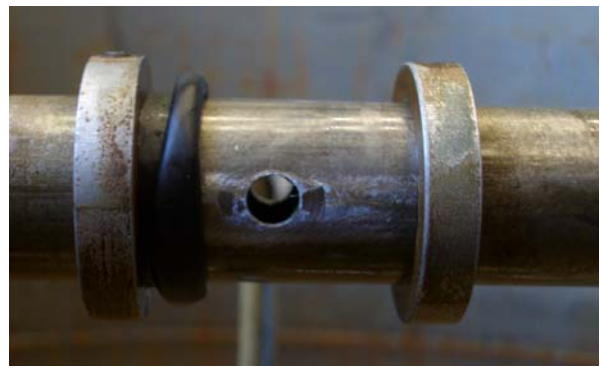


Figure 6-13 Two injection openings of 7mm are horizontally situated.

Furthermore, test 2 is performed under the same conditions as test 1 except for the adjustments to the injection opening.

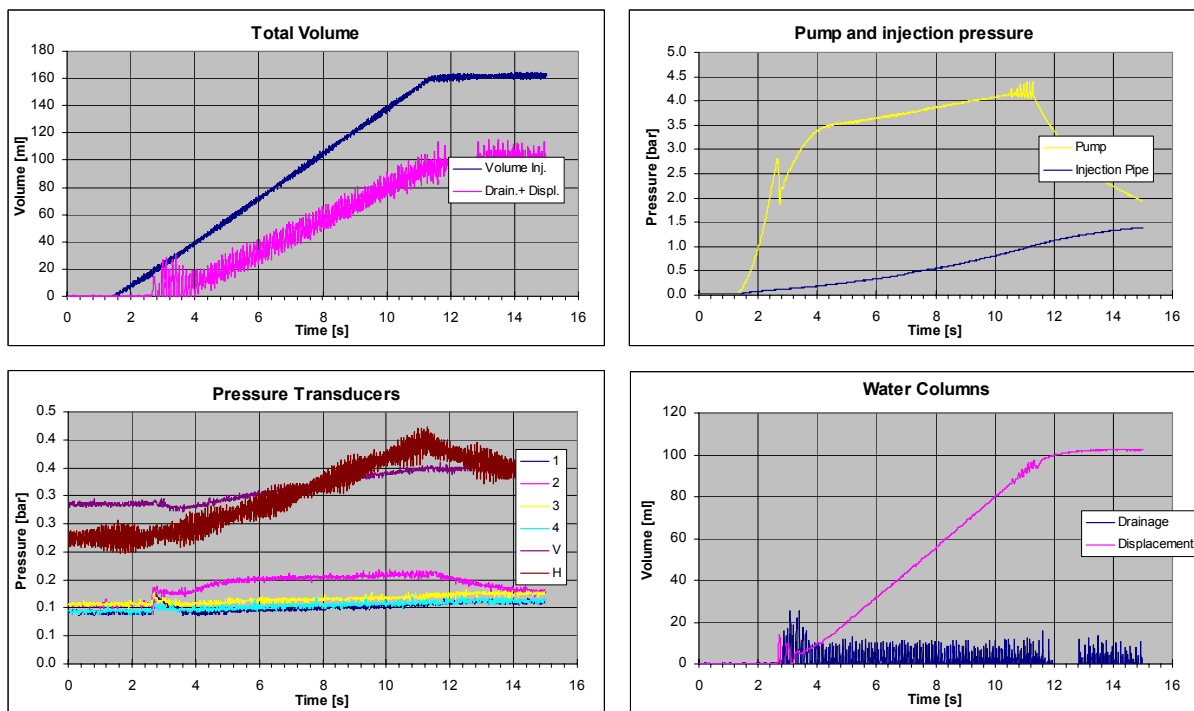


Figure 6-14 Results test 2.

Total Volume diagram

From the line *volume injected*, it is noticed that a volume of 167ml is injected in a time of 10 seconds. The Oscillation in the *Drain. + Displ.* plot are caused by the air in the drainage system. Air bubbles influence the transducer as can be seen from the *Drainage* line in the Water Columns diagram. Because of the air in the drainage system, the *Drain. + Displ.* plot does not match the volume injected. Therefore, it is not possible to make a good volume balance.

Pump and injection pressures diagram

At $t=2.8s$ it is concluded from the pressure drop that the rubber sleeve opens at a pressure of 2.8bar. At $t=3.6s$ the pressure increases at a lower pace. A reason for this could be the opening of the second hole under the rubber sleeve. In this test the injection pressure in relation to the pump pressure has too large of a delay compared to the calibration test with water. The filter in front of the transducer is blocked by cement grains. Consequently, a better system to measure grout pressures in the injection pipe was devised. A silicone gel prevents the grout from coming into direct contact with the transducer. This gel passes the pressure on to the transducer.

Pressure Transducers diagram

PPT-2 is located 5cm below the injection opening. It shows a higher water pressure than would be suspected from the drainage water level raise. The increase of water pressure is caused by drainage water being pressed away by the injected grout. After the excess pore water pressure has flown away the PPT2 shows an decrease of the pressure towards the pressure of PPT 1,3 and 4.

Water Columns diagram

The displacement line shows once more an oscillation, probably coming from the PVC-piston plate floating on the drainage water. Additionally, as said before, there is noise in the drainage line because of air in the system.



Figure 6-15 Top view, result of test 2: low injection rate, compaction grouting



Figure 6-16 Side view of hardened grout injection of test 2 (excavated and detached from the injection pipe)

The bulb created in test 2 as shown in Figure 6-15 was not the expected fracture that was predicted by the analytical model. This spherical shaped bulb is more the effect of compaction grouting as models in literature show [Stoel⁵]. To create more of a fracture instead of a bulb, various options were considered. A less viscous grout could be used, which is able to penetrate the sand better. However, a less viscous grout means more water is added and therefore more bleeding is to be expected. More bleeding involves a less effective injection. Additionally the possibility of injecting

more volume was considered, since this shape could be the first step in fracturing. According to fracture theory, the bulb could be a cavity expansion. An easy step to reduce bleeding and inject more grout is to enlarge the injection rate.

To calculate the bleeding in test 2, the one-dimensional approach with a constant load is used (the same method as used in chapter 4). The thickness of the bled layer can be described as:

$$x = \sqrt{2k \frac{1 - n_i}{n_i - n_e} \Delta\phi t} \quad [6.2]$$

With:

| | | |
|--------------|----------------------------------|--------------------------|
| x | : thickness of the bled layer | |
| k | : permeability of the bled layer | $1.76 \cdot 10^{-7}$ |
| n_i, n_e | : initial and end porosity | $n_i = 0.74, n_e = 0.53$ |
| $\Delta\phi$ | : pressure head difference | 50m |
| t | : time | 10s |

This gives an x of 14mm (see Figure 6-16), which is about the thickness of the bulb itself. This illustrates that a lot of bleeding occurs when the grout is injected. Time is a factor which can be influenced easily by the injection rate; a higher rate can inject more volume in a shorter time, which consequently gives the grout less opportunity to bleed. The volume injected is also adapted; in test 3 twice the amount of grout is injected.

6.8 Test 3 Injection Rate 10 l/min

Test 3 is as test 2 but the injection rate is ten times as large to prevent the grout from bleeding too fast and there is double the amount injected.

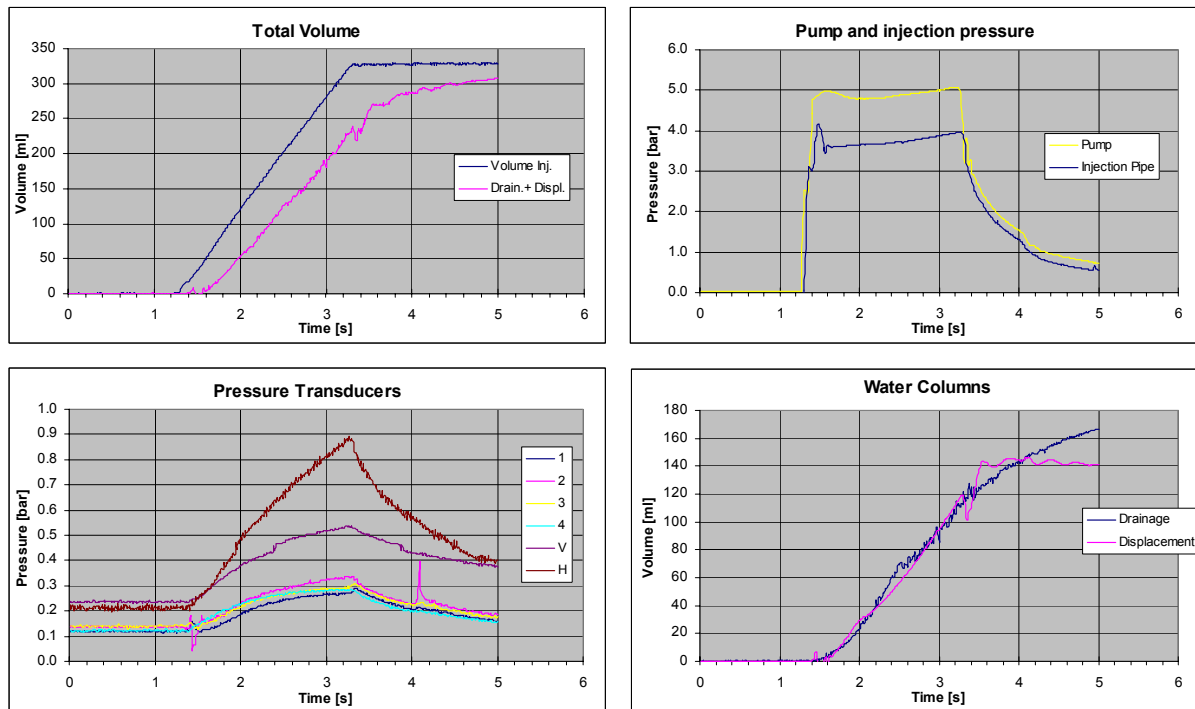


Figure 6-17 Results test 3

Total Volume diagram

This time 333ml grout is injected in 2 seconds, a rate of 10 liter per minute. The volume balance can be made; the *Drain + Displ.* plot approaches the total volume line and it is still climbing. As can be observed from the Water Columns diagram the *drainage* line is still climbing, because the excess pore water pressure needs time to flow of to top and bottom of the sand sample.

Pump and injection pressures diagram

As a change of pressure occurs in the injection pipe, the pressure in the pump changes as well and vice versa. However, these pressures do not change simultaneously, but with a small delay. This can be seen from two phenomena. First, the pressure increase in the pump starts earlier than the pressure increase in the injection pipe. Second, the pressure drop in the injection pipe can be seen in the *pump pressure* line as well but with a short delay. This is logical as the transducers react on changes in pressure. If something occurs in the injection pipe or in the pump the other end experiences it as well but with a delay in time. The grout experiences friction to the injection pipe as well. The friction is the difference in pressure between t=2s and t=3s, both pressures go up at the same speed but differing in size. The pressure drop can be distinguished well in the *injection pipe* pressure line. The rubber sleeve opens at a pressure of 3.1bar at t=1.4s, this can be seen at the first interruption of the straight line going up. The moment the injection stops at t=3s the pressure drops rapidly.

Pressure Transducers Diagram

The Vertical total pressure transducer (V) starts at 0.24bar and the Horizontal total pressure transducer (H) starts at 0.22bar, $K_0 \approx 1$. H runs up immediately at the first opening of the rubber sleeve at $t=1.4s$ and grows faster than V because the steel cylinder confines the sand sample in the horizontal direction. In the vertical direction the sand sample is not confined but the vertical pressure does increase due to the large horizontal pressure; the vertical pressure runs up along with it. The 140ml the *displacement* line (Water Columns diagram) shows as a maximum movement of the PVC-piston plate (PVC-p), is a total ‘stiff’ vertical movement of the PVC-piston plate of 0.02cm ($140cm^3 / \text{Area PVC-p} (\pi 45cm^2)$). In conclusion, this is nothing more than an initial bend of the PVC-piston plate. The ppts 1-4 start at the same pressure of 0.12bar. PPT 2 shows an underpressure owed to dilatation of the sand. The jump at $t=4.1s$ is not understood.

Water Columns diagram

From $t=1.6s$ to $t=3.4s$ an amount of 120ml water has drained away from the sample. This makes a rate of 66ml/s.

The oscillation in the *displacement* line is initiated by the end of injection; the pump has finished its stroke at that time. The frequency of that oscillation is 2.5Hz, which is the same frequency as in test 2. As stated before, it was not possible to inject at an overburden of 100kPa with the pump used in test 1 – test 5. Therefore, the air pressure was released to zero. With the consequence of the water level in the measuring tube *drainage* started working as a communicating vessel with the measuring tube *displacement*, pushing the PVC-piston plate up (Figure 6-18). The ‘floating’ PVC-piston plate between the drainage water and the water chamber is the cause of the 2.5Hz oscillation. This is also confirmed by the fact that the PVC-piston plate from tests 6 – test 10 was not floating because of the overburden applied by the air pressure.

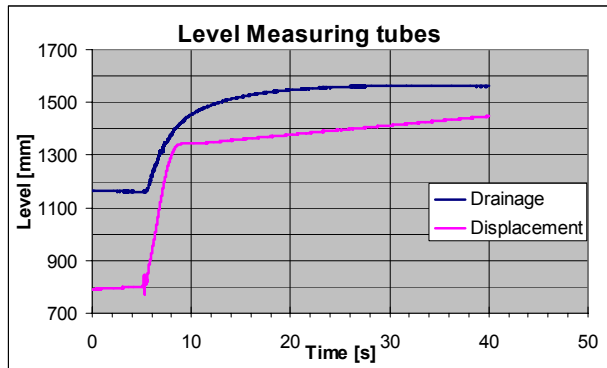


Figure 6-18 The water level in the two measuring tubes with the injection pipe level as a reference height



Figure 6-19 Test 3 after excavation

The sand is penetrated more by the grout and a sort of path has formed towards the sand away from the steel injection pipe (Figure 6-19). To call this a fracture is too premature but the results look promising. In test 4 it is tried to influence the bleeding factor even more by doubling the injection rate from 10l/min to 20l/min.

6.9 Test 4 Injection Rate 20l/min

The only difference between tests 3 and 4 is the injection rate. However, this does affect the results enormously. Pressures increase extremely fast and the rubber sleeve does not have the opportunity to close off the injection holes after injection, which leads to water and sand leaking back through the injection holes (see Figure 6-21)

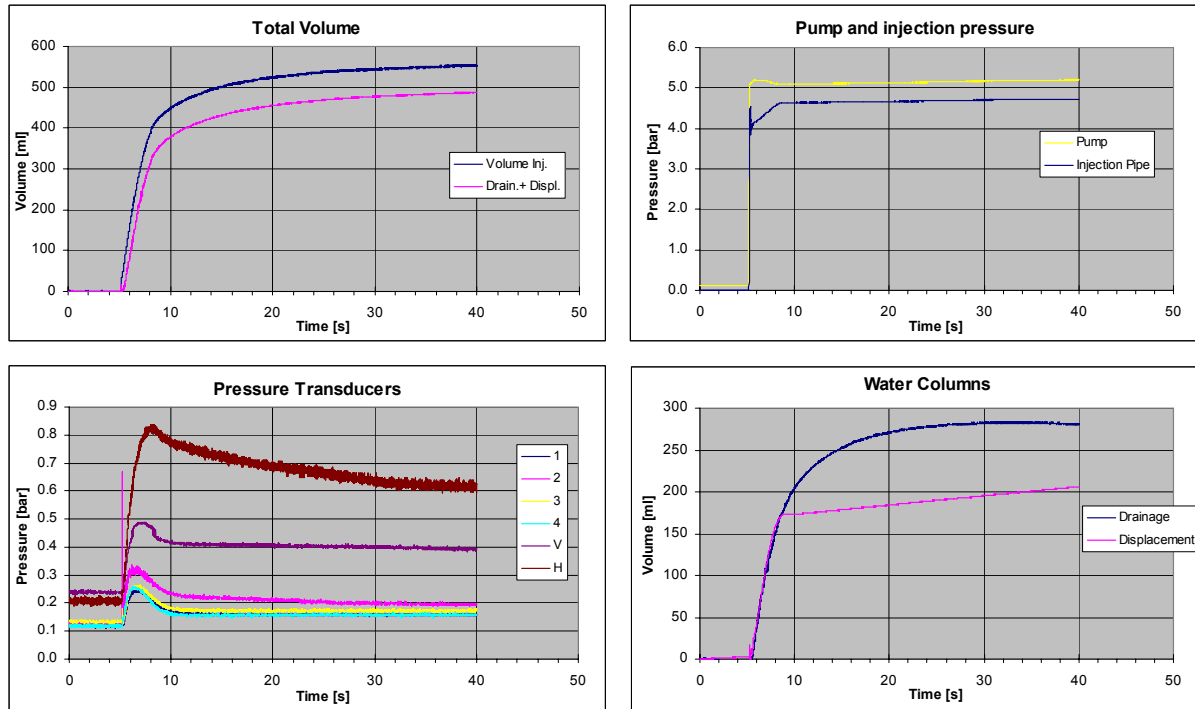


Figure 6-20 Results test 4

Total Volume diagram

At $t=5s$ the pump starts to move and inject at a rate of 333ml/s. The pump can maintain this rate until it is at the maximum pressure of 5bar. The rubber sleeve has opened and the grout volume can be injected but the grout cannot keep penetrating the sand. The pump cannot sustain this rate and the gradient of the line *volume injected* declines. From that point volume injection declines.

Pump and injection pressures diagram

It can be seen from the pressure drop in the *injection pipe* pressure line that the rubber sleeve opens at 4.5bar and is followed by a gradual increase of the *injection pipe* pressure to the maximum the pump can produce. The lack of capacity of the pump is the reason the volume does not penetrate the sand at the rate enforced. Therefore, the pump is misfiring at a pressure of 5.1bar; grout volume does not flow into the sand but it does experience a pressure of 5.1bar. Consequently it bleeds the whole volume to an end porosity which makes the injection less efficient. This bleeding makes the grout very viscous, which is the reason for the rubber sleeve not being able to close off the injection holes after injection (see Figure 6-23).

Pressure Transducers Diagram

TPT-V starts at 0.24bar and TPT-H at 0.21bar, $K_0 \approx 1$. H runs up immediately at the first opening of the rubber sleeve at $t=5s$. PPT-2 shows a leap, after which the excess pore water pressure is flowing of. TPT-V also has a saltation in pressure, this is when the PVC-piston plate is pushed up and creates heave. *The vertical total pressure (V)* runs off horizontally after the displacement has taken a twist at $t=8.6s$ and not a lot of heave is being created because of a lack of extra volume injected.

Water Columns diagram

At $t=8.6s$ a twist in the *displacement* line occurs because of the abrupt decrease of injecting volume by the pump. The *drainage* line shows the consolidation of the drainage water in the sand sample, when injecting decreases water drainage also decreases.



Figure 6-21 Test 4 Sand surface after the test.



Figure 6-22 Top view test 4 after excavation



Figure 6-23 Closer picture of the bulb with the rubber sleeve blown up.

After this test it became clear that a stronger pump was needed if more tests were to be performed with this set-up. The desire for a higher overburden was the most important reason for a stronger pump. Nevertheless the set-up was ready for another test with the same properties, and while a pump with more power was prepared, a fifth test was performed. Test 5 was executed with a lower injection rate than 20l/min because the pump was not strong enough. To reduce the bleeding an amount of 7% bentonite is added to the grout mixture.

6.10 Test 5 More Bentonite Added (7%)

The reason for doing this test is to show that the injection rate of 10l/min is a better rate than the high rate of test 4. In test 4 the rubber sleeve did not close because of the high injection rate of 20l/min. Therefore, the expectation is that the rubber sleeve will close and it still is a large enough rate to prevent a lot of bleeding. Another important figure to reduce bleeding is the percentage of bentonite; more bentonite will hold the water better, which leads to a higher efficiency. This time the percentage bentonite was 7% while in the previous tests 5% (mass percentage of water) bentonite was added to the grout.

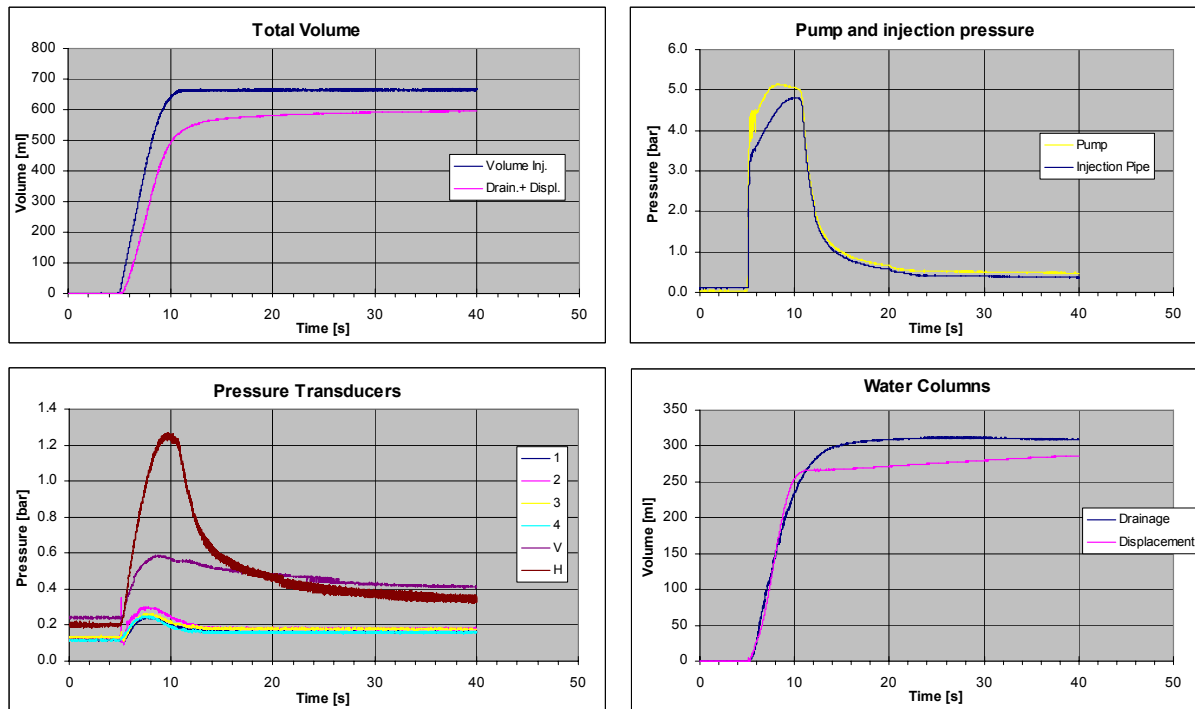


Figure 6-24 Results Test 5

Total Volume diagram

Injecting starts at t=5s; it is injection rate controlled until t=8s. After eight seconds the pressure has become too high and the pump is incapable of injecting grout at a constant rate of 167ml/s. However, the pump is able to inject the pre-set end amount at a slower pace. This shows once again that a stronger pump is needed for tests 6 -10. The volume balance is made but because of the limited length of the measuring tube _{drainage} some volume is missing. In test 7, the drainage measurements have more capacity.

Pump and injection pressures diagram

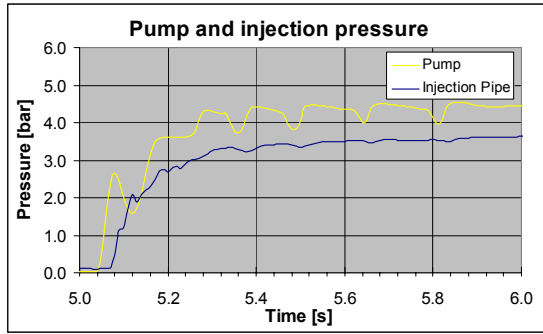


Figure 6-25 enlarged part Pump and injection pressure diagram between t=5s and t=6s

The *pump pressure* line shows a first pressure drop at t=5.1s of 2.6bar (Figure 6-25), an identical pressure as where the rubber sleeve opened in test 3 (the same test properties except for the percentage of added bentonite). In the Pump and injection pressure diagram in Figure 6-24 can be seen that after opening of the rubber sleeve, pressure keeps rising at a constant rate towards the maximum capacity of the pump. From that point on (t=8s), the injection rate decreases, as can be distinguished from the *volume injected* line in the diagram Total Volume in Figure 6-24.

The fluctuation in pressure distinguished from the *Pump* line in Figure 6-25 are probable slip stick reactions of the rubber ring around the piston in the water plunger-pump

Pressure Transducers Diagram

The *PPT 2* first shows a positive pulse because of excess pore water pressure, followed by a drop caused by dilatation. The other PPTs show the same behavior but less pronounced. *TPT-H* increases very rapidly as in every test, and it takes the vertical pressure along. The peak in *TPT-V* is reached before the injection is completed. The reason for this is the slower injection rate when injection progresses. *TPT-H* resides at its peak when injection slows down and stays there until the total volume is injected.

Water Columns diagram

The volume controlled injection begins to tumble at t=8s, and as a result the *displacement* line makes a twist a little after t=8.5s. The continued climbing of the *displacement* line could be the effect of vertical total pressure decreasing, so a release of the sand grains with the effect of elastic swell passed on to the PVC-piston plate.



Figure 6-26 Top view excavated grout fracture in Test 5. The Rubber sleeve closes after injection

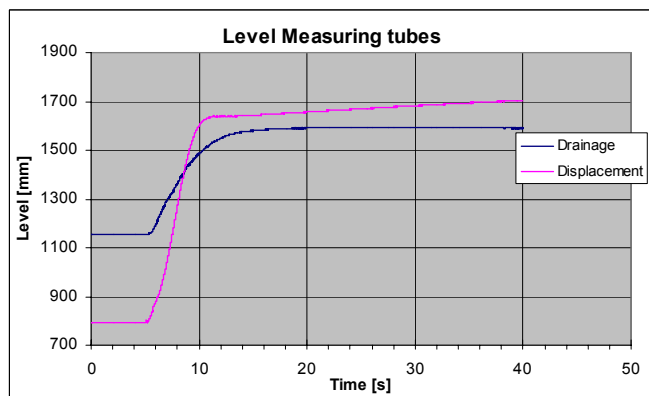


Figure 6-27 The water level in the two measuring tubes with the injection pipe level as a reference height.

6.10.1 Conclusion Tests 1-5 Leads to Test 6

After 5 tests the idea is still that it would be possible to create small, thin fractures in sand if certain parameters could be controlled better. It is understood that two factors are of importance, the bleeding and the overburden. Bleeding is the dominating factor in the efficiency of grout injections. Also the idea still holds that the bleeding factor has a strong influence on the fracture pattern. To reduce this bleeding several measures can be taken such as decreasing the permeability of the bled layer. This is done by letting the bentonite hydrate in water before adding the cement to the water, which gives a four times smaller permeability than when mixed directly with cement and water.

The other factor, the overburden, creates stiffness to the sand sample, which it needs in order to fracture. The overburden is responsible for the effective stresses. The current effective stresses (tests 1-5) at the level of the injection pipe are 10kPa; in test 6 this can be twice as high because the pump capacity has doubled. Another doubling of the effective stresses (effective stresses are managed by the overburden) can be performed when the injection opening becomes larger, as more area creates larger forces. This is achieved by adding two extra holes of 7mm (from 2x7mm holes to 4x7mm). An effective stress of 40kPa at injection pipe level can be achieved, plus 12kPa water pressure, which gives a total stress of 52kPa.

Injecting more volume could lead to fracturing the sand, as the first amount of any volume injected is needed to pre-stress the sand in the container horizontally. After this has been done the grout can create fractures. The maximum amount injected in test 1 through test 5 was 667ml. A quantity of 1000ml is the limit of the experimental set-up.

6.11 Test 6 Pump Upgrade 10bar, 4 Injection Holes

A new series of tests starts, with the following adjustments:

- Two extra holes in the injection pipe of 7mm each to create an easier escape route for the grout.
- Larger capacity of the water plunger-pump (10bar instead of 5bar)
- Consequently the overburden can be larger (40kPa instead of no air pressure applied)
- Use a mixture with 5% bentonite which has hydrated overnight.

A grout mixture with hydrated bentonite and a WCR of 1 gives too large yield stress, which could give problems when pumping, therefore a mixture with a larger WCR (more water added) is used.

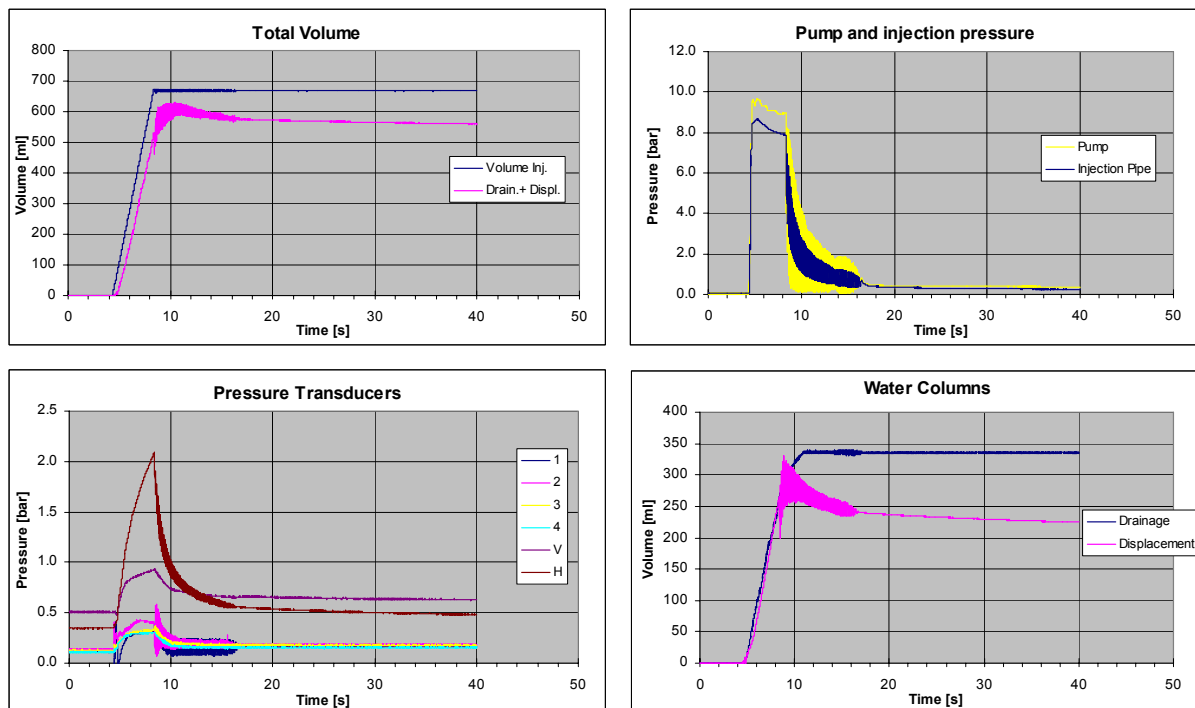


Figure 6-28 Results test 6

Total Volume diagram

A volume of 667ml is injected at a rate of 10 liter/minute; the water plunger-pump does not have any difficulty injecting the total amount as it had in the previous tests. *Volume injected* in time is a straight line with a sharp angle at the end of the injection at t=8.2s. Recapitulating: a strictly volume-controlled injection. The volume balance is made again but the sum is not zero. The reason for this is the over flow of the measuring tube _{drainage}. The new pump was not accurate; when set in a standstill position it keeps vibrating when it is supposed to hold its position. This is the reason for the high frequent oscillation which can be discerned from the Pump and injection pressure diagram.

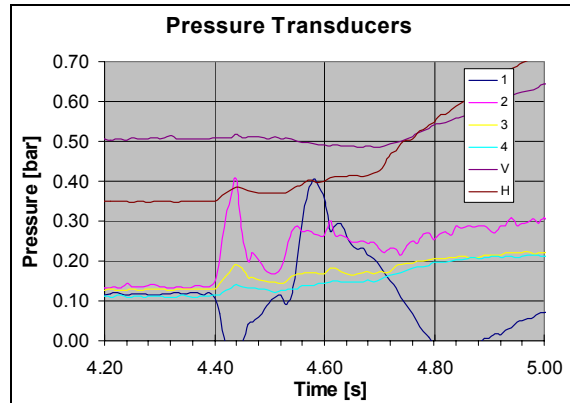
Pump and injection pressures diagram

The first interruption in the injection pipe pressure occurs at t=4.5s with a pressure of 2.3bar but the actual opening of the rubber sleeve does not take place until t=4.6s at a pressure of 8.5bar. This is concluded because after the first hiccup pressure immediately starts rising again. The fast fluctuation of the piston in the water plunger-pump is carried through to all the transducers. Even

small movement of the piston causes pressure fluctuation because of the incompressibility of water.

Pressure Transducers Diagram

The total vertical pressure (*V*) is set at 0.5bar. An attempt was made to inject the grout at 1bar total vertical pressure but the water plunger-pump was not strong enough for such an overburden.



The horizontal pressure runs up immediately after the injection starts. For a better analysis there is zoomed in to this diagram at the point the injection starts $t=4.4s$. A leap in *PPT2* shows the instant reaction to excess pore pressures, whereas *PPT1* shows a decrease of pressure due to the effect of dilatation.

Figure 6-29 Close-up of the Pressure Transducer diagram at the start of injection of test 6.

Water Columns diagram

From the point the injection starts until the point the pre-set volume is injected with a constant rate of 167ml/s (10l/min), the amount of drainage water and the volume due to displacement follow each other directly. The moment the injection stops, the displacement stops occurring as well. At that point the drainage is still rising because the effective vertical stresses are still applying a pressure on the grout which causes bleeding and therefore drainage water to flow of.

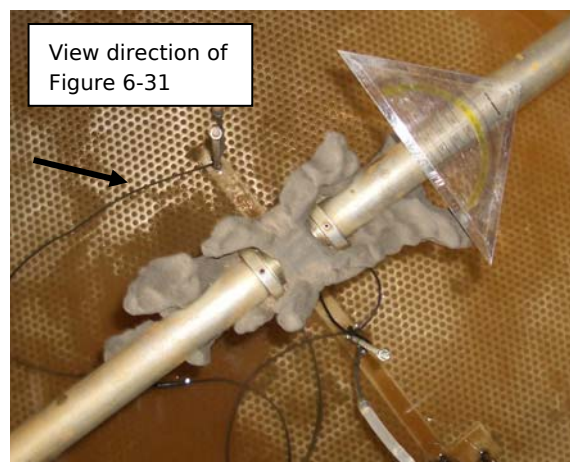


Figure 6-30 Top view of the excavated grout in test 6

Figure 6-31 Side view of the grout fracture

The fracture as shown in the pictures above is vertical orientated.

6.12 Test 7 pump Upgrade 15 bar

In test 6 it was possible to inject the grout whereas the overburden causes a total vertical pressure of 0.5bar. In test 7 the overburden is set at 100kPa

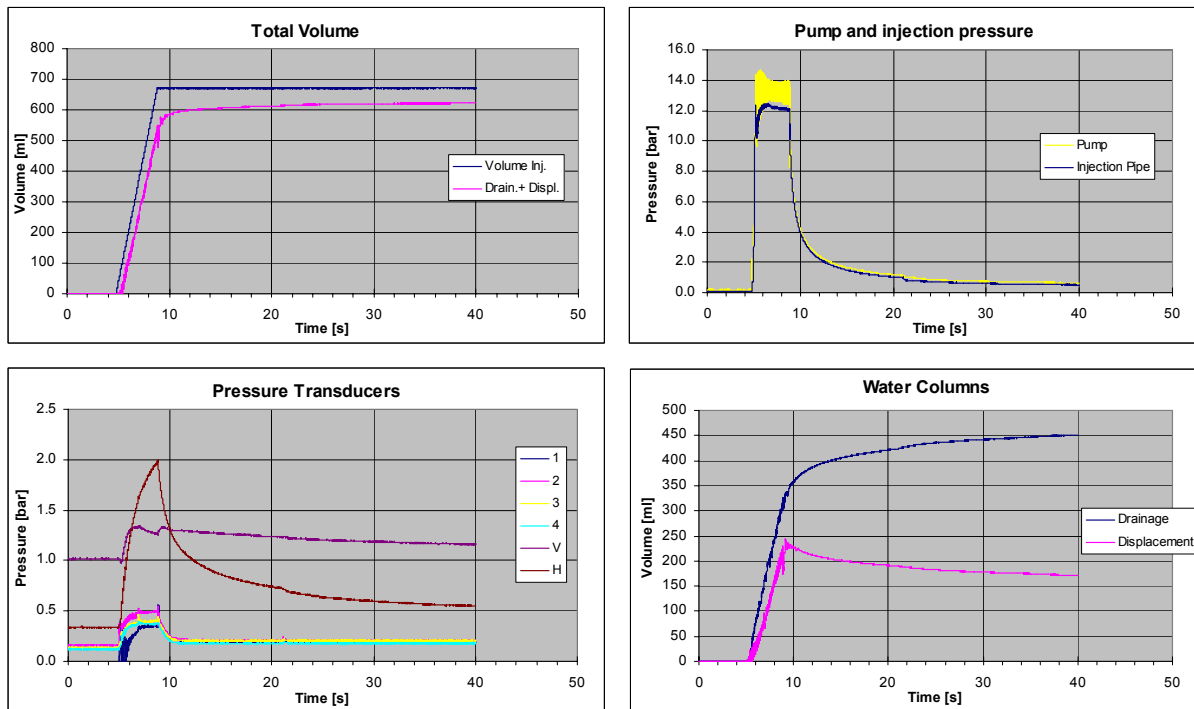


Figure 6-32 Results test 7

Total Volume diagram

With the exception of 50ml is the volume balance correct.

Pump and injection pressures diagram

The water plunger-pump at the maximum pressure of 14bar gives high frequent fluctuations which are to blame on the electronically control of the water plunger-pump.

Pressure Transducers Diagram

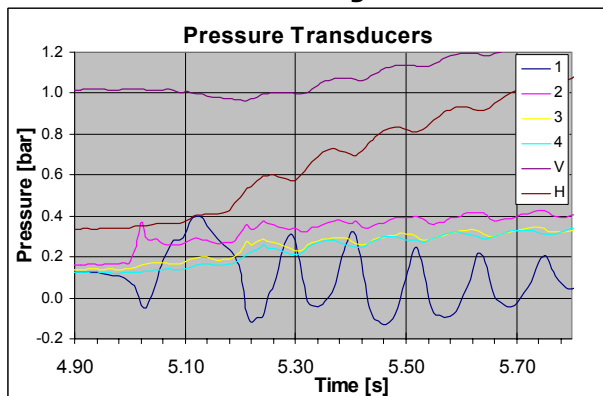


Figure 6-33 Close-up of the Pressure Transducer diagram at the start of injection of test 7

The frequent fluctuations (9Hz) in water pressure in Figure 6-33 are compared to the 2.5Hz of the Water Columns Diagram in test 1 (Figure 6-7) relative high frequent. These oscillations are attributed to the electronic operation devices. In the Diagram Pump and Injection pressures (Figure 6-32) is the 'high' frequent oscillation distinguished in the *pump pressure* line.

Water Columns diagram

The decline in displacement after $t=9s$ is the consequence of the vertical pressure (see *TPT V* line) still existing and therefore accommodating the bleeding. The bleeding causes the decline in the *displacement line* and increase in the *drainage line*.

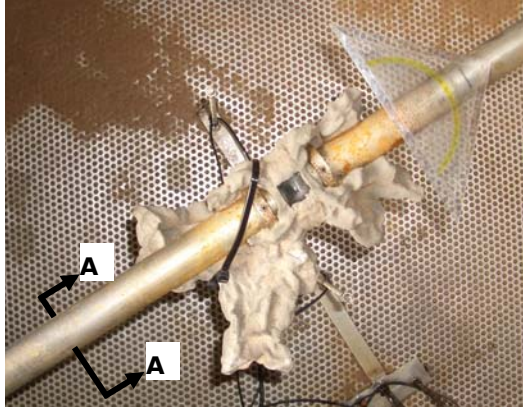


Figure 6-34 Excavated grout fracture of test 7



Figure 6-35 View A-A below injection pipe

The fracture as shown in the pictures above is horizontally orientated. This makes it to be expected that the horizontal fracture away from the injection pipe is created at the point the horizontal stresses are higher than the vertical stresses.

6.13 Test 8 Large Volume Injection (1 liter)

This test is done to examine the influence of a large amount of grout injected in the sand. A volume of 1 liter of grout is injected. The subject of fracture initiating and then propagating could be an issue of injecting enough volume. This suspicion is dispelled by this test. The geometry is similar to the fracture in test 3 where only 333ml was injected.

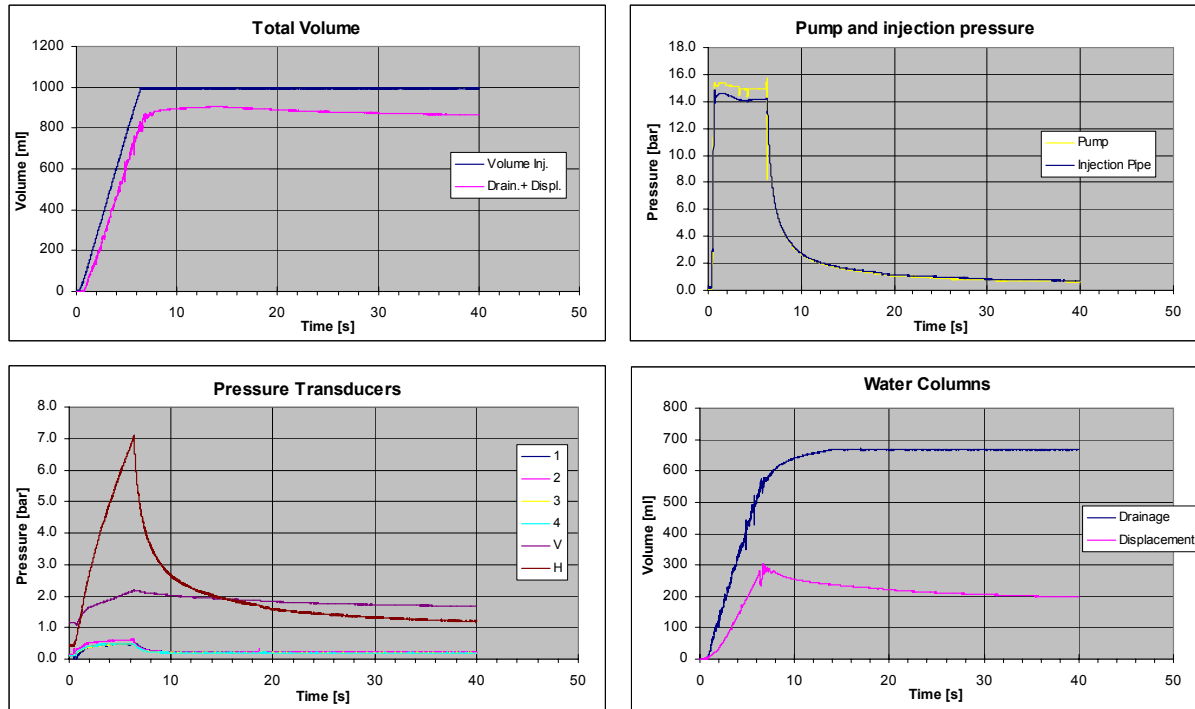


Figure 6-36 Results test 8

Total Volume diagram

An amount of 1000ml is injected at a rate of 10liter/minute. The volume balance misses 100ml caused by the lost of drainage water. The measuring tube *drainage* can only measure an amount of maximum 672ml.

Pump and injection pressures diagram

The pressure record show a similar trend as found in the DLR¹⁴, these records are compared with eachother in chapter 7.

Pressure Transducers Diagram

The high horizontal pressure is owing to the large amount of grout injected. The sand sample is horizontally confined for that reason can it build up large pressures between the steel container walls. The K_0 reaches a value of 4.5 which is extremely high.

Water Columns diagram

The line *drainage* runs of horizontally after $t=14s$ which means the measuring tube *drainage* is over flown after that point. The decline in displacement after $t=6s$ is the consequence of the vertical pressure (see *TPT V* line) still existing and therefore accommodating the bleeding. The bleeding causes the decline in the *displacement line* and over flown (horizontally run off) of the *drainage line*.



Figure 6-37 Top view of the grout fracture

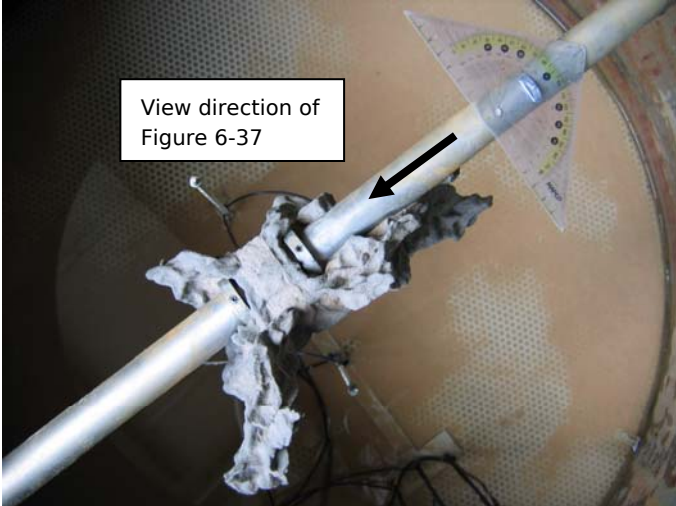


Figure 6-38 Test 8 after excavation

6.14 Test 9 Dense Sand

To examine the influence of the density of the sand sample on the fracture geometry, two tests with a different density of the sand are executed test 9 with a relative density of 75% and test 10 with a density of 40%. At test 9, with the high relative density, was it not possible to inject with an overburden applied by air pressure. Therefore the vertical pressure is set at 25kpa at the start of the test (see the Pressure Transducers diagram).

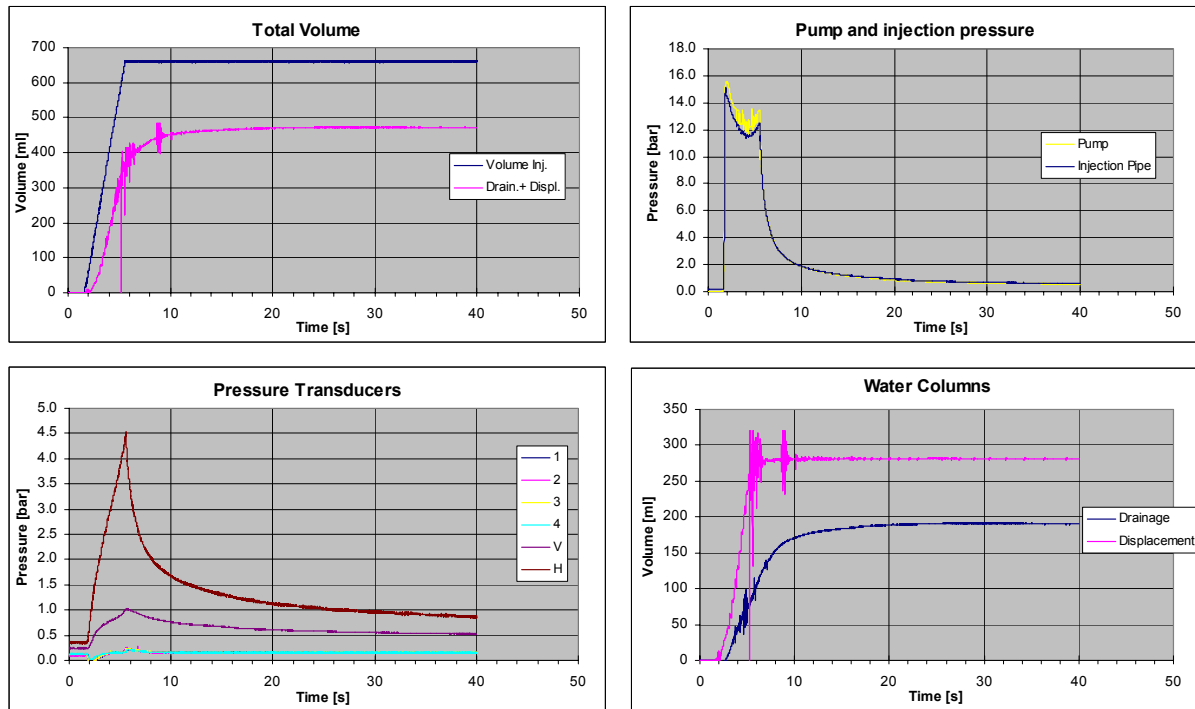


Figure 6-39 Results test 9

Total Volume diagram

A volume of 667ml is injected at a rate of 10liter/minute. The volume balance is disturbed by the overflow of the measuring tube displacement.

Pump and injection pressures diagram

The rubber sleeve opens at 15bar. After that the injection pressure decreases. The initial opening of the rubber sleeve requires the highest pressure.

Pressure Transducers Diagram

The horizontal pressures have been larger than the vertical pressure throughout the whole test. Consequently the fracture is horizontal orientated his can be seen from Figure 6-40 and Figure 6-41

Water Columns diagram

The volume injected in relation to the volume of heave created by the grout injection is called the efficiency. Very dense sand experiences less volume changes from injection and is therefore creating a large amount of heave which makes the efficiency very high (see Table 6-7).By consequence is the measuring tube displacement overflowing. This can be seen from the fierce fluctuations in the line Displacement.

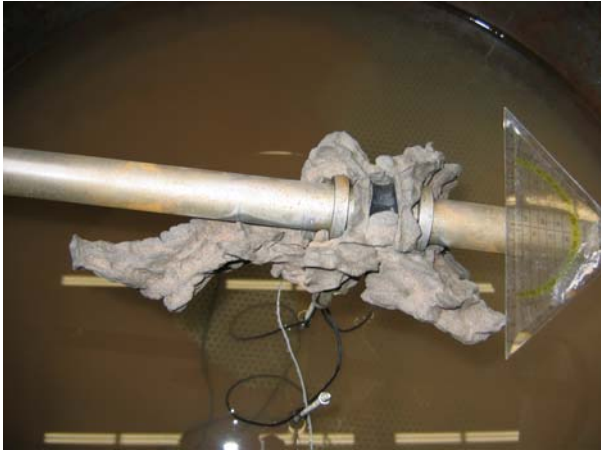


Figure 6-40 Horizontal orientated fracture of test 9



Figure 6-41 Excavated grout fracture in test 9

6.15 Test 10 Loose Sand

Test 10 is the counterpart of test 9, because test 9 is done with a sand density of 75% and test 10 with a sand density of 40%

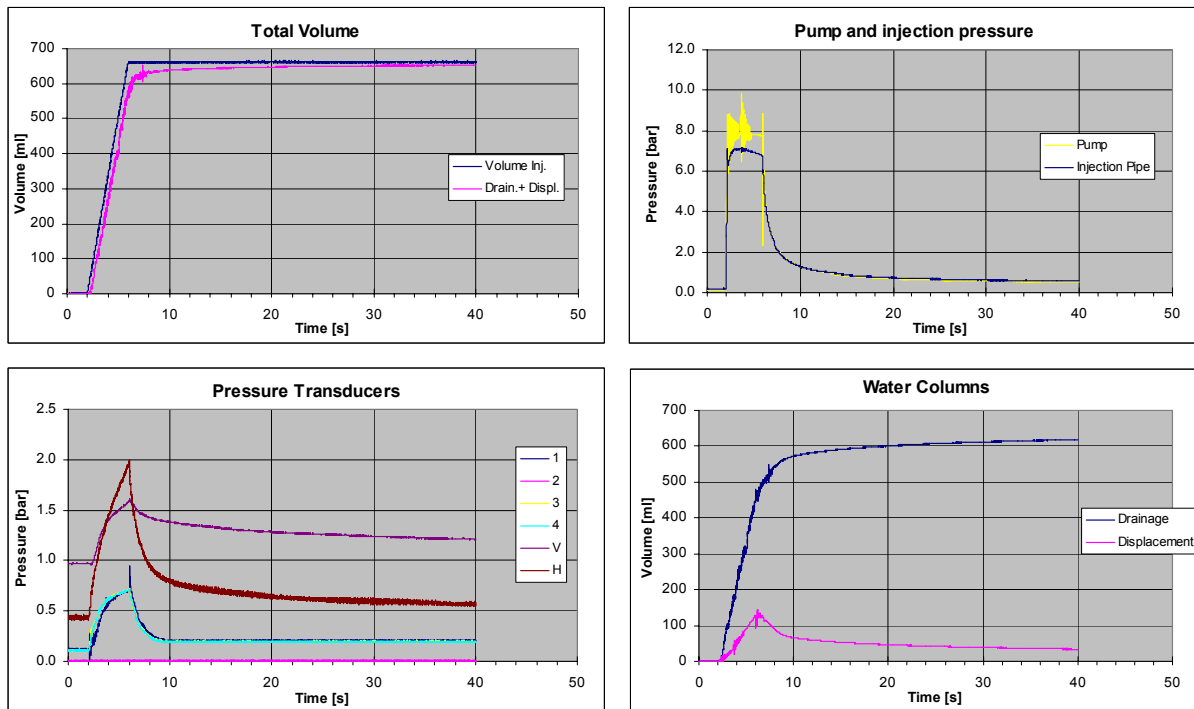


Figure 6-42 Results test 10

Total Volume diagram

A volume of 667ml is injected at a rate of 10 liter/minute. The volume balance is perfectly matched. All the drainage water flow of, plus the volume change due to the heave of the PVC piston plate, perfectly match the volume injected. This proves the accuracy of the measuring system. This test 10 proves, when in all preceding tests the volume balance was not corresponding with the volume injected, there must be an explanation for a not matching volume balance.

Pump and injection pressures diagram

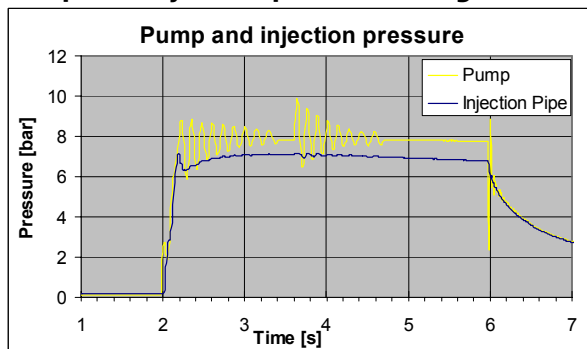


Figure 6-43 Zoomed in pressure records of test 10

The rubber sleeve opens at a lower pressure (7bar) than in test 9 because of the low density of the sand. The oscillations with a frequency of 8.5Hz are ascribed to electronically control of the water plunger-pump. The pressure in the *Injection Pipe* line does not show such a behavior. Therefore it is blamed on not properly functioning of the water plunger-pump.

Pressure Transducers Diagram

The vertical pressures are larger than the horizontal pressures up to $t=4s$. Half the volume is injected at that time. Consequently the fracture is vertically orientated this can be seen in Figure 6-44 and Figure 6-45.

Water Columns diagram

The volume injected in relation to the volume of heave created by the grout injection is called the efficiency. Very loose sand experiences a lot of compaction when injected by grout and is therefore not creating heave which makes the efficiency very low (see Table 6-7).

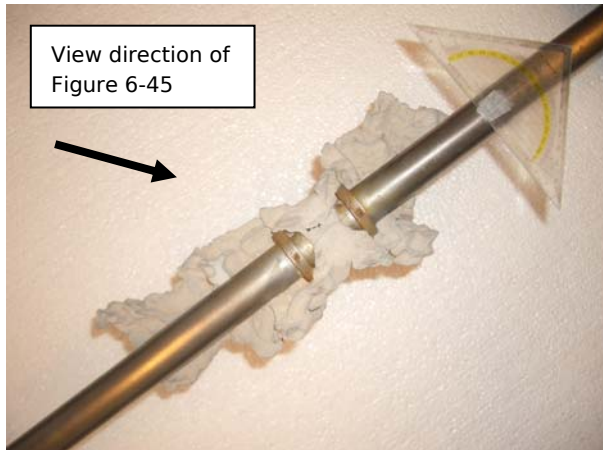


Figure 6-44 Excavated grout fracture test 10



Figure 6-45 Side view of the grout fracture

7 Discussion

An upper limit of efficiency was calculated to compare these numbers with the values found in the experiment. The injected volume is assumed to be a sphere with a bled outer layer x .

7.1 Theoretical Maximum Efficiency of the Injection

During injection of the grout, water bleeding occurs, which decreases the effectiveness of the injected volume (V_0). The theoretical maximum heave caused by the grout injection is the total volume injected minus the bled water, assumed that no densification of the sand sample occurs. The amount of bled water is calculated in the next paragraph. The shape of the volume injected is assumed to be a sphere.

V_0 formed as a sphere:

$$V_0 = \frac{4}{3} \pi r_0^3 \tag{7.1}$$

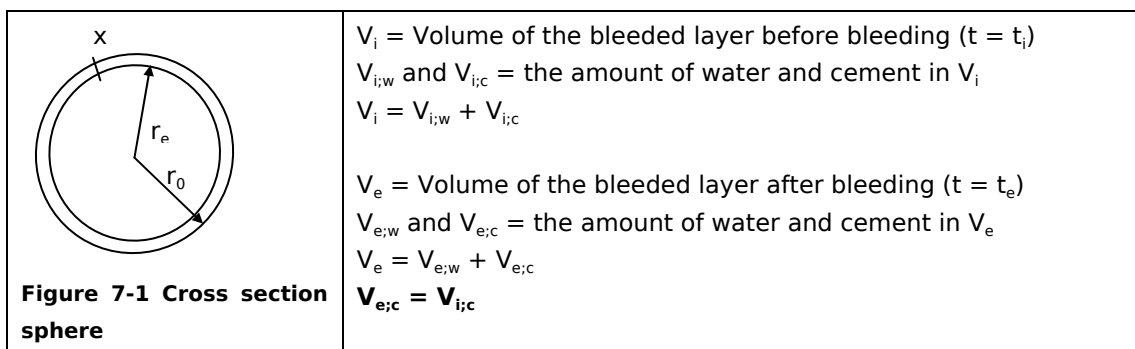
Then the radius of the sphere is r_0

$$r_0 = \sqrt[3]{\frac{3 \cdot V_0}{4\pi}} \tag{7.2}$$

This volume grout (V_0) bleeds over a thickness x from initial porosity (n_i) to end porosity (n_e)

$$n_i = \frac{V_{i:w}}{V_{i:w} + V_{i:c}} \qquad n_e = \frac{V_{e:w}}{V_{e:w} + V_{e:c}} \tag{7.3}$$

The shell with bled grout has a thickness x . The experiments show that in the end porosity stage the cement grains are packed closer together than in the initial porosity stage. However, the amount of cement in both stages is assumed the same. The difference is the water that bled out of the fresh grout into the sand.



x = thickness of the bled layer

The volume of the bled layer after bleeding:

$$V_e = \frac{4}{3} \pi (r_0^3 - r_e^3) \tag{7.4}$$

During bleeding the porosity of the bled layer reduces from n_i to n_e , so the volume of water that is lost to bleeding is calculated:

The amount of water in V_e at $t = t_e$:

$$V_{e;w} = n_e \cdot V_e \tag{7.5}$$

The amount of cement in V_e at $t = t_e$:

$$V_{e;c} = V_e - V_{e;w} \tag{7.6}$$

The amount of water in V_i at $t = t_i$:

$$V_{i;c} = V_{i;c} \quad V_{i;w} = \frac{n_i \cdot V_{e;c}}{1 - n_i} \tag{7.7}$$

The volume of water that bled to the sand is lost water:

$$V_{w;lost} = V_{i;w} - V_{e;w} \tag{7.8}$$

Effective volume, which created heave V_h :

$$V_h = V_0 - V_{w;lost} \tag{7.9}$$

Efficiency:

$$\frac{V_h}{V_0} \cdot 100\% \tag{7.10}$$

This calculation is done for every test performed and it gives reliable values when compared to the measured efficiencies.

x is calculated by
$$x = \sqrt{2 \cdot k \frac{1 - n_i}{n_i - n_e} \cdot \Delta\phi \cdot t} \tag{4.13}$$

For $\Delta\phi$, the maximum obtained pump pressure in the experiment is taken, and for the time t, the injection time. This is an assumption because pressure records show that after injection the pressure is not immediately zero.

The pictures in Figure 6-16, Figure 7-2 and Figure 7-3 show the **bled layer x** in cross sections of grout fractures in a number of tests.

| Test | n_e | n_i | Pressure [bar] | Time [s] | Permeability [m/s] | Bled layer x [mm] | V_0 [ml] | r_0 [mm] |
|------|-------|-------|----------------|----------|----------------------|-------------------|------------|------------|
| 1 | 0.53 | 0.74 | 50 | 10 | $1.76 \cdot 10^{-7}$ | 14.7 | 50 | 22.9 |
| 2 | 0.53 | 0.74 | 40 | 10 | $1.76 \cdot 10^{-7}$ | 13.2 | 167 | 34.2 |
| 3 | 0.53 | 0.74 | 50 | 2 | $1.76 \cdot 10^{-7}$ | 6.6 | 333 | 43.0 |
| 4 | 0.53 | 0.74 | 50 | 2 | $1.76 \cdot 10^{-7}$ | 6.6 | 667 | 54.2 |
| 5 | 0.53 | 0.74 | 50 | 4 | $9.56 \cdot 10^{-8}$ | 6.9 | 667 | 54.2 |
| 6 | 0.55 | 0.77 | 100 | 4 | $4.70 \cdot 10^{-8}$ | 6.1 | 667 | 54.2 |
| 7 | 0.55 | 0.77 | 140 | 4 | $4.70 \cdot 10^{-8}$ | 7.2 | 667 | 54.2 |
| 8 | 0.59 | 0.80 | 150 | 6 | $2.67 \cdot 10^{-8}$ | 6.7 | 1000 | 62.0 |
| 9 | 0.59 | 0.80 | 154 | 4 | $1.38 \cdot 10^{-8}$ | 4.0 | 667 | 54.2 |
| 10 | 0.59 | 0.80 | 87 | 4 | $1.38 \cdot 10^{-8}$ | 3.0 | 667 | 54.2 |

Table 7-1 Results calculation maximum theoretical efficiency [1]

The calculations give numbers for the theoretical maximum efficiency. An important remark is that the calculated efficiency does not take into account the compaction of the sand sample. Only the bleeding of the grout contributes to the lost volume compared to the volume injected, not the densification of the sand.

| Test | r_e [mm] | V_i [ml] | $V_{e;c}$ [ml] | $V_{e;w}$ [ml] | $V_{i;w}$ [ml] | $V_{i;w} - V_{e;w}$ [ml] | Efficient Volume Injected [ml] | Theoretical Efficiency |
|------|---------------|---------------|-------------------|-------------------|-------------------|-----------------------------|-----------------------------------|---------------------------|
| 1 | 8.1 | 48 | 22 | 25 | 64 | 39 | 11 | 23% |
| 2 | 21.0 | 128 | 60 | 68 | 172 | 104 | 63 | 38% |
| 3 | 36.4 | 131 | 62 | 69 | 175 | 106 | 227 | 68% |
| 4 | 47.6 | 215 | 101 | 114 | 288 | 174 | 493 | 74% |
| 5 | 47.3 | 223 | 105 | 118 | 299 | 181 | 486 | 73% |
| 6 | 48.1 | 201 | 91 | 110 | 313 | 202 | 465 | 70% |
| 7 | 47.0 | 233 | 105 | 128 | 362 | 234 | 433 | 65% |
| 8 | 55.3 | 291 | 121 | 171 | 480 | 309 | 691 | 69% |
| 9 | 50.2 | 137 | 57 | 80 | 226 | 146 | 521 | 78% |
| 10 | 51.2 | 105 | 44 | 62 | 173 | 112 | 555 | 83% |

Table 7-2 Results calculation maximum theoretical efficiency [2]

For example: Test 2 gives a calculated theoretical efficiency of 38%. Concluded from this calculation is that the 62% that was measured in test 2 (See paragraph 6.7) is too high a value. This is due to the air in the drainage system. Air in the drainage system pushes the PVC-piston plate up which measures the heave.

To validate the bleeding theory a number of cross sections are examined, see below.

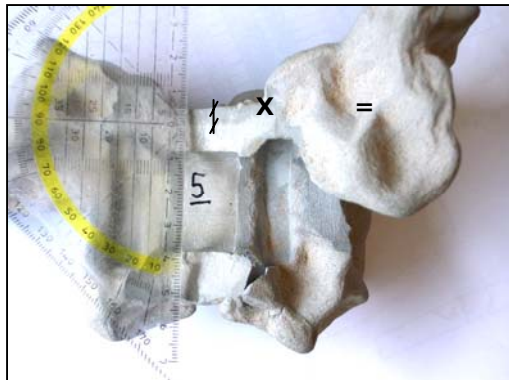


Figure 7-2 Test 5, bleeding layer x (the total fracture of test 5 is shown)



Figure 7-3 Test 7 and 10 bleeding layer (cross sections of the fracture)

The thicknesses of the bled layer in the pictures above do correspond to the thickness of the layer calculated in Table 7-1. The differences can be explained by inaccuracies in the measurements of the permeability of the bled layer.

7.2 Cement Efficiency

A comparison was done to calculate the efficiency of the volume of cement that was injected. The WCR was not the same in every test therefore the interest goes to the relationship between the volume of heave and the volume of cement grains injected. A short and straightforward calculation is made.

Weight of the grout injected:

$$W_{grout} = V_0 \cdot \gamma_{grout} \quad [7.11]$$

Weight of the cement grains in the volume of grout (V_0) injected:

$$W_{cement} = \frac{W_{grout}}{WCR + 1} \quad [7.12]$$

Volume cement grains in the volume of grout injected (V_0) injected:

$$V_{cement} = \frac{W_{cement}}{\gamma_{cement}} \quad [7.13]$$

Volume heave per volume cement grain injected:

$$Cement\ efficiency = \frac{V_h}{V_{cement}} \quad [7.14]$$

Table 7-3 below shows the cement efficiency calculated for every test. In column 4 (Efficiency η) the measured efficiency ($V_h/\Delta V_0$) is also given. The $\gamma_{fracture}$ is measured after excavation of the grout fractures. For test 1 through test 5 the $\gamma_{fracture}$ is larger than the γ_{grout} (= density fresh grout). The reason for this is the significant amount of water bled from the grout fracture. Grout from which water has bled away has a lower end porosity (n_e) which gives it consequently a higher density. In test 1 through test 5 the permeability of the bled layer is larger than in test 6 through test 10. In Test 6 through test 10 the permeability of the bled layer is limited; consequently the bled layer becomes thinner. This makes the density in tests 6-10 of the fracture ($\gamma_{fracture}$) the same as the density of the grout (γ_{grout}) before injecting. From test 6 on, the bentonite hydrated for at least 24 hours, which made the permeability of the bled layer considerably smaller.

| Test | V_h [ml] | ΔV_0 [ml] | Efficiency η Measured | WCR [-] | γ_{grout} [gr/ml] | $\gamma_{fracture}$ [gr/ml] | W_{grout} [gram] | W_{cement} [gram] | V_{cement} [ml] | Cement efficiency |
|------|---------------|----------------------|-------------------------------|------------|-----------------------------|--------------------------------|-----------------------|------------------------|----------------------|----------------------|
| 1 | 3 | 50 | 6% | 1 | 1.48 | 1.91 | 74 | 37 | 13 | 23% |
| 2 | 103 | 167 | 62% | 1 | 1.48 | 1.74 | 247 | 124 | 43 | 238% |
| 3 | 140 | 333 | 42% | 1 | 1.48 | 1.48 | 493 | 246 | 86 | 162% |
| 4 | 246 | 667 | 37% | 1 | 1.48 | 1.78 | 987 | 494 | 173 | 143% |
| 5 | 287 | 667 | 43% | 1 | 1.48 | 1.55 | 987 | 494 | 173 | 166% |
| 6 | 225 | 667 | 34% | 1.2 | 1.42 | 1.43 | 947 | 431 | 151 | 149% |
| 7 | 175 | 667 | 26% | 1.2 | 1.42 | 1.44 | 947 | 431 | 151 | 116% |
| 8 | 200 | 1000 | 20% | 1.4 | 1.37 | 1.35 | 1370 | 571 | 200 | 100% |
| 9 | 281 | 667 | 42% | 1.4 | 1.37 | 1.38 | 914 | 381 | 133 | 211% |
| 10 | 38 | 667 | 6% | 1.4 | 1.37 | 1.31 | 914 | 381 | 133 | 29% |

Table 7-3 Summary of calculated efficiency in every test.

In conclusion, changing the WCR does not affect the efficiency, only the density of the sand and the effective stress at injection opening have an influence on this. Therefore, the WCR should become as large as possible on condition that the permeability of the bleded layer is limited.

7.3 Pressure Records

According to te Grotenhuis' model, which holds the assumption that the Moseley¹³ pressure records are applicable here, peak pressures occurring after initial opening of the rubber sleeve are reactions of additional fractures (see left-hand diagram of Figure 1-4). The DLR¹⁴ do not show a clear fracture initiation pressure, they only show a constant pressure when injection progresses.

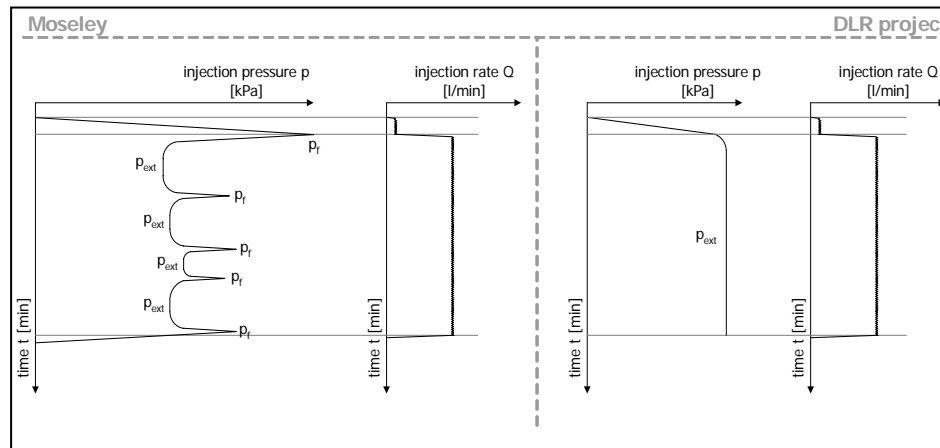


Figure 7-4 Pressure records Moseley¹³ (left) DLR¹⁴ (right) [te Grotenhuis⁴]

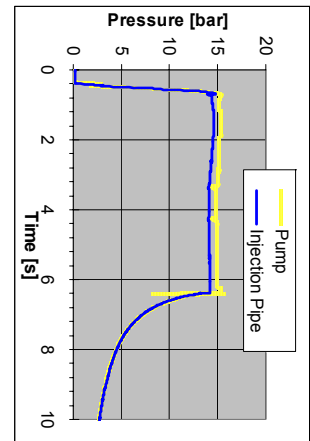


Figure 7-5 Pressure records (test 8)

Figure 7-5 shows the pressure records as found in the experiment plotted. These records correspond more with the tendency of the DLR¹⁴ project records than with the records of Moseley¹³.

Fluctuations in the pressure records were not found in the compensation grouting experiments, which makes the assumption of additional fracture paths not plausible. The outcome of the pressure records in the experiment do not confirm the pressure records (as stated in te Grotenhuis' model) as Moseley¹³ found them. It should be reconsidered if the theory of fracture propagation and new fractures originating can be hanged on the peak pressure records of Moseley¹³. The conditions of the laboratory test, dense sand with a moderate overburden and a grout mixture of WCR = 1.4, do not create the fractures as expected.

8 Conclusions and Recommendations

In order to formulate a well-founded conclusion of this research, the objective as stated in the introduction is reviewed here.

8.1 Introduction

Problem analysis

How does a grout injection behave (fracture propagation and fracture growth in diameter) while injected at a controlled flow? Examine possibilities to influence length and exterior of the fracture, which means borehole expansion and fracture propagation, by changing the rheology parameters of the grout mixture. This is all done in order to control the settlements by compensation grouting at foundation level along the route of the Noord/Zuidlijn in Amsterdam.

Objective

The main objective of this research is to set up an experiment, where by means of grout injection the geometry and the propagation of a grout fracture in sand can be examined. This gives a better understanding of the technique of compensation grouting. An analytical model was made to describe the propagation and stagnation of a fracture. The experiments can validate the model for use in practice and can be useful for making an injection strategy.

8.2 Conclusions

8.2.1 Set-up

One can conclude that the main objective of the research has been achieved. A set-up of an experiment, where by means of grout injection the geometry of and the propagation of a grout fracture in sand can be examined, was made. Additionally, the set-up of the experiment was equipped with a system which could precisely measure the heave of the sand sample while injecting a grout mixture. Ten grout injections were completed. The grout injections were performed with similar grout as used in practice. Furthermore, adjustments were made to the grout mixture to improve the behavior of the grout injection to create more of an actual fracture. The geometrical outline of the fracture was examined by excavation, which increased the understanding of the compensation grouting technique.

8.2.2 Model Validation

The fracture propagation model developed by [te Grotenhuis⁴] has been validated. According to the model, the grout injections are influenced by three essential processes:

1. The friction of propagating grout (related to shear stress)
2. Bleeding of the injected grout mixture (related to the permeability of the bled layer)
3. The response of the sand

All three processes in the model are evaluated and examined to see if they give a realistic description of the actual process.

The friction of propagating grout

The friction side of the propagating grout model states:

When grout is injected into a single channel, injection proceeds until the grout stops because the shear force along the wall of the channel balances the driving pressure. The model assumes that the grout behaves as a Bingham fluid, which means that the shear force per unit area of contact between the

grout and the fracture channel wall is constant along the length of the fracture.

[Stille et al. 1992¹⁰]

Evidently, the grout experiences friction, shear stresses within the fluid, during injection. All fluids experience internal shear stress when flowing. In this experiment, this phenomenon only occurs in the injection pipe system and not in the fractures itself as the excavated fractures show. The geometry of the fracture is not a long thin tube as was assumed in the fracture model. Grout flowing in a thin long tube might experience friction when flowing; however, the friction does not balance the driving pressure from the pump. The driving pressure from the pump is mainly determined by the sand properties such as grain size distribution, relative density (this influences the stiffness of the sand sample) and the effective stresses in the soil. Friction in the injection pipe is only a small part in this.

Bleeding of the injected grout mixture

It is assumed that fracture propagation stagnates whenever the size of the inner core of fresh grout is decreasing. Consequently, a new fracture branch originates if the grout injection flow is continued. [te Grotenhuis 2004⁴]

The model assumes the fresh grout fracture channel gets silted up by bled grout. This could be the case when modeling a grout fracture in sand as a channel but this was not the geometry found in the experiment. Therefore, bleeding is mainly an event which influences the efficiency of the compensation grouting injections. The bleeding of the grout plays a key role in the injection experiment in sand. This has been confirmed by the results that show that the theory on bleeding grout did fairly good correspond with the bleeding of grout in the experiments.

The difference in scale between the model and the experiment is given in Figure 8-1 and Figure 8-2. The explanation for this is the mistaken assumption that the fracture would become a channel in sand. The surface of the grout injection that is in contact with the sand and has the opportunity to bleed is, according to the experiments, irrelevant in comparison to the total volume of grout. In the model the opposite is the case. The ratio fracture surface/volume (specific surface?) in the model is such that the silting up of the fracture is a dominant phenomenon. The test results, however, do not confirm this.

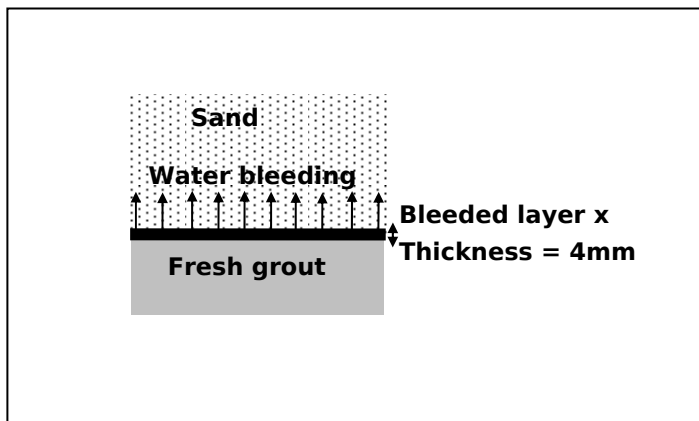


Figure 8-1 1D Model of the grout injection in the experiment.

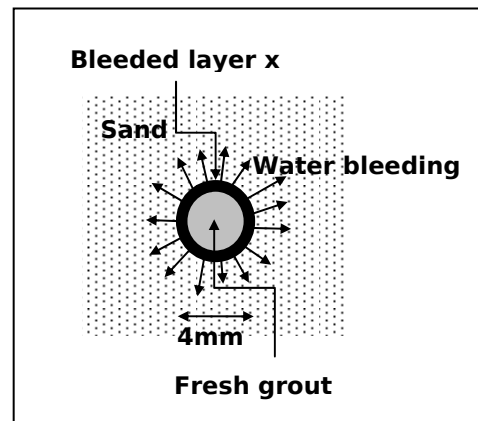


Figure 8-2 Assumption of the fracture grouting model.

The response of the sand

The model does not quantify soil response, but with the measurements done it is possible now to introduce this into a model. A couple of the findings are:

- The injected grout fails to penetrate the sand to the extent that a fracture is created. Instead, excavation shows that the grout mixture forms a bulb which pushes the sand away rather than fracturing it.
- The relative density (the stiffness of the sand) has an enormous influence on the efficiency. The denser the sand the stiffer it performs and therefore the greater the efficiency.
- Both the level of effective stresses in the sand and the density of the sand influence the opening pressure of the rubber sleeve. The opening pressure of the rubber sleeve rises as density and effective stresses increase.

8.2.3 Technical Achievements

Water Cement Ratio

The grout injections have been kept processible by varying the WCR. The other reason for varying the ratio of water and cement in a grout mixture is to analyze what influence the WCR has on the geometry of the grout fracture. The difference in fracture geometry and fracture pressure characteristics is negligible when comparing two tests with different WCRs. Test 7 WCR 1.2; Test 8 WCR 1.4.

Pre conditioning

Pre conditioning is an important part of the compensation grouting process. Horizontal stresses have been made larger than the vertical stresses to create horizontal fractures. This pre conditioning is done artificially in the experiment by pre stressing the sand and unloading to get an over consolidated sand, creating a $K_0 \approx 1$. This did not succeed, but as soon injection started in the experiment, the horizontal stresses rose to a level higher than the vertical stresses, resulting in a K_0 larger than 1. Consequently, a preconditioned sand sample was created after all. Another dominant factor is the low stress zone underneath the injection pipe, due to the densification process that is applied in the test procedure.

Fluctuations in pressure record

The fluctuations in pressure records were a part of the fracture grouting model. This was not found in the pressure records in the experiment. New fractures do not occur during injection; as excavated fractures show, it is more likely that the existing fracture keeps on growing by pushing the sand away.

Bentonite

The bentonite does have a large influence on the grout injections' material behavior. This does not necessarily play a part when more bentonite is added, but rather when the bentonite that is added has hydrated for more than 24 hours before mixing cement. The permeability of the bled layer is measured to become four times smaller in mixtures where the bentonite had 24 hours time to interact with the water. The mixture is more capable of holding water. However, when bentonite hydrates for 24 hours it thickens the grout mixture and therefore the WCR must increase to keep the grout mixture processible. Increasing the WCR adds more water to the mixture; this water can bleed again and consequently is not improving the efficiency.

Volume balance can be made.

A volume balance can be made. This was not observed in every test but that can be assigned to unexpectedly high pressures needed to inject the grout at low pressures of the sand sample. When this took place the air pressure was taken off the water chamber, which consequently resulted in the drainage water helping to push the PVC-piston plate up. In test 10 an exact volume balance is pointed out.

Lesson learned

When doing an experiment one should realize that if the test program is not totally clear yet because expected outcomes are uncertain, due to assumptions made when modeling the process, one should take enough time to analyze the results after each test before jumping to the next test and hoping the outcome is what was expected.

8.3 Recommendations

The compensation grouting laboratory experiments in sand have not given the expected outcomes as predicted by te Grotenhuis' model. Fortunately, a lot of experimental data is generated which can support further research.

8.3.1 Further Research

Set-up

The set-up of the compensation grouting experiment is adequate and sufficient for the experiments done on grout injections. This was not the case for the first serie of tests; therefore, some adjustments were made during the experimental process and the test set-up is satisfactory for its purpose. One of the important adjustments was the injection opening. This aspect has evolved by trial and error and no further adjustments on this point are necessary. The other adjustment was made to the grout pump. In test 9, which was done with very dense sand (relative density of at least 75%), the grout pump was not able to inject the grout when the overburden was generating an effective stress of 100kPa. Therefore, the overburden was lowered to 25kPa effective stress. The overburden was and still is a parameter which is supposed to have a strong influence on fracturing of sand (see for example the experiments of de Pater⁸).

The recommendation would be to do a test where the grout pump is not the weakest link. Inject at an overburden of at least 100kPa in a dense sand sample (relative density minimal 75%). The expected geometry of the fracture would be the same shape as created in all the other tests but it would take away the uncertainty and speculations of fractures being created by grout injected in saturated sand. During this test an extreme watery mixture should be used of a Water Cement Ratio of 1.6.

Analysis

The generated data can still be analyzed in more detail and on more aspects. The experiment has produced a considerable amount of data which can be used for a more comprehensive analytically analysis. The following issues are possibilities for further analysis:

- **The soil response**

The heave of the soil and the amount of drainage water being pressed out of the saturated sand sample has been measured during injection and during consolidation of the sand sample. These soil responses need to be analyzed more to be able to give a better explanation for the behavior of the fracture.

- **Fracture geometry**

The worm or bulb of grout that formed in the sand was not the expected fracture as modeled. The question still remains what influences this geometry besides the bleeding of the grout and the soil stresses in the sand sample. Check theoretically whether it is physically possible to fracture sand with a fluid existing of granular material like cement.

- **The order of origination of the grout bulbs**

The order of originating of the fracture is an interesting point for further research. An interesting question would be whether little 'fractures' develop first which then fill up with the injected grout, or whether a filter cake (bleeded layer) develops during the injection which pushes the sand away.

8.3.2 Practical Performance Compensation Grouting

Injection strategy

The exterior of the fracture geometry gives an opportunity to regulate the injection grout bulbs when injected, no long fracture channels do develop, so no grout is lost. Therefore, a fan of pipes is installed beneath a foundation with an injection point at every meter in the pipe. This is a method that is already being performed in practice. The outcome of the experiment encourages this approach (bulbs originate instead of long fractures). It will keep the process of compensation grouting controllable.

Bentonite

The addition of bentonite to the grout mixture is a method already used in practice to prevent the grout from bleeding, and thus makes grout injection more efficient. In the experiment, bentonite was added to the grout mixture and subsequently left to hydrate (ripe) for 24 hours. The hydration had a positive influence on the permeability (became lower) of the bled layer which prevented bleeding. In practice this should also be done by having a silo on site where a 24 hour hydrated mixture of bentonite (5%) and water is available. This saves cement.

Appendices

Appendix A:

Summary Report Fracture Grouting in Theory

[te Grotenhuis, 2004⁴]

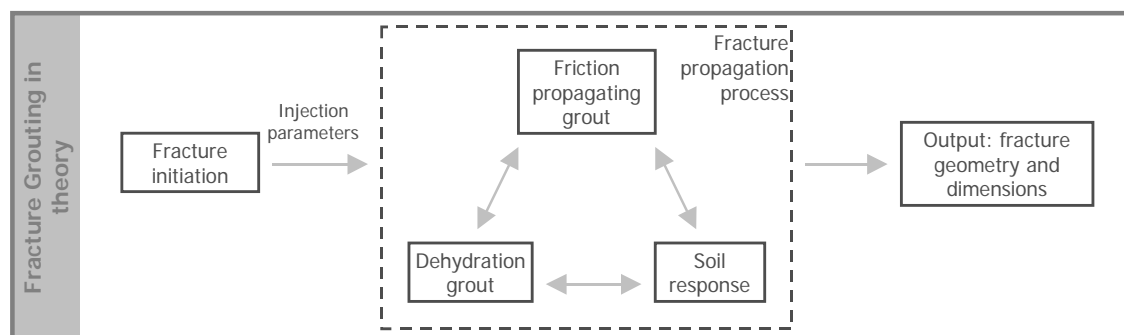
Introduction

The construction of a new metro line in the city centre of Amsterdam, the so-called Noord/Zuidlijn, is a challenging job as many buildings along the route are sensitive to settlement and angular distortion. Furthermore, many of these buildings have a monumental status. To prevent damage, settlement criteria are very strict and mitigating measures are necessary at several locations to meet the criteria. One of the measures that will be taken is the use of Fracture Grouting.

This technique has been successfully applied in soil tunneling projects abroad. Therefore it is a promising measure for the situation in Amsterdam. Nevertheless, soil conditions (soft soil) and foundation configuration (pile foundation) are significantly different in the Amsterdam situation. In order to see whether Fracturing Grouting can be used in these conditions, a full-scale Compensation Grouting Trial (CGT) has been performed under comparable conditions.

The trial showed that Fracture Grouting in sand underneath the pile foundation can be used to control the vertical movement of wooden pile foundations. Nevertheless, the grouting efficiency fluctuated considerably during the trial. Grouting efficiency is the ratio between heave volume to volume of the injected grout. It can be concluded that hydraulic fracture initiation and fracture propagation in sand are theoretically not well understood. Consequently the hydraulic fracture dimensions in sand are not actively controlled. For this reason the grouting efficiency of Fracture Grouting in sand is suboptimal. Objective of this study is to find methods that can be used in order to actively control fracture growth.

To enlarge the understanding of hydraulic fracture initiation and propagation a literature study has been performed. The results were used to model fracture initiation and propagation in sand. The fracture propagation model has consequently been used to study the effect of changing input parameters, like variation of the grout properties. Additionally, several laboratory experiments were done to find realistic values for several input parameters of the model. A schematic outline of the research is presented below.



Results Fracture Grouting in Theory

The results of this research on Fracture Grouting in theory are presented in accordance with the schematic outline of the research.

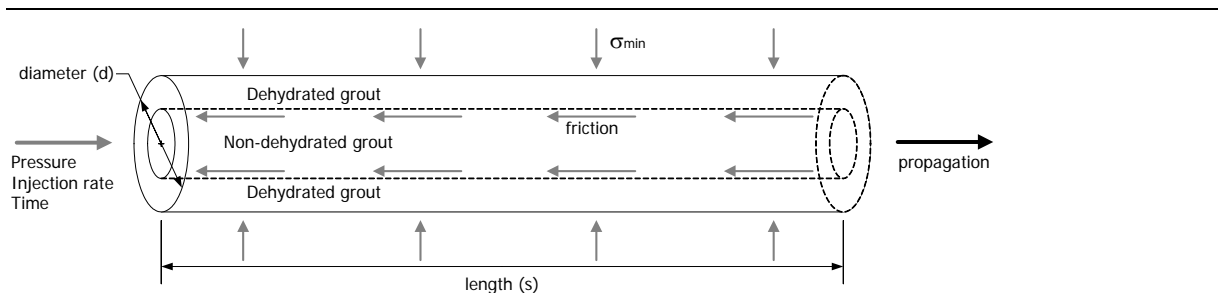
Fracture initiation

- The fracture initiation pressure is a function of several parameters. The most important parameters are:
 - The minimal principal stress or so-called confining stress. Meaning that increasing stress results in increasing fracture initiation pressure.
 - The rheological parameters and the gradation of the injection fluid. Some fluids leak off completely at high pressure, hampering fracture initiation (concerning fracturing in and). For effective fracturing one should use a good wall-building fluid.
- Given the project description and soil properties (TAM level NAP -16 m, pile foundations and fracturing in medium to coarse sand) it is possible to use the ratio of fracture (injection) pressure p_f to confining stress σ_c in order to predict the fracture pressure. A reasonable value for this ratio is $p_f / \sigma_c \approx 5$

Fracture propagation

- Hydraulic fracture development in sand is certainly not restricted to radial or non-radial planes. The length over which fractures propagate is considerable. Additionally, development often has a certain, or preferred, direction. 'Fracture paths', instead of 'fracture planes', do better reflect the shape of fractures that can be found as a result of Fracture Grouting in sand. Therefore a tube has been used to represent a propagating hydraulic fracture in sand during fracture propagation modelling.
- The fracture process is affected by three constituent processes:
 - The friction of propagating grout (related to rheological parameters and resulting shear stress)
 - Dehydration of injected grout (related to permeability) and accompanying development of a dehydrated layer at the outer ring of the fracture tube.
 - The response of surrounding soil

These processes take place at the same time and do together result in a particular fracture geometry with accompanying dimensions. The first two processes have been quantified and turned into a model; see the figure below. The latter process could not be quantified. It is assumed that fracture propagation stagnates whenever the size of the inner core of non-dehydrated grout is decreasing. Consequently, a new fracture branch originates if the grout injection flow is continued.



Output of fracture propagation process

- During experiments specific properties of fracture grout have been determined. Representative yield point and plastic viscosity appeared to be respectively 17 Pa and 0.012 Pa*s. This results in a representative shear stress of 25 Pa. The initial porosity is 0.75, while the end-porosity after dehydration is about 0.50. The permeability of the dehydrated grout filter is about $5 \cdot 10^{-9}$ m/s.
- The grouting efficiency varies considerably and is substantially less than 1 due to several reasons. Most important reasons are:
 - Interaction of the fracture with the adjacent soil (when the grout displaces the surrounding soil, the ground is compacted).
 - Water expulsion or so-called leak-off, or dehydration, from the injected grout.
- Dehydration or water expulsion from the grout results in a volume loss of the injected volume of grout. Complete dehydration would result in a total volume loss of 50% of the total injected volume. The inner core of the fracture does not completely dehydrate. However, a volume loss of 40% is still reasonable. This means grouting efficiency has already been reduced to 60% without even taking into account the other causes for efficiency loss. The fracture length is particularly affected by this volume loss.
- A calculation with the fracture propagation model, based on the Fracture Grouting parameters, initially results in a fracture propagation process that stagnates just after about 1 or 2 seconds. In those seconds, fractures with a thickness of about 4 mm and a length of 10 m are created. The moment of propagation stagnation seems to appear very soon. Nevertheless, the fracture dimensions are realistic compared to results found at Fracture grouting works in sand in practice.

Conclusion Fracture Grouting in Theory

The previous information leads to the most important conclusion of this MSc thesis research. Studying of hydraulic fracture initiation and propagation in sand has certainly resulted in enlarged understanding of hydraulic fracturing. Three constituent processes have been defined that affect fracture propagation. Considering these processes it seems possible to influence the output of the fracture propagation process in order to increase grouting efficiency:

- Grouting efficiency is increased whenever injected grout can be retained under the foundation of a building. It is favourable to limit the fracture length and to maximise the fracture thickness. There are two theoretical methods to influence the output of the fracture process. These methods can be used to increase grouting efficiency:
 - Reducing the Water Solids Factor (WSF) or increasing the amount of angular aggregate material in the fracture grout increases the shear stress. This results in decreasing fracture length and increasing thickness. It should be realised there is a lower limit to the WSF in order to facilitate fracture initiation in the fracture tip.
 - By changing the amount of bentonite in the fracture grout, the moment of propagation stagnation can be affected. The grouting efficiency can be affected indirectly when taking the foundation configuration into account. Stimulating propagation stagnation reduces the fracture length. Injected grout will be concentrated under the foundation piles. Consequently, more of the injected grout contributes to the objective of fracture grouting: creation of heave of a building. In other words, the amount of bentonite can theoretically be used to tune the fracture length to the foundation configuration.

Recommendations Fracture Grouting in Theory

Further improvement of the fracture propagation model will be a difficult exercise. It is therefore recommended to focus on practical experiments. These experiments will directly show if gained understanding is (partly) right. Subsequently, it will directly result in practical recommendations for the execution of Fracture Grouting in sand. Experiments should be performed in such a way that fracture dimensions can be checked by excavation of the sample afterwards. During the experiments on fracture propagation the intended objectives should be:

- To create hydraulic fracturing in sand with a regular composed fracture grout.
- To study the geometrical shape of the created fractures.
- To see whether soil conditions and properties change due to repetitive grout injections and to study the effect on fracture propagation.
- To reduce the Water Solids Factor (WSF) of the fracture grout, or to increase the amount of angular aggregate material in the fracture grout in order to see whether fracture dimensions change significantly by the increased shear stress in the grout. Subsequently it would be interesting to find the lower limit of the WSF at which fracture initiation does not occur anymore.
- To vary the percentage of bentonite in the fracture grout to see whether the moment of propagation stagnation can be controlled and to see whether the fracture pattern has been influenced.

In all cases it is necessary to permanently record the injection pressure (preferably at the injection point) and the accompanying injection rate.

Appendix B:

Review All Ten Tests

References

- ¹ Noord/Zuidlijn website, www.noordzuidlijn.nl
- ² Vliet, M.J.; *The influence Zone and Effectiveness of Fracture Grouting on Piled Foundations*, MSc. thesis TU Delft, April 2002
- ³ Kummerer, C.; Numerical modelling of displacement grouting and application to case histories. PhD thesis, University Graz, October 2003
- ⁴ Te Grotenhuis, R.; *Fracture grouting in Theory*, M.Sc. Thesis, TU Delft, November 2004
- ⁵ Stoel, A.E.C. van, der; *Grouting for Pile Foundation Improvement*, PhD thesis TU Delft, September 2001
- ⁶ Cheong, M.T., Au, S.K.A., Soga, K., Mair, R.J., Bolton, M.D.; *Fundamental Study of Compensation Grouting in Clay*, University of Cambridge, Department of Engineering, http://www-civ.eng.cam.ac.uk/geotech_new/posters/meicheong.pdf
- ⁷ Haasnoot, J.K., Stoel, A.E.C. van, der, Kaalberg; *Full-scale compensation grouting trial North/South line Amsterdam; Spatial relationship of fracture grouting injection pressures*, F.J.; Proc. XIIIth European Conference on soil mechanics and geotechnical engineering, Prague 2003
- ⁸ Pater, de, H.J., Bohloli, B.; *Fracturing Unconsolidated Rock*, Delft, October 2003
- ⁹ Bezuijen, A.; *Hydraulic Fracture Experiments at low stresses in sand*, Delft 2003
- ¹⁰ National research council; *Rock fractures and fluid flow*; National academy press; 1996
- ¹¹ Bezuijen, A., Talmon, A.M.; *Groutdrukken Sophia spoortunnel, Metingen en analyse beide buizen*; Delft Cluster; November 2003
- ¹² Schiereck, G.J.; *Introduction to bed, bank and shore protection*, Delft University Press, 1993
- ¹³ Moseley, M.P.; *Ground Improvement*; Chapman & Hall; 1993
- ¹⁴ Sugiyama, T., Nomoto, M., Hagiwara, T., Mair, R.J., Bolton, M.D., Soga, K.; *Compensation Grouting at the Docklands Light Railway Lewisham Extension project*; Proc. Geotechnical aspects of Underground Construction in Soft Ground, p 319-324; 2000